



Diversity of Sporocadaceae (pestalotioid fungi) from Rosa in China

C. Peng¹, P.W. Crous^{2,3,4}, N. Jiang⁵, X.L. Fan¹, Y.M. Liang⁶, C.M. Tian^{1,*}

Key words

Amphisphaerales
Ascomycota
new taxa
phylogeny
taxonomy

Abstract *Rosa* (Rosaceae) is an important ornamental and medicinal plant genus worldwide, with several species being cultivated in China. Members of Sporocadaceae (pestalotioid fungi) are globally distributed and include endophytes, saprobes but also plant pathogens, infecting a broad range of host plants on which they can cause important plant diseases. Although several Sporocadaceae species were recorded to inhabit *Rosa* spp., the taxa occurring on *Rosa* remain largely unresolved. In this study, a total of 295 diseased samples were collected from branches, fruits, leaves and spines of eight *Rosa* species (*R. chinensis*, *R. helenae*, *R. laevigata*, *R. multiflora*, *R. omeiensis*, *R. rugosa*, *R. spinosissima* and *R. xanthina*) in Gansu, Henan, Hunan, Qinghai, Shaanxi Provinces and the Ningxia Autonomous Region of China. Subsequently 126 strains were obtained and identified based on comparisons of DNA sequence data. Based on these results 15 species residing in six genera of Sporocadaceae were delineated, including four known species (*Pestalotiopsis chamaeropis*, *Pes. rhodomyrthus*, *Sporocadus sorbi* and *Spo. trimorphus*) and 11 new species described here as *Monochaetia rosarum*, *Neopestalotiopsis concentrica*, *N. subepidermalis*, *Pestalotiopsis tumida*, *Seimatosprium centrale*, *Seim. gracile*, *Seim. nonappendiculatum*, *Seim. parvum*, *Seiridium rosae*, *Sporocadus brevis*, and *Spo. spiniger*. This study also represents the first report of *Pes. chamaeropis*, *Pes. rhodomyrthus* and *Spo. sorbi* on *Rosa*. The overall data revealed that *Pestalotiopsis* was the most prevalent genus, followed by *Seimatosprium*, while *Pes. chamaeropis* and *Pes. rhodomyrthus* were the two most prevalent species. Analysis of Sporocadaceae abundance on *Rosa* species and plant organs revealed that spines of *R. chinensis* had the highest species diversity.

Citation: Peng C, Crous PW, Jiang N, et al. 2022. Diversity of Sporocadaceae (pestalotioid fungi) from Rosa in China.

Persoonia 49: 201–260. <https://doi.org/10.3767/persoonia.2022.49.07>.

Effectively published online: 12 December 2022 [Received: 8 May 2022; Accepted: 18 September 2022].

INTRODUCTION

Sporocadaceae (Xylariales, Sordariomycetes) is a well-known fungal family containing pestalotioid fungi. Traditionally, pestalotioid fungi are circumscribed as a group of coelomycetous fungi having fusoid or nearly fusoid, multi-septate conidia, with appendages at one or both ends (Nag Raj 1993, Maharachchikumbura et al. 2014, Liu et al. 2019).

Pestalotioid fungi were previously classified in Amphisphaeriaceae, Amphisphaerales (Eriksson 1986, Samuels et al. 1987). Subsequently, several studies suggested that Amphisphaerales should not be accepted due to the lack of stable phylogenetic support, and hence it was treated as synonym of Xylariales (Eriksson 1987, Kang et al. 1999, Smith et al. 2003). Later, Senanayake et al. (2015) revised Xylariomycetidae and transferred several important genera of pestalotioid fungi from Am-

phisphaeriaceae to three new families, Bartaliniaceae, Discosiacae and Pestalotiopsidaceae. Genera such as *Bartalinia* and *Broomella* were transferred to Bartaliniaceae, Discosia and *Seimatosprium* to Discosiacae, and *Neopestalotiopsis*, *Pestalotiopsis*, *Pseudopestalotiopsis*, *Monochaetia* and *Seiridium* to Pestalotiopsidaceae. Crous et al. (2015a) introduced a new family Robillardaceae to accommodate *Robillarda*. Subsequently, Jaklitsch et al. (2016) grouped the pestalotioid fungi into a single family and revived the older family name Sporocadaceae. Therefore, Bartaliniaceae, Discosiacae, Pestalotiopsidaceae and Robillardaceae became synonyms of Sporocadaceae. These families were classified in Amphisphaerales which was resurrected instead of Xylariales (Senanayake et al. 2015). Recently, several studies treated Amphisphaerales as a distinct order (Senanayake et al. 2015, Samarakoon 2016, Hongsanan et al. 2017, Wijayawardene et al. 2020). Based on multi-locus phylogenetic analyses with morphological characters, Liu et al. (2019) confirmed the natural taxonomic status of Sporocadaceae, which currently contains 33 genera (Liu et al. 2019, Wijayawardene et al. 2020).

Sporocadaceae contains many important plant pathogens associated with diseases on a wide range of plant hosts worldwide (Maharachchikumbura et al. 2014, Liu et al. 2019, Norphanphoun et al. 2019). Within the family, pestalotiopsis-like taxa (*Neopestalotiopsis*, *Pestalotiopsis* and *Pseudopestalotiopsis*) are the group that has received the most attention (Maharachchikumbura et al. 2014, Wang et al. 2019b, Gualberto et al. 2021). For example, *N. mangiferae* and *N. palmarum* cause leaf

¹ The Key Laboratory for Silviculture and Conservation of the Ministry of Education, Beijing Forestry University, Beijing 100083, China;
corresponding author e-mail: chengmt@bjfu.edu.cn.

² Westerdijk Fungal Biodiversity Institute, Uppsalaalaan 8, 3584 CT Utrecht, The Netherlands.

³ Wageningen University and Research Centre (WUR), Laboratory of Phytopathology, Droevedaalsesteeg 1, 6708 PB Wageningen, The Netherlands.

⁴ Microbiology, Department of Biology, Utrecht University, Padualaan 8, 3584 CH Utrecht, The Netherlands.

⁵ Key Laboratory of Forest Protection of National Forestry and Grassland Administration, Institute of Forest Ecology, Environment and Nature Conservation, Chinese Academy of Forestry, Beijing 100091, China.

⁶ Museum of Beijing Forestry University, Beijing Forestry University, Beijing 100083, China.

diseases on a variety of cash crops in Brazil, South Africa and India, weakening tree vigour, and even reducing yield in severe cases (Spaulding 1949, Mendes et al. 1998, Crous et al. 2000). *Pestalotiopsis pini* is an emerging pathogen causing shoot blight and stem necrosis on *Pinus pinea* (Silva et al. 2020), while in Australia, *Pes. telopeae* causes a serious leaf spot disease of *Telopea* spp. (Maharachchikumbura et al. 2014). Furthermore, pestalotiopsis-like fungi are widespread, occur on many hosts in Proteaceae, and are generally regarded to be saprobic or weakly pathogenic (Crous et al. 2013). *Neopestalotiopsis protearum* was recorded as causing leaf spots and blight on several *Protea* and *Leucospermum* hosts in Zimbabwe (Swart et al. 1999, Crous et al. 2011b). This species is also reported from Australia and Proteaceae in the Western Cape Province of South Africa (Crous et al. 2013). *Neopestalotiopsis protearum* is probably only a problem of commercial importance in summer rainfall areas and it has been intercepted at quarantine inspection points (Taylor 2000). *Pestalotiopsis montellicoides* was isolated from *Protea cynaroides* leaves from South Africa (Mordue 1986), and a *Pestalotiopsis* sp. (asexual *Pestalosphaeria leucospermi*), was described from living leaves of a *Leucospermum* sp. in New Zealand (Samuels et al. 1987). In Portugal and the Canary Islands, a species of *Pestalotiopsis* is commonly associated with tip blight and leaf spot symptoms on *Protea*, *Leucospermum* and *Leucadendron* species, although pathogenicity studies have not yet been conducted (Crous et al. 2013). Members of *Pseudopestalotiopsis* are cosmopolitan in distribution and have often been regarded as leaves spot pathogens occurring on a broad host range, e.g., *Pse. elaeidis* and *Pse. theae* cause foliar diseases in more than 60 hosts around the world in tropical and subtropical areas (Maharachchikumbura et al. 2014, Liu et al. 2019). In addition to pestalotiopsis-like species, the diseases caused by other groups of Sporocadaceae cannot be underestimated. Cypress canker is caused by several species of *Seiridium* (Bonthond et al. 2018), *Allelochaeta* is an important foliar pathogen of eucalypts (Crous et al. 2019b), and some species of *Distononappendiculata* and *Truncatella* cause diseases on a wide range of hosts (Crous et al. 2011a, 2013, Liu et al. 2019).

Sporocadaceae has an extremely rich species diversity in China. The investigation of the biodiversity of plant-associated pestalotioid fungi in China date back as far as 1886, when Patouillard collected and described many species from Yunnan (Patouillard 1886). With subsequent research, a total of 310 species belonging to 22 genera were reported in China, inhabiting many hosts, especially in *Juglandaceae*, *Myrtaceae*, *Pinaceae*, *Podocarpaceae*, *Rhododendronaceae*, *Rosaceae*, *Theaceae* and *Vitaceae* (Chen 2003, Ge et al. 2009, Liu et al. 2019). Most of the previous studies on *Sporocadaceae* in China focused on *Pestalotiopsis*. Previous investigations on *Pestalotiopsis* in China were summarised by Tai (1979), in which 38 species from 52 plant hosts were listed. A wider survey included 153 species obtained from at least 406 plant species, 67 of which are endemic to China (Ge et al. 2009). Hitherto 203 species have been reported in China, accounting for more than 65 % of the total records of this family in China. However, the distribution of 11 genera in China is still unknown, i.e., *Ciliochorella*, *Clypeosphaeria*, *Diploceras*, *Disaeta*, *Distononappendiculata*, *Heterotruncatella*, *Hyalotilla*, *Morinia*, *Nonappendiculata*, *Parabartalinia* and *Xenseimatosporium*. Furthermore, many species of *Sporocadaceae* can also cause serious plant diseases in China. *Pseudopestalotiopsis cameliae-sinensis* is responsible for grey blight of tea plants and causes serious losses in some tea-growing regions of China (Wang et al. 2019b), while *Pes. apiculata* causes severe top blight of cedar seedlings (Ge et al. 2009). *Monochaetia kansensis* and *M. monochaeta* cause leaf spots on a variety of

Quercus and *Castanea* plants (Teng 1996, Chen et al. 2002, Chen 2003), and *Truncatella laurocerasi* causes grey blight and leaf spot on *Eriobotrya* in China (Tai 1979). Considering the importance of pestalotioid fungi, it is necessary to clarify the species diversity and distribution of *Sporocadaceae* in China in a modern taxonomic framework.

Rosa (Rosaceae) is widely distributed in tropical to cold temperate regions of the Northern Hemisphere, including approximately 200 species (Bruneau et al. 2007, Fougère-Danezan et al. 2015). China is the main distribution area of *Rosa* plants globally (Wu et al. 2003). There are currently 95 *Rosa* spp. in China (65 of which are endemic), accounting for about 41 % of the global total (Jin 2020). *Rosa* species are widely cultivated and are of immense economic importance in China (Liu 2016). As important ornamental plants, *Rosa* spp. play a key role in Chinese landscaping (Zhang et al. 2009). Furthermore, *Rosa* species are important raw materials for the spice and food industry, and a rose industry has been established in many parts of China, generating huge income for the local economy (Wang 2021). Most *Rosa* spp. can be used in traditional Chinese medicines, having great nutritional and medicinal value (Wang 2021). In addition to these, *Rosa* spp. are important resource species for ecological and vegetation restoration, having great ecological value in China, because many rose species have strong resistance to stress and can survive in harsh environments (Liu 2016).

Many fungal taxa such as *Botryosphaeria dothidea*, *Botrytis cinerea*, *Chaetomella raphigera*, *Colletotrichum siamense*, *Cytospora* spp., *Diplocarpon rosae*, *Elsinoe rosarum* and *Lasio-diplodia theobromae* have in the past been identified as the causal agents of various diseases of *Rosa* spp. in China, and severely limited their production. (Zhang et al. 2014, Babsic et al. 2016, Chen et al. 2016, Debener 2019, Feng et al. 2019 Jia et al. 2019, Munoz et al. 2019, Pan et al. 2020). Members of *Sporocadaceae* have also been reported to cause diseases on *Rosa* spp. Examples include cankers caused by *N. rosicola*, dieback caused by *Ciliochorella mangiferae* and *Robillarda sessilis*, stem lesions caused by *N. rosae* and *R. sessilis*, and leaf spots caused by *Diploceras discosiodes*, *Discosia artocreas* and *Truncatella angustata* (Weiss 1950, Mathur 1979, Peregrine & Ahmad 1982, Eken et al. 2009, Maharachchikumbura et al. 2014, Jiang et al. 2018). Furthermore, *Rosa* has proven to represent a rich niche of undescribed species of *Sporocadaceae*, with many remaining poorly identified, as the generic concepts have been in flux until recently (Liu et al. 2019). Therefore, conducting detailed surveys of pestalotioid fungi from *Rosa* spp. in China was necessary. The aims of the present study were thus to identify these fungi based on phylogenetic analyses and morphological comparisons, describe the species new to science, and gain a better understanding of the diversity and prevalence of *Sporocadaceae* associated with *Rosa* spp. in China.

MATERIALS AND METHODS

Sampling and isolation

A total of 295 *Rosa* samples (branches, fruits, leaves and spines) showing disease symptoms (Fig. 1) were collected from five provinces (Gansu, Henan, Hunan, Qinghai and Shaanxi) and the Ningxia Autonomous Region of China, which are the main production areas of *Rosa* plants in China. The *Rosa* species sampled include *R. chinensis*, *R. helenae*, *R. laevigata*, *R. multiflora*, *R. omeiensis*, *R. rugosa*, *R. spinosissima* and *R. xanthina*.

A total of 126 strains were obtained by removing the spore mass from conidiomata and generating single spore colonies, or plating superficially sterilised diseased tissue on potato



Fig. 1 Disease symptoms on *Rosa* associated with infection by Sporocadaceae. a–c. Leaves spots on *Rosa rugosa* caused by *Pestalotiopsis rhodomyrti*; d–e. lesion developing on the fruits of *Rosa laevigata* infected by *Seimatosporium nonappendiculatum*; f. dying bush; g–h. dieback on (g) *Rosa rugosa* and (h) *Rosa xanthina* caused by *Seiridium rosae* and *Sporocadus sorbi*; i–j. sporocarps of *Pestalotiopsis chamaeropis* and *Seimatosporium centrale* on the spines of (i) *Rosa rugosa* and (j) *Rosa chinensis*.

Table 1 PCR reaction primers (forward and reverse) for amplification of gene loci of each fungal genus.

Genus	Loci used for amplification					References
	ITS	LSU	RPB2	TEF	TUB	
<i>Monochaetia</i>	ITS1/ITS4	LROR/LR5	RPB2-5F2/fRPB2-7cR			Liu et al. (2019), Jiang et al. (2021)
<i>Neopestalotiopsis</i>	ITS1/ITS4	LROR/LR5	RPB2-5F2/fRPB2-7cR	EF1-728F/EF-2	T1/Bt2b	Liu et al. (2019), Norphanphoun et al. (2019), Jiang et al. (2021)
<i>Pestalotiopsis</i>	ITS1/ITS4	LROR/LR5	RPB2-5F2/fRPB2-7cR	EF1-728F/EF-2	T1/Bt2b	Liu et al. (2019), Norphanphoun et al. (2019), Jiang et al. (2021)
<i>Seimatosporium</i>	ITS1/ITS4	LROR/LR5	RPB2-5F2/fRPB2-7cR			Goonasekara et al. (2016), Wijayawardene et al. (2016a), Liu et al. (2019)
<i>Seiridium</i>	ITS1/ITS4	LROR/LR5	RPB2-5F2/fRPB2-7cR	EF1-728F/EF-2	T1/Bt2b	Jiang et al. (2019), Liu et al. (2019), Marin-Felix et al. (2019)
<i>Sporocadus</i>	ITS1/ITS4	LROR/LR5	RPB2-5F2/fRPB2-7cR	EF1-728F/EF-2	T1/Bt2b	Liu et al. (2019)

Table 2 Isolates sequenced and used for phylogenetic analyses in the current study.

Table 2 (cont.)

Species ¹	Culture no.	Status ²	Host	Tissues	Origin	ITS	LSU	RPB2	TEF	TUB	GenBank accession no.
<i>Pes. rhodomyrtus</i> (cont.)											
	ROC 356		<i>Rosa chinensis</i>	branches	Changsha, Hunan	OK560606	OL814520	OM158170			
	ROC 357		<i>Rosa chinensis</i>	branches	Changsha, Hunan	OK560607	OL814521	OM158171			
	ROC 358		<i>Rosa chinensis</i>	branches	Changsha, Hunan	OK560608	OL814522	OM158172			
	ROC 359		<i>Rosa chinensis</i>	branches	Changsha, Hunan	OK560609	OL814523	OM158173			
<i>Pes. tumida</i>	CFCC 55158 = ROC 110	T	<i>Rosa chinensis</i>	spines	Tianshui, Gansu	OK560610	OL742142	OM158174			
	ROC 109		<i>Rosa chinensis</i>	spines	Tianshui, Gansu	OK560611	OL742143	OM158175			
	ROC 108		<i>Rosa chinensis</i>	spines	Tianshui, Gansu	OK560612	OL742144	OM158176			
	CFCC 55159 = ROC 234		<i>Rosa chinensis</i>	branches	Tianshui, Gansu	OK560613	OL742145	OM158177			
	ROC 235		<i>Rosa chinensis</i>	branches	Tianshui, Gansu	OK560614	OL742146	OM158178			
	ROC 236		<i>Rosa chinensis</i>	branches	Tianshui, Gansu	OK560615	OL742147	OM158179			
	ROC 237		<i>Rosa chinensis</i>	spines	Tianshui, Gansu	OK560616	OL742148	OM158180			
	ROC 238		<i>Rosa chinensis</i>	spines	Tianshui, Gansu	OK560617	OL742149	OM158181			
	ROC 240		<i>Rosa chinensis</i>	branches	Tianshui, Gansu	OK560618	OL814532	OM158182			
	CFCC 55166 = ROC 003	T	<i>Rosa chinensis</i>	spines	Tianshui, Gansu	OK560629	OM986918	OM301641			
	ROC 001		<i>Rosa chinensis</i>	spines	Tianshui, Gansu	OK560630	OM986919	OM301642			
	ROC 002		<i>Rosa chinensis</i>	spines	Tianshui, Gansu	OK560631	ON055449	OM301643			
	CFCC 55169 = ROC 014		<i>Rosa chinensis</i>	spines	Baoji, Shaanxi	OK560632	ON055449	OM301644			
	ROC 015		<i>Rosa chinensis</i>	spines	Baoji, Shaanxi	OK560633	ON055450	OM301645			
	ROC 016		<i>Rosa chinensis</i>	spines	Baoji, Shaanxi	OK560634	ON055452	OM301646			
	ROC 145		<i>Rosa chinensis</i>	spines	Tianshui, Gansu	OK560635	ON055453	OM301647			
	ROC 146		<i>Rosa chinensis</i>	spines	Tianshui, Gansu	OK560636	ON055454	OM301648			
	ROC 147		<i>Rosa chinensis</i>	spines	Tianshui, Gansu	OK560637	ON055455	OM301649			
	CFCC 55167 = ROC 004	T	<i>Rosa xanthina</i>	spines	Tianshui, Gansu	OK560638	ON055456	OM301650			
	ROC 005		<i>Rosa xanthina</i>	spines	Tianshui, Gansu	OK560639	ON055457	OM301651			
	ROC 006		<i>Rosa xanthina</i>	spines	Tianshui, Gansu	OK560640	ON055458	OM301652			
	ROC 007		<i>Rosa xanthina</i>	spines	Tianshui, Gansu	OK560641	ON055459	OM301653			
	ROC 008		<i>Rosa xanthina</i>	spines	Tianshui, Gansu	OK560642	ON055460	OM301654			
	ROC 009		<i>Rosa xanthina</i>	spines	Tianshui, Gansu	OK560643	ON055461	OM301655			
	ROC 010		<i>Rosa xanthina</i>	spines	Tianshui, Gansu	OK560644	ON055462	OM301656			
	ROC 011		<i>Rosa xanthina</i>	spines	Tianshui, Gansu	OK560645	ON055463	OM301657			
	ROC 012		<i>Rosa xanthina</i>	spines	Tianshui, Gansu	OK560646	ON055464	OM301658			
	CFCC 55168 = ROC 377	T	<i>Rosa laevigata</i>	fruits	Guyuan, Ningxia	OK560657	ON055465	OM301659			
	ROC 378		<i>Rosa laevigata</i>	fruits	Guyuan, Ningxia	OK560658	ON055466	OM301670			
	ROC 379		<i>Rosa laevigata</i>	fruits	Guyuan, Ningxia	OK560659	ON055467	OM301671			
	ROC 380		<i>Rosa laevigata</i>	fruits	Guyuan, Ningxia	OK560660	ON055468	OM301672			
	ROC 381		<i>Rosa laevigata</i>	fruits	Guyuan, Ningxia	OK560661	ON055469	OM301673			
	CFCC 55164 = ROC 038	T	<i>Rosa spinosissima</i>	spines	Huangnan, Qinghai	OK560647	ON055475	OM301674			
	ROC 039		<i>Rosa spinosissima</i>	spines	Huangnan, Qinghai	OK560648	ON055476	OM301675			
	ROC 040		<i>Rosa spinosissima</i>	spines	Huangnan, Qinghai	OK560649	ON055477	OM301676			
	ROC 041		<i>Rosa spinosissima</i>	spines	Huangnan, Qinghai	OK560650	ON055478	OM301677			
	ROC 042		<i>Rosa spinosissima</i>	spines	Huangnan, Qinghai	OK560651	ON055479	OM301678			
	ROC 043		<i>Rosa spinosissima</i>	spines	Huangnan, Qinghai	OK560652	ON055480	OM301679			
	CFCC 55165 = ROC 017	T	<i>Rosa heleneae</i>	spines	Guyuan, Ningxia	OK560653	ON055481	OM301680			
	ROC 044		<i>Rosa heleneae</i>	spines	Guyuan, Ningxia	OK560654	ON055482	OM301681			
	ROC 045		<i>Rosa heleneae</i>	spines	Guyuan, Ningxia	OK560655	ON055483	OM301682			
	ROC 046		<i>Rosa heleneae</i>	spines	Guyuan, Ningxia	OK560656	ON055484	OM301683			
	ROC 047		<i>Rosa heleneae</i>	spines	Guyuan, Ningxia	OK560657	ON055485	OM301684			
	ROC 048		<i>Rosa heleneae</i>	spines	Guyuan, Ningxia	OK560658	ON055486	OM301685			
	ROC 049		<i>Rosa heleneae</i>	spines	Guyuan, Ningxia	OK560659	ON055487	OM301686			
	ROC 050		<i>Rosa rugosa</i>	branches	Guyuan, Ningxia	OK560681	ON055488	OM301687			
	ROC 209		<i>Rosa rugosa</i>	branches	Guyuan, Ningxia	OK560682	ON055489	OM301688			
	CFCC 55175 = ROC 267		<i>Rosa rugosa</i>	branches	Guyuan, Ningxia	OK560683	ON055490	OM301689			
	ROC 268		<i>Rosa rugosa</i>	branches	Guyuan, Ningxia	OK560684	ON055491	OM301690			
	ROC 051		<i>Rosa spinosissima</i>	spines	Gannan, Gansu	OK560685	ON055492	OM301691			
	ROC 052		<i>Rosa spinosissima</i>	spines	Gannan, Gansu	OK560686	ON055493	OM301692			
	ROC 053		<i>Rosa spinosissima</i>	spines	Gannan, Gansu	OK560687	ON055494	OM301693			
<i>Seiridium rosae</i>											
	CFCC 55174 = ROC 208	T	<i>Rosa rugosa</i>	branches	Guyuan, Ningxia	OK560688	OL814533	OM313314			
	ROC 209		<i>Rosa rugosa</i>	branches	Guyuan, Ningxia	OK560689	OL742152	OM313315			
	CFCC 55175 = ROC 267		<i>Rosa rugosa</i>	branches	Guyuan, Ningxia	OK560690	OL742153	OM313316			
	ROC 268		<i>Rosa rugosa</i>	branches	Guyuan, Ningxia	OK560691	OL742154	OM313317			
	ROC 054		<i>Rosa spinosissima</i>	spines	Gannan, Gansu	OK560692	OL814535	OM401669			
	ROC 055		<i>Rosa spinosissima</i>	spines	Gannan, Gansu	OK560693	OL814536	OM401670			
	ROC 056		<i>Rosa spinosissima</i>	spines	Gannan, Gansu	OK560694	OL814537	OM401671			
<i>Sporocadus brevis</i>											
	CFCC 55170 = ROC 091	T	<i>Rosa spinosissima</i>	spines	Gannan, Gansu	OK560695	OL814538	OM401669			
	ROC 092		<i>Rosa spinosissima</i>	spines	Gannan, Gansu	OK560696	OL814539	OM401670			
	ROC 093		<i>Rosa spinosissima</i>	spines	Gannan, Gansu	OK560697	OL742157	OM401671			

Table 2 (cont.)

Species ¹	Culture no.	Status ²	Host	Tissues	Origin	ITS	LSU	RPB2	TEF	TUB	GenBank accession no.
<i>Sporocadus brevis</i> (cont.)											
<i>Spo. sorbi</i>	ROC 094	RO	<i>Rosa spinosissima</i>	spines	Gannan, Gansu	OK655783	OL742158	OL814540	OM401662		
	ROC 095	OC	<i>Rosa spinosissima</i>	spines	Gannan, Gansu	OK655784	OL742159	OL814541	OM401663		
	ROC 105	OC	<i>Rosa xanthina</i>	branches	Lanzhou, Gansu	OK655785	OL742160	OL814542	OM401664		
	ROC 102	OC	<i>Rosa xanthina</i>	branches	Lanzhou, Gansu	OK655786	OL742161	OL814543	OM401665		
	ROC 103	OC	<i>Rosa xanthina</i>	branches	Lanzhou, Gansu	OK655787	OL742162	OL814544	OM401666		
	ROC 159	OC	<i>Rosa xanthina</i>	spines	Gannan, Gansu	OK655788	OL742163	OL814545	OM401667		
	ROC 159	OC	<i>Rosa xanthina</i>	spines	Gannan, Gansu	OK655789	OL742164	OL814546	OM401668		
	ROC 160	OC	<i>Rosa xanthina</i>	spines	Gannan, Gansu	OK655790	OL742165	OL814547	OM401669		
	ROC 161	OC	<i>Rosa omeiensis</i>	spines	Lanzhou, Gansu	OK655791	OL742166	OL814548	OM401670		
	ROC 119	OC	<i>Rosa omeiensis</i>	spines	Lanzhou, Gansu	OK655792	OL742167	OL814549	OM401671		
	ROC 120	OC	<i>Rosa omeiensis</i>	spines	Lanzhou, Gansu	OK655793	OL742168	OL814550	OM401672		
	ROC 121	OC	<i>Rosa omeiensis</i>	spines	Lanzhou, Gansu	OK655794	OL742169	OL814551	OM401673		
	ROC 122	OC	<i>Rosa omeiensis</i>	spines	Lanzhou, Gansu	OK655795	OL742170	OL814552	OM401674		
	ROC 123	OC	<i>Rosa omeiensis</i>	spines	Lanzhou, Gansu	OK655796	OL742171	OL814553	OM401675		
	ROC 124	OC	<i>Rosa omeiensis</i>	spines	Lanzhou, Gansu	OK655797	OL742172	OL814554	OM401676		
	ROC 125	OC	<i>Rosa omeiensis</i>	spines	Lanzhou, Gansu	OK655798	OL742173	OL814555	OM401677		
			<i>Rosa xanthina</i>	branches	Lanzhou, Gansu	OK6560389	OL742174	OL814556	OM401678		
			<i>Rosa xanthina</i>	branches	Lanzhou, Gansu	OK655800	OL742175	OL814557	OM401679		
			<i>Rosa xanthina</i>	branches	Lanzhou, Gansu	OK655801	OL742176	OL814558	OM401680		
			<i>Rosa xanthina</i>	branches	Lanzhou, Gansu	OK655802	OL742177	OL814559	OM401681		
<i>Spo. trimorphus</i>											
	CFCC 55171 = ROC 112										
	ROC 113										
	ROC 114										
	ROC 115										
	ROC 116										

¹ Newly described taxa and deposited sequences are in bold.² T: ex-type.

dextrose agar (PDA, 20 % diced potatoes, 2 % agar and 2 % glucose) and incubating Petri dishes at 25 °C in the dark for 2–3 d. When colonies just formed, they were hyphal-tipped and transferred to fresh PDA Petri dishes (Crous et al. 2019a). Type specimens of new species from this study were deposited in the Museum of the Beijing Forestry University (BJFC), and ex-type living cultures were deposited in the China Forestry Culture Collection Centre (CFCC), Beijing, China.

Morphological analyses

Cultures were incubated on PDA at 25 °C in a 12 h day/night regime (Crous et al. 2019a). After 15 d, colony diameters were measured and colony colours were rated according to Rayner (1970). Slide preparations were mounted in lactic acid or water, from colonies sporulating on PDA, autoclaved pine needles on 2 % tap water agar (Smith et al. 1996), and incubated at 25 °C under continuous nuv-light to promote sporulation. Sections through stromata were made by hand. Observations were made with a Leica DM 2500 dissecting microscope (Wetzlar, Germany), and with a Nikon Eclipse 80i compound microscope using differential interference contrast (DIC) illumination and images recorded on a Nis DS-Ri2 camera with the Nikon Nis-Elements F4.30.01 software. Conidial length was measured from the base of the basal cell to the base of the apical appendage, and conidial width was measured at the widest point of the conidium (Bonhond et al. 2018). Taxonomic novelties were deposited in MycoBank (Crous et al. 2004).

DNA extraction, PCR amplification and sequencing

Total genomic DNA was extracted from axenic cultures using a modified cetyltrimethylammonium bromide (CTAB) protocol (Doyle & Doyle 1990). DNA products were stored at -20 °C. The extracted DNA was used as template for the polymerase chain reaction (PCR). PCR reaction primers (forward and reverse) of each fungal genus are found in Table 1. PCR parameters were initiated with 95 °C for 5 min, followed by 34 cycles of denaturation at 95 °C for 30 s, annealing at a suitable temperature for 30 s (56 °C for ITS and LSU, 52 °C for TEF, 52 °C for RPB2 and 60 °C for TUB), and extension at 72 °C for 30 s, and terminated with a final elongation step at 72 °C for 10 min. The final PCR products were examined by electrophoresis in 2 % agarose gels. The amplified PCR products were sent to a commercial sequencing provider (Tsingke Biotechnology Co. Ltd, Beijing, China).

Phylogenetic analyses

All nucleotide sequences generated from different primer pairs in this study were deposited in GenBank (Table 2). Sequences were BLASTn searched in NCBI to obtain the related sequences from recent publications and were analysed (Table 3). Sequences were aligned in MAFFT v. 7 at the web server (<http://mafft.cbrc.jp/alignment/server>) (Katoh & Standley 2013, Katoh et al. 2019) and manually adjusted in MEGA v. 6 (Tamura et al. 2013).

Seven phylogenetic analyses were conducted based on both individual and combined loci for one family (Sporocadaceae) and six genera (*Monochaetia*, *Neopestalotiopsis*, *Pestalotiopsis*, *Seimatosporium*, *Seiridium* and *Sporocadus*). Maximum Parsimony (MP) was used to construct phylogenies using PAUP v. 4.0b10 (Swofford 2003), Maximum Likelihood (ML) was executed in RAxML (Dean et al. 2014) implemented in raxmlGUI v. 1.5b1 (Silvestro & Michalak 2012) and MrBayes v. 3.1.2 was used for Bayesian analyses (BA) (Huelsenbeck & Ronquist 2001).

Trees were visualised with FigTree v. 1.4.0 (<http://tree.bio.ed.ac.uk/software/figtree/>), and additional layout was done with Adobe Illustrator CS v. 5. Maximum-likelihood bootstrap values (MLBP)

Table 3 Isolates from previous studies used in the phylogenetic analyses in the current study.

Species	Strain number ¹	Status ²	Country	Substrate	GenBank accession no.				References
					ITS	LSU	RPB2	TEF	
<i>Alliochaea acuta</i>	CPC 16629	ET	Australia	<i>Eucalyptus dives</i>	MH554086	MH554297	MH555000	–	Crous et al. (2018)
<i>All. elegans</i>	CBS 187.81	ET	Australia	<i>Melaleuca lanceolata</i>	MH554014	MH554234	MH554927	–	Crous et al. (2018)
<i>All. falcata</i>	CPC 13580	ET	Australia	<i>Eucalyptus alligatrix</i>	MH554073	MH554284	MH554985	–	Crous et al. (2018)
<i>All. fusispora</i>	CBS 13117	ET	Australia	<i>Eucalyptus alligatrix</i> sp.	MH553999	MH554217	MH554907	–	Crous et al. (2018)
<i>All. fusispora</i>	CPC 17616	IT	Australia	<i>Eucalyptus polyanthemos</i>	MH554094	MH554304	MH555008	–	Crous et al. (2018)
<i>All. kriegeriana</i>	CBS 810.73	IT	Australia	<i>Callistemon sieberi</i>	MH554067	MH554279	MH554920	–	Crous et al. (2018)
<i>All. neocauta</i>	CBS 188.81	T	South Africa	<i>Eucalyptus smithii</i>	MH554235	MH554235	MH554928	–	Crous et al. (2018)
<i>All. neodilophospora</i>	CBS 115131	T	South Africa	<i>Eucalyptus smithii</i>	JN871209	MH554998	–	Crous et al. (2018)	
<i>All. neocauta</i>	CBS 110733	T	South Africa	<i>Callistemon pinifolius</i>	JN871201	MH554999	–	Crous et al. (2018)	
<i>All. neocauta</i>	CPC 17161	T	Australia	<i>Eucalyptus regnans</i>	MH554090	MH554300	MH555004	–	Crous et al. (2018)
<i>All. neocaularis</i>	CPC 13581	T	Australia	<i>Eucalyptus obliqua</i>	MH554074	MH554285	MH554986	–	Crous et al. (2018)
<i>All. obliquae</i>	CPC 20191	T	Australia	<i>Corymbia henryi</i>	MH554105	MH554315	MH555018	–	Crous et al. (2018)
<i>All. orbicularis</i>	CBS 131118	ET	Australia	<i>Melaleuca ericifolia</i>	MH554000	MH554218	MH554908	–	Crous et al. (2018)
<i>All. paralegans</i>	CBS 150.71	T	Australia	<i>Eucalyptus sp.</i>	MH554077	MH554228	MH554923	–	Crous et al. (2018)
<i>All. pseudowalkeri</i>	CPC 17043	T	Australia	<i>Eucalyptus sparsifolia</i>	MH554089	MH554299	MH555003	–	Crous et al. (2018)
<i>All. sparsifoliae</i>	CPC 14529	T	Australia	<i>Eucalyptus sparsifolia</i>	MH554083	MH554294	MH554995	–	Crous et al. (2018)
<i>Bartalinia bella</i>	CPC 14502	T	Australia	<i>Eucalyptus sparsifolia</i>	MH554082	MH554293	MH555018	–	Crous et al. (2018)
<i>Bartalinia bella</i>	CBS 125525	T	South Africa	<i>Maytenus abbotii</i>	GU291796	MH554214	MH554904	–	Liu et al. (2019)
<i>Bar. pini</i>	CBS 464.61	T	Brazil	Air	MH554051	MH554264	MH554964	–	Liu et al. (2019)
<i>Bar. robillardoides</i>	CBS 143891	T	Uganda	<i>Pinus patula</i>	MH554125	MH554330	MH555033	–	Liu et al. (2019)
<i>Bar. robillardoides</i>	CBS 144141	T	USA	<i>Acacia koa</i>	MH554170	MH554364	MH555067	–	Liu et al. (2019)
<i>Beltrania pseudothomombica</i>	CBS 122705	ET	Italy	<i>Lepioglossus occidentalis</i>	LT853104	KJ104386	LT853152	–	Liu et al. (2019)
<i>Beltrania pseudothomombica</i>	CBS 122615	ET	South Africa	<i>Cupressus lusitanica</i>	MH553989	MH554207	MH554897	–	Liu et al. (2019)
<i>Beltrania pseudothomombica</i>	CPC 23656	T	China	<i>Pinus tabulaeformis</i>	MH554124	KJ869215	MH555032	–	Crous et al. (2014a), Liu et al. (2019)
<i>Bel. rhombica</i>	CBS 123.58	T	Mozambique	Sand near mangrove swamp	MH553990	MH554209	MH554899	–	Liu et al. (2019)
<i>Broomella vitaliae</i>	HPC 1154	ET	–	–	MH554173	MH554367	–	–	Liu et al. (2019)
<i>Ciliochorella phanercola</i>	MFLUCC 13-0798	ET	Italy	<i>Clematis vitalba</i>	NR_153610	KP757749	–	–	Liu et al. (2019)
<i>Ciliochorella phanercola</i>	MFLUCC 12-0310	ET	Thailand	Dead leaves	KF827444	KF827445	KF827479	–	Hyde et al. (2016)
<i>Ciliochorella phanercola</i>	MFLUCC 14-0844	T	Thailand	<i>Phanera purpurea</i>	KX789680	KX789681	–	–	Hyde et al. (2016)
<i>Clypeosphaeria uniseptata</i>	CBS 114967	T	Hong Kong, China	Wood	MH553979	MH554197	MH554878	–	Liu et al. (2019)
<i>Diploceras hypericumum</i>	CBS 109058	T	New Zealand	<i>Hypericum sp.</i>	MH553956	MH554178	MH554852	–	Liu et al. (2019)
<i>Diploceras hypericumum</i>	CBS 492.97	T	Netherlands	<i>Hypericum perforatum</i>	MH554054	MH554267	MH554967	–	Liu et al. (2019)
<i>Diploceras hypericumum</i>	CBS 197.36	ET	Switzerland	<i>Hypericum sp.</i>	MH554017	MH554237	MH554930	–	Liu et al. (2019)
<i>Diploceras hypericumum</i>	CBS 138885	ET	Netherlands	<i>Hypericum perforatum</i>	MH554108	MH554316	MH555019	–	Liu et al. (2019)
<i>Diploceras hypericumum</i>	CBS 143903	ET	Australia	<i>Acacia pycnantha</i>	MH554148	MH554346	MH555050	–	Liu et al. (2019)
<i>Diploceras hypericumum</i>	CBS 124848	ET	Germany	<i>Fagus syvatica</i>	MH553994	MH554213	MH555003	–	Liu et al. (2019)
<i>Disaeta arbuti</i>	NTCLQ95	T	Thailand	Dead leaf	KF827433	KF827437	KF827474	–	Liu et al. (2019)
<i>Disaeta arbuti</i>	NTCLQ97-2	T	Thailand	Dead leaf	KF827434	KF827438	KF827475	–	Liu et al. (2019)
<i>Discozia sp. 6</i>	CBS 241.66	T	South Africa	Acacia karroo	KF827432	KF827436	KF827473	–	Liu et al. (2019)
<i>Discozia sp. 7</i>	CBS 684.70	T	Netherlands	<i>Aesculus hippocastanum</i>	MH554022	MH554244	MH554933	–	Liu et al. (2019)
<i>Dist. casuarinae</i>	CPC 17658	T	Australia	<i>Banksia marginata</i>	MH554064	MH554277	MH554978	–	Liu et al. (2019)
<i>Dist. verocreas</i>	CBS 143906	T	Australia	<i>Banksia marginata</i>	MH554097	MH554307	MH555011	–	Liu et al. (2019)
<i>Distoniamappendiculata banksiae</i>	CBS 143884	T	Australia	<i>Casuarina sp.</i>	JQ044422	JQ044422	MH554909	–	Liu et al. (2019)
<i>Dis. brasiliensis</i>	CBS 144032	T	USA	<i>Banksia marginata</i>	MH554104	MH554314	MH555017	–	Liu et al. (2019)
<i>Dis. brasiliensis</i>	CBS 302.86	T	Australia	<i>Casuarina sp.</i>	MH554093	MH554303	MH555007	–	Liu et al. (2019)
<i>Heterotruncatella lutea</i>	CBS 349.73	T	USA	<i>Banksia marginata</i>	MH554163	MH554359	MH555062	–	Liu et al. (2019)
<i>Heterotruncatella lutea</i>	CBS 123029	T	South Africa	<i>Soil</i>	MH554028	MH554247	MH554941	–	Liu et al. (2019)
<i>He. proteicola</i>				<i>Acacia pycnantha</i>	LT853099	DO414833	LT853146	–	Liu et al. (2019)
<i>He. proteicola</i>				<i>Protea acaulis</i>	MH553993	MH554212	MH554902	–	Liu et al. (2019)

Table 3 (cont.)

Species	Strain number ¹	Status ²	Country	Substrate	GenBank accession no.				References
					ITS	LSU	RPB2	TEF	
<i>Het. restionacearum</i>	CBS 119210		South Africa	<i>Ischyrolepis cf. gaudichaudiana</i>	DQ278915	DQ278929	MH554892	–	Liu et al. (2019)
	CBS 118150		South Africa	<i>Restio filiformis</i>	DQ278914	MH554233	MH554889	–	Liu et al. (2019)
<i>Het. spadicea</i>	CBS 118148		South Africa	<i>Rhodocoma capensis</i>	DQ278913	DQ278928	MH554888	–	Liu et al. (2019)
	CBS 118144		South Africa	<i>Ischyrolepis</i> sp.	DQ278921	DQ278926	MH554886	–	Liu et al. (2019)
<i>Hyalotella spartii</i>	MFLUCC 13-0397	T	Italy	<i>Spartium junceum</i>	KP757756	KP757752	–	–	Li et al. (2015)
<i>Hyalotella transvalensis</i>	CBS 303.65	T	South Africa	Soil	MH554029	MH554248	MH554942	–	Liu et al. (2019)
<i>Hymenopeltella austroafricana</i>	CBS 143886	T	South Africa	<i>Glechis tricantths</i>	MH554115	MH554230	MH555023	–	Liu et al. (2019)
	CBS 144027	T	Zambia	<i>Combretum hereroense</i>	MH554119	MH554324	MH555027	–	Liu et al. (2019)
<i>Hym. endophytica</i>	CBS 144026	T	South Africa	<i>Bridelia mollis</i>	MH554117	MH554322	MH555025	–	Liu et al. (2019)
<i>Hym. hippophaeae</i>	EMLAS5-1	T	Korea	<i>Abies firma</i>	KX216520	KX216518	–	–	Liu et al. (2019)
<i>Hym. hippophaeae</i>	CBS 113687	T	Sweden	<i>Hippophae rhamnoides</i>	MH553969	MH554188	MH554863	–	Jaklitsch et al. (2016)
<i>Hym. lakefuxianensis</i>	CBS 140410	ET	Austria	<i>Hippophae rhamnoides</i>	KT949901	MH554224	MH554919	–	Jaklitsch et al. (2016)
<i>Hym. polysyphata</i>	HKUCC 7303	T	China	Submerged wood	–	AF452047	–	–	Liu et al. (2019)
<i>Hym. subcylindrica</i>	CBS 143887	T	South Africa	<i>Combretum</i> sp.	MH554116	MH554321	MH555024	–	Liu et al. (2019)
<i>CBS 164.77</i>	CBS 164.77	T	India	<i>Cocos nucifera</i>	MH554009	MH554230	MH554925	–	Liu et al. (2019)
<i>CBS 647.74</i>	CBS 647.74	T	India	<i>Glycosphila</i> seeds	MH554062	MH554275	MH554976	–	Liu et al. (2019)
<i>MAFF 2422781</i>	MAFF 2422781		Japan	Unknown dead leaves	AB594793	AB593725	–	–	Tanaka et al. (2011)
<i>NBRC 104197</i>	NBRC 104197		Japan	<i>Ardisia japonica</i>	AB594792	AB593724	–	–	Tanaka et al. (2011)
<i>CBS 140409</i>	CBS 140409	NT	Belgium	<i>Tilia cordata</i>	NR_154123	KT949902	MH554918	–	Liu et al. (2019)
<i>CBS 131707</i>	CBS 131707	T	UK	<i>Sambucus nigra</i>	NR_154124	MH554219	MH554911	–	Liu et al. (2019)
<i>CBS 125585</i>	CBS 125585	T	Austria	<i>Lycopodium annotinum</i>	KP859016	KP858952	KP859125	–	Hernández-Restrepo et al. (2016), Liu et al. (2019)
<i>Microdochium lycopodiinum</i>				<i>Puccinia teleutosorus</i>	KP859013	KP858949	KP859122	–	Hernández-Restrepo et al. (2016), Liu et al. (2019)
<i>Mic. phragmitis</i>	CBS 285.71	ET	Poland	<i>Maize</i> kernels	KP859375	KP858974	KP859147	–	Liu et al. (2019)
<i>Mic. semincola</i>	CBS 139951	T	Switzerland					–	Liu et al. (2019)
<i>Immersidiscosia eucaalypti</i>								–	Liu et al. (2019)
<i>Leptothypha fuckelii</i>								–	Liu et al. (2019)
<i>Lep. sambuci</i>								–	Liu et al. (2019)
<i>Monochaetia camelliae</i>	PSH20001-151		China	<i>Camellia hongkongensis</i>	AY682948	–	–	–	Liu et al. (2019)
<i>M. castaneae</i>	PSH20001-146		China	<i>Camellia pitardii</i>	AY682947	–	–	–	Liu et al. (2019)
	CFCC 54354 = SM9-1	T	China	<i>Castanea mollissima</i>	MW166222	–	–	–	Jiang et al. (2021)
	SM9-2		China	<i>Castanea mollissima</i>	MW166223	–	–	–	Jiang et al. (2021)
<i>M. dimorphospora</i>	NBRC 9960		Japan	<i>Castanea pubinervis</i>	LC146750	–	–	–	De Silva et al. (2018)
	NIBNBRFG396		Korea	Fresh water	MT271967	–	–	–	De Silva et al. (2018)
	CBS 101009		Japan	Air	MH553953	MH554176	MH554849	–	Liu et al. (2019)
<i>M. junipericola</i>	KUMCC 15-0520	T	China	<i>Ilex</i> sp.	KX984153	–	–	–	Liu et al. (2019)
	CBS:143391		Germany	<i>Juniperus communis</i>	MH107900	–	–	–	Liu et al. (2019)
	ZJLQ468		China	<i>Pseudotaxus chienii</i>	KC345692	–	–	–	De Silva et al. (2018)
	PSHI2004Endo1030		China	<i>Cyclobaliopsis</i> sp.	DQ534044	–	–	–	De Silva et al. (2018)
	PSHI2004Endo1031		China	<i>Quercus aliena</i>	DQ534045	–	–	–	De Silva et al. (2018)
	CBS 315.54		England	<i>Quercus</i> sp.	MH554030	MH554249	MH554943	–	Liu et al. (2019)
	CBS 658.95		Netherlands	<i>Quercus robur</i>	MH554063	MH554276	MH554977	–	Liu et al. (2019)
	CBS 115004		Netherlands	<i>Culture contaminant</i>	AY853243	MH554198	MH554879	–	Liu et al. (2019)
	CBS 546.80		Netherlands	<i>Quercus pubescens</i>	MH554056	MH554270	MH554969	–	Liu et al. (2019)
	CBS 199.82		Italy	Unknown plant	MH554018	MH554238	MH554931	–	Liu et al. (2019)
	M18		Italy	<i>Quercus eduardii</i>	JX262802	–	–	–	Liu et al. (2019)
	CBS 144034 = CPC 29514	T	Mexico	<i>Quercus eduardii</i>	MH554365	MH555068	–	–	De Silva et al. (2018)
	CBS 144034 = CPC 29515	T	Mexico	<i>Schima superba</i>	NR_161110	–	OK104874	OK104867	De Silva et al. (2018)
	SAUCC212201	T	China	<i>Schima superba</i>	MZ577565	–	OK104875	OK104868	Zhang et al. (2022)
	SAUCC212202		China	<i>Schima superba</i>	MZ577567	–	OK104876	OK104869	Zhang et al. (2022)
	SAUCC212203		China	<i>Quercus</i> sp.	NR_161064	–	–	–	De Silva et al. (2019)
	HKAS 10065		China	<i>Quercus</i> sp.	MH_15996	–	–	–	De Silva et al. (2020)

Table 3 (cont.)

Species	Strain number ¹	Status ²	Country	Substrate	GenBank accession no.				References
					ITS	LSU	RPB2	TEF	
<i>Morina acaciae</i>	CBS 100230 CBS 137994	T	New Zealand France	<i>Prunus salicina</i> cv. 'Omega' <i>Acacia melanoxylon</i>	MH553950 MH554002	MH554174 MH554221	MH554847 MH554914	—	Liu et al. (2019)
<i>Mor. crini</i>	CBS 143888	T	South Africa	<i>Crinum bulbispermum</i>	MH554118	MH554323	MH555026	—	Liu et al. (2019)
<i>Mor. longipendiculata</i>	CBS 117603	T	Spain	<i>Calluna vulgaris</i>	AY929324	MH554202	MH554885	—	Collado et al. (2006), Liu et al. (2019)
<i>Mor. pestalozzoides</i>	F090354	ET	Spain	<i>Sedum seiforme</i>	AY929325	—	—	—	Liu et al. (2019)
<i>Neopestalozziopsis acrostichi</i>	MFLUCC 17-1754	T	Thailand	<i>Acrostichum aureum</i>	MK764272	—	—	MK764316	Norphanphon et al. (2019)
<i>N. alpapicalis</i>	MFLUCC 17-1755	T	Thailand	<i>Acrostichum aureum</i>	MK764273	—	—	MK764317	Norphanphon et al. (2019)
<i>N. longipendiculata</i>	MFLUCC 17-2844	T	Thailand	<i>Rhizophora mucronata</i>	MK357772	—	—	MK463547	Kumar et al. (2019)
<i>N. aotearoa</i>	MFLUCC 17-2845	T	Thailand	<i>Rhizophora apiculata</i>	MK357773	—	—	MK463548	Kumar et al. (2019)
<i>N. aotearoa</i>	CBS 367-54	T	New Zealand	<i>Canvas</i>	KM199369	—	—	KM199454	Maharachchikumbura et al. (2014)
<i>N. asiatica</i>	MFLUCC 12-0286	T	China	Leaves	JX398883	—	—	JX398049	Maharachchikumbura et al. (2014)
<i>N. australis</i>	CBS 114-159	T	Australia	<i>Telopea</i> sp.	KM199348	—	—	KM199537	Maharachchikumbura et al. (2014)
<i>N. brachiatia</i>	MFLUCC 17-1555	T	Thailand	<i>Rhizophora apiculata</i>	MK764274	—	—	MK764318	Maharachchikumbura et al. (2014)
<i>N. brasiliensis</i>	COAD 2166	T	Brazil	<i>Psidium guajava</i>	MG686469	—	—	MG692402	Norphanphon et al. (2019)
<i>N. camelliæ-oleiferæ</i>	CSUFTCC81	T	China	<i>Camellia oleifera</i>	OK493555	—	—	OK562360	Bezerra et al. (2018), Li et al. (2021)
<i>N. cavernicola</i>	KUMCC 20-0289	T	China	Cave rock surface	MW545802	—	—	MW550735	Liu et al. (2021)
<i>N. chiangmaiensis</i>	MFLUCC 18-0113	T	Thailand	Dead leaves	—	—	—	MH412725	Tibpromma et al. (2018)
<i>N. chrysea</i>	MFLUCC 12-0261	T	China	<i>Pandanus</i> sp.	JX398895	—	—	JX399020	Maharachchikumbura et al. (2014)
<i>N. clavigpora</i>	MFLUCC 12-0281	T	China	<i>Magnolia</i> sp.	JX398797	—	—	JX399014	Maharachchikumbura et al. (2014)
<i>N. coccos</i>	MFLUCC 15-0152	T	Thailand	<i>Cocos nucifera</i>	KX78987	—	—	KX789869	Hyde et al. (2016)
<i>N. coffeee-arabicae</i>	HGUP 4019	T	China	<i>Coffea arabica</i>	KF412649	—	—	KF412646	Song et al. (2013)
<i>N. cubana</i>	CBS 600-96	T	Cuba	Leaf litter	KM199347	MH554973	—	KM199538	Maharachchikumbura et al. (2014)
<i>N. dendrobi</i>	MFLUCC 14-0106	T	Thailand	<i>Dendrobium cariniferum</i>	MK993571	—	—	MK975835	Ma et al. (2019)
<i>N. drenthii</i>	BRIP 72264a	T	Australia	<i>Macadamia integrifolia</i>	MZ303787	—	—	MZ312680	Prasannath et al. (2021)
<i>N. egyptica</i>	CBS 140-162	T	Egypt	<i>Mengifera indica</i>	KP943747	—	—	KP943748	Crous et al. (2015b)
<i>N. ellipsospora</i>	CBS 115-113	T	China	Dead plant material	KM199343	—	—	KM199544	Maharachchikumbura et al. (2014)
<i>N. eucommiae</i>	MFLUCC 12-0283	T	China	<i>Dead plant material</i>	JX398980	—	—	JX399047	Maharachchikumbura et al. (2014)
<i>N. eucommiae</i>	CBS 294-37	T	Portugal	<i>Eucalyptus globulus</i>	KM199376	MH554935	—	KM199531	Maharachchikumbura et al. (2014)
<i>N. eucommiae</i>	CBS 147-684	T	China	<i>Eucalyptus globulus</i>	MW794103	—	—	MW802841	Diogo et al. (2021)
<i>N. foedans</i>	CGMCC 3.9123	T	China	Mangrove plant	JX398987	—	—	JX399053	Maharachchikumbura et al. (2014)
<i>N. formicarum</i>	CBS 362-72	T	Cuba	Plant debris	MH860500	—	—	KM199517	Maharachchikumbura et al. (2014)
<i>N. guajavæ</i>	FMBCC 11.1	T	Pakistan	<i>Psidium guajava</i>	MFT830395	—	—	MH460888	Maharachchikumbura et al. (2014)
<i>N. guajavæ</i>	FMBCC 11.4	T	Pakistan	<i>Hadrolaelia jongheana</i>	MK454709	—	—	MH460873	Ui Haq et al. (2021)
<i>N. hadroelaie</i>	COAD 2637	T	Brazil	<i>Ilex chinensis</i>	OK087294	—	—	MK465122	Freitas et al. (2019)
<i>N. haikouensis</i>	SAUCC212271	T	China	<i>Ilex chinensis</i>	OK087295	—	—	OK104877	Zhang et al. (2022)
<i>N. hispanica</i>	SAUCC212272	T	China	<i>Eucalyptus globulus</i>	MW794107	—	—	OK104878	Zhang et al. (2022)
<i>N. honoluluana</i>	CBS 147-686	T	Portugal	<i>Eucalyptus globulus</i>	KM199364	—	—	MW802840	Diogo et al. (2021)
<i>N. hydeana</i>	MFLUCC 20-0132	T	Thailand	<i>Artocarpus heterophyllus</i>	MW266069	—	—	MW251119	Huanliek et al. (2021)
<i>N. iberica</i>	CBS 147-688	T	Portugal	<i>Eucalyptus globulus</i>	MW794111	—	—	MW802844	Diogo et al. (2021)
<i>N. iraniensis</i>	CBS 137768	T	Iran	<i>Fragaria x ananassa</i>	KM074045	—	—	KM074056	Norphanphon et al. (2019)
<i>N. javaensis</i>	CBS 257-31	T	Indonesia	<i>Cocos nucifera</i>	KM199357	—	—	KM199543	Prasannath et al. (2021)
<i>N. longipendiculata</i>	CBS 147-690	T	Portugal	<i>Eucalyptus globulus</i>	MW794112	—	—	MZ344167	Maharachchikumbura et al. (2014)
<i>N. lusitanica</i>	CBS 147-692	T	New South Wales	<i>Eucalyptus globulus</i>	MW794110	—	—	KF582791	KM199441
<i>N. macadamiae</i>	BRIP 63737C	T	Australia	<i>Macadamia integrifolia</i>	KX186604	—	—	KX186627	KM199441
<i>N. maddoxii</i>	MFLUCC 12-0652	T	France	<i>Pteridium</i> sp.	MZ230372	—	—	MZ312675	Maharachchikumbura et al. (2014)
<i>N. magna</i>	CBS 336-86	T	Iraq	<i>Pinus brutia</i>	KM199362	—	—	KF789685	KY789686
<i>N. musae</i>	MFLU 16-1279	T	Thailand	<i>Musa</i> sp.	KY789683	—	—	KM199522	KM199466
<i>N. natalensis</i>	CBS 138-41	T	South Africa	<i>Acacia mollissima</i>	KM199377	—	—	—	—

Table 3 (cont.)

Species	Strain number ¹	Status ²	Country	Substrate	GenBank accession no.				References
					ITS	LSU	RPB2	TEF	
<i>N. nebuloides</i>	BRIP 66617	T	Australia	<i>Sporobolus elongatus</i>	MK966338	–	–	MK977633	Crous et al. (2020)
<i>N. olumiæde</i>	BRIP 72273a	T	Australia	<i>Macadamia integrifolia</i>	MZ303790	–	–	MZ312683	Prasarnith et al. (2021)
<i>N. palmatum</i>	PSHI2004Endo458	T	Cuba	<i>Zalacca wallichiana</i>	DQ813426	–	–	–	Liu et al. (2010)
	PSHI2004Endo454	T	Cuba	<i>Rcytstonea regia</i>	DQ813427	–	–	DQ787837	Liu et al. (2010)
<i>N. pandanicola</i>	KUMCC 17-0175	T	Brazil	<i>Pandanus</i> sp.	–	–	–	MH388389	MH412220
<i>N. permambucana</i>	URM 7148-01	T	Pakistan	<i>Vismia guianensis</i>	KJ792466	–	–	KU306739	Tibpromma et al. (2018)
<i>N. perukeae</i>	FMBCC 11-3	T	Thailand	<i>Psidium guajava</i>	MH299077	–	–	MH423647	Silvério et al. (2016)
<i>N. petila</i>	MFLUCC 17-1738	T	Thailand	<i>Rhizophora mucronata</i>	MK764275	–	–	MH764319	Ul Haq et al. (2021)
	MFLUCC 17-1737	T	Thailand	<i>Rhizophora mucronata</i>	MK764276	–	–	MK764320	Norphanphoun et al. (2019)
<i>N. phangngaensis</i>	MFLUCC 18-0119	T	–	<i>Pandanus</i> sp.	MH388354	–	–	MH388390	Norphanphoun et al. (2019)
<i>N. pieceana</i>	CBS 394.48	T	UK	<i>Picea</i> sp.	KM199368	–	–	KM199527	MH412221
<i>N. protearum</i>	CBS 114178	T	Zimbabwe	<i>Leucospermum cuneiforme</i>	JN712498	MH554873	LT853201	KM199453	Maharachchikumbura et al. (2014)
<i>N. psidii</i>	FMBCC 11-2	T	Pakistan	<i>Psidium guajava</i>	MF783082	–	–	MH460874	Ul Haq et al. (2021)
<i>N. rhipidis</i>	GUCC 21501	T	China	<i>Rhododendron simsii</i>	MW931620	–	–	MW980442	Yang et al. (2021)
<i>N. rhizophorae</i>	MFLUCC 17-1551	T	Thailand	<i>Rhizophora mucronata</i>	MK764277	–	–	MK764321	Norphanphoun et al. (2019)
	MFLUCC 17-1550	T	Thailand	<i>Rhizophora mucronata</i>	MK764278	–	–	MK764322	Norphanphoun et al. (2019)
<i>N. rhododendri</i>	GUCC 21504	T	China	<i>Rhododendron simsii</i>	MW979577	–	–	MW980444	Yang et al. (2021)
<i>N. roseæ</i>	CBS 101057	T	New Zealand	<i>Rosa</i> sp.	KM199359	KM116245	MH554850	KM199463	Maharachchikumbura et al. (2014)
	CBS 124745	T	USA	<i>Paonia suffruticosa</i>	KM199360	–	–	KM199430	Maharachchikumbura et al. (2014)
	CRM-FRC AC50	T	Mexico	<i>Fragaria × ananassa</i>	MN357178	–	–	MN268532	Rebolledo-Alvite et al. (2020)
	CFCC 51992	T	Italy	<i>Rosa americana</i>	ON117810	–	–	ON209165	Alberto et al. (2022)
	CFCC 51993	T	China	<i>Rosa chinensis</i>	KY885239	–	–	KY885245	Jiang et al. (2018)
<i>N. semaragenensis</i>	MFLUCC 12-0233	T	Thailand	<i>Rosa chinensis</i>	KY885240	–	–	KY885246	Jiang et al. (2018)
<i>N. saprophytica</i>	MFLUCC 12-0282	T	China	<i>Syzygium samarangense</i>	KM199365	–	–	KM199447	Norphanphoun et al. (2019)
<i>N. scalariensis</i>	CAA1029	T	Portugal	<i>Magnolia</i> sp.	KY606286	–	–	JX399048	Maharachchikumbura et al. (2014)
<i>N. sichuanensis</i>	CFFC 51993 = SM15-1	T	China	<i>Vaccinium corymbosum</i>	MW969748	–	–	MW959100	Santos et al. (2022)
	SM15-1C	T	China	<i>Castanea mollissima</i>	MW166223	–	–	MW199750	Jiang et al. (2021)
<i>N. sicilianna</i>	AC46	T	Italy	<i>Castanea mollissima</i>	MW166232	–	–	MW218524	Jiang et al. (2021)
	AC48	T	Italy	<i>Persea americana</i>	ON117813	–	–	ON209162	Alberto et al. (2022)
	AC49	T	Italy	<i>Persea americana</i>	ON117812	–	–	ON209163	Alberto et al. (2022)
	MFLUCC 17-1744	T	Thailand	<i>Sonneratia alba</i>	MK764279	–	–	ON209164	Alberto et al. (2022)
	MFLUCC 17-1745	T	Colombia	<i>Sonneratia alba</i>	MK764280	–	–	MK764323	Norphanphoun et al. (2019)
	VRes4	T	Colombia	Scab disease of Guava	KR493566	–	–	MK764346	Norphanphoun et al. (2019)
	BPca2	T	Colombia	Scab disease of Guava	KR493569	–	–	KR493628	Kumar et al. (2019)
	VieP	T	Colombia	Scab disease of Guava	KR493570	–	–	KR493627	Kumar et al. (2019)
	VTran4	T	Colombia	Scab disease of Guava	KR493574	–	–	KR493666	Kumar et al. (2019)
	BVayr1	T	Colombia	Scab disease of Guava	KR493575	–	–	KR493671	Kumar et al. (2019)
	BRIP 63740a	T	Australia	Scab disease of Guava	KR493579	–	–	KR493724	Kumar et al. (2019)
	BRIP 63745a	T	India	Dry flower	KX186617	–	–	KR493739	Kumar et al. (2019)
	CBS 119.75	T	Brazil	Dry flower	KX186614	–	–	KR493739	Kumar et al. (2019)
	CMM 1363	T	China	<i>Acras sapota</i>	KM199356	–	–	KR493744	Kumar et al. (2019)
	LC6489	T	China	<i>Opuntia stricta</i>	KY549599	–	–	KL184189	Kumar et al. (2019)
	MFLUCC 12-0614	T	Midi-pyrénées	<i>Camellia</i> sp.	KX895020	–	–	KU252390	Kumar et al. (2019)
	MMf0011	T	Japan	Unidentified host	KX816919	–	–	KU252477	Kumar et al. (2019)
	SC2A3	T	China	<i>Lilium speciosum</i>	LC184188	–	–	KM199434	Kumar et al. (2019)
	CBS 164.42	T	France	Tea plant	KU252210	–	–	KM199520	Kumar et al. (2019)
	CBS 266.80	T	India	Sand dune	KM199367	–	–	KM199532	Kumar et al. (2019)
	CBS 361.61	T	Guinea	<i>Vitis vinifera</i>	KM199352	–	–	KM199440	Kumar et al. (2019)
	IM 192475	T	Netherlands	<i>Cinchona</i> sp.	KM199346	–	–	KM199460	Kumar et al. (2019)
			Australia	<i>Cissus</i> sp.	KM199355	–	–	KF582794	Maharachchikumbura et al. (2014)
				<i>Eucalyptus viminalis</i>	KF582792	–	–		

Table 3 (cont.)

Species	Strain number ¹	Status ²	Country	Substrate	GenBank accession no.				References
					ITS	LSU	RPB2	TEF	
<i>N. surinamensis</i>	CBS 450.74	T	Suriname	Soil	KM199351	KM116258	MH554962	KM199518	KM199465
<i>N. thailandica</i>	MFLUCC 17-1730	T	Thailand	<i>Rhizophora mucronata</i>	MK764281	—	MK764325	MK764347	Maharachchikumbura et al. (2014)
<i>N. umbribinospora</i>	MFLUCC 12-0285	T	China	Dead leaves	JX398884	—	JX399050	JX399019	Norphanphoun et al. (2019)
<i>N. vaccinii</i>	CAA1059	T	Portugal	<i>Vaccinium corymbosum</i>	MW969747	—	MW959099	MW934610	Norphanphoun et al. (2019)
<i>N. vaccinifolia</i>	CAA1055	T	Portugal	<i>Vaccinium corymbosum</i>	MW969751	—	MW959103	MW934614	Santos et al. (2022)
<i>N. versicolor</i>	CBS 303.49	T	China	<i>Myrica rubra</i>	MH856535	—	—	—	Santos et al. (2022)
<i>N. wheeneae</i>	BRIP 72293a	T	Australia	<i>Macadamia integrifolia</i>	MZ303792	—	MZ344177	MZ312685	Prasannath et al. (2021)
<i>N. vitis</i>	MFLUCC 15-1265	T	China	<i>Vitis vinifera</i>	KU140684	—	KU140676	KU140685	Jayawardena et al. (2016)
<i>N. zakeelii</i>	BRIP 72282a	T	Australia	<i>Macadamia integrifolia</i>	MZ303789	—	MZ344174	MZ312682	Prasannath et al. (2021)
<i>N. zimbabwana</i>	CBS H-21769	T	Zimbabwe	<i>Leucospermum cuneiforme</i>	—	JX556249	MH554855	KM199456	Maharachchikumbura et al. (2014)
<i>Nonappendiculata quercina</i>	CBS 116061	T	Italy	<i>Quercus suber</i>	MH553982	MH554199	MH554882	—	Liu et al. (2019)
<i>Parabartalinia lateralis</i>	CBS 270.82	T	South Africa	<i>Quercus pubescens</i>	MH554025	MH554246	MH554937	—	Liu et al. (2019)
<i>Pestalotiopsis abietis</i>	CBS 399.71	T	China	<i>Acacia karroo</i>	MH554043	MH554256	MH554954	—	Liu et al. (2019)
<i>Pes. adusta</i>	CFCC 53011	T	China	<i>Abies fargesii</i>	MK397013	—	MK622277	MK622280	Gu et al. (2021)
<i>Pes. aggregatum</i>	CFCC 53012	T	China	<i>Abies fargesii</i>	MK397014	—	MK622278	MK622281	Gu et al. (2021)
<i>Pes. anacardiacearum</i>	CFCC 53013	T	Fiji	<i>Abies fargesii</i>	MK397015	—	MK622279	MK622282	Gu et al. (2021)
<i>Pes. arctothibii</i>	ICMP 6088	T	Netherlands	Refrigerator door PVC gasket	JX399006	—	JX399070	JX399037	Norphanphoun et al. (2019)
<i>Pes. arengae</i>	CBS 263.33	T	China	<i>Rhododendron ponticum</i>	KM199316	—	KM199489	KM199414	Norphanphoun et al. (2019)
<i>Pes. australasiae</i>	LC6301	T	China	<i>Camellia sinensis</i>	KX895015	—	KX895348	KX895348	Liu et al. (2017)
<i>Pes. australis</i>	IFRDCC 2397	T	USA	<i>Mangifera indica</i>	KC247154	—	KC247156	Maharachchikumbura et al. (2013b)	Maharachchikumbura et al. (2013b)
<i>Pes. arctothibii</i>	CBS 433.65	T	USA	<i>Arcuetobium campylospodium</i>	MH554046	—	MH554481	MH554722	Maharachchikumbura et al. (2014)
<i>Pes. arctothibii</i>	CBS 434.65	T	USA	<i>Arcuetobium campylospodium</i>	MH199341	—	MH554481	MH554722	Maharachchikumbura et al. (2014)
<i>Pes. arctothibii</i>	CBS 331.92	T	Singapore	<i>Arrenga undulatifolia</i>	MH199340	—	MH554481	MH554722	Maharachchikumbura et al. (2014)
<i>Pes. austroalasiae</i>	CBS 114.126	T	New Zealand	<i>Knighlia sp.</i>	KM199297	KM116218	MH554867	KM199499	Maharachchikumbura et al. (2014)
<i>Pes. austroalasiae</i>	CBS 114.141	T	Australia	<i>Protea</i> cv. 'Pink Ice'	KM199298	—	KM199501	KM199410	Maharachchikumbura et al. (2014)
<i>Pes. austroalasiae</i>	CBS 114.193	T	Australia	<i>Grevillea</i> sp.	KM199332	KM116197	MH554875	KM199475	Maharachchikumbura et al. (2014)
<i>Pes. austroalasiae</i>	CBS 119350	T	South Africa	<i>Braebium stellatifolium</i>	KM199333	—	KM199476	KM199383	Maharachchikumbura et al. (2014)
<i>Pes. austroalasiae</i>	MEAN 1096 = CPC 36750 = CBS 146843	T	Portugal	<i>Pinus pinea</i>	MT374679	—	MT374692	KM199384	Maharachchikumbura et al. (2014)
<i>Pes. austroalasiae</i>	MEAN 1109	T	Portugal	<i>Pinus pinea</i>	MT374683	—	MT374708	Silva et al. (2020)	Silva et al. (2020)
<i>Pes. austroalasiae</i>	MEAN 1110	T	Portugal	<i>Pinus pinea</i>	MT374684	—	MT374696	MT374709	Silva et al. (2020)
<i>Pes. austroalasiae</i>	MEAN 1111	T	Portugal	<i>Pinus pinea</i>	MT374685	—	MT374697	MT374710	Silva et al. (2020)
<i>Pes. austroalasiae</i>	MEAN 1112	T	Portugal	<i>Pinus pinea</i>	MT374686	—	MT374698	MT374711	Silva et al. (2020)
<i>Pes. biciliata</i>	CBS 124463	T	Slovakia	<i>Platanus × hispanica</i>	KM199308	—	KM199505	KM199399	Maharachchikumbura et al. (2014)
<i>Pes. brachiatia</i>	CBS 236.38	T	Italy	<i>Paonia</i> sp.	KM199309	—	KM199506	KM199401	Maharachchikumbura et al. (2014)
<i>Pes. brachiatia</i>	MEAN 1168	T	Portugal	<i>Pinus pinea</i>	MH174690	—	MT374702	MT374715	Maharachchikumbura et al. (2014)
<i>Pes. brachiatia</i>	LC2988	T	China	<i>Camellia</i> sp.	KX894933	—	KX895150	KX895265	Maharachchikumbura et al. (2014)
<i>Pes. brachiatia</i>	CBS 170.26	T	New Zealand	<i>Brassica napus</i>	KM199379	—	KM199558	—	Maharachchikumbura et al. (2014)
<i>Pes. brachiatia</i>	CBS 443.62	T	Turkey	<i>Camellia sinensis</i>	KM199336	—	KM199512	KM199424	Zhang et al. (2012b)
<i>Pes. camelliae-oleiferae</i>	MFLUCC 12-0277	T	China	<i>Camellia japonica</i>	JX399010	—	MT374693	JX399074	Zhang et al. (2012b)
<i>Pes. camelliae-oleiferae</i>	CSUFTCC08	T	China	<i>Camellia oleifera</i>	OK493593	—	OK507963	OK562368	Li et al. (2021)
<i>Pes. camelliae-oleiferae</i>	CSUFTCC09	T	China	<i>Camellia oleifera</i>	OK493594	—	OK507964	OK562369	Li et al. (2021)
<i>Pes. camelliae-oleiferae</i>	CSUFTCC10	T	China	<i>Camellia oleifera</i>	OK493595	—	OK507965	OK562370	Li et al. (2021)
<i>Pes. chamaeropis</i>	CBS 113607	T	—	<i>Chamaerops humilis</i>	KM199325	—	KM199424	KM199390	Maharachchikumbura et al. (2014)
<i>Pes. chiaroscuro</i>	CBS 186.71	T	Italy	<i>Sporobolus natalensis</i>	KM199326	—	KM199473	KM199473	Maharachchikumbura et al. (2014)
<i>Pes. clavata</i>	BRIP 72970	T	Australia	<i>Buxus</i> sp.	OK422510	—	OK562368	OK562368	Crous et al. (2022)
<i>Pes. colombiensis</i>	MFLUCC 12-0268	T	China	<i>Eucalyptus eurograndis</i>	JX398990	—	JX399056	JX399025	Maharachchikumbura et al. (2012)
<i>Pes. digitalis</i>	CBS 118553	T	Colombia	<i>Digitalis purpurea</i>	KM199307	—	KM199488	KM199421	Maharachchikumbura et al. (2014)
<i>Pes. diplocistiae</i>	ICMP 5434	T	New Zealand	<i>Diplocloisia glaucescens</i>	KP781887	—	KP781883	KP781883	Liu et al. (2015)
<i>Pes. diplocistiae</i>	CBS 115587	T	Hong Kong, China	<i>Diplocloisia glaucescens</i>	KM199320	—	KM199486	KM199419	Maharachchikumbura et al. (2014)

Table 3 (cont.)

Species	Strain number ¹	Status ²	Country	Substrate	GenBank accession no.				References
					ITS	LSU	RPB2	TEF	
<i>Pes. disseminata</i>	CBS 118552 CBS 143904		New Zealand New Zealand	<i>Eucalyptus botryoides</i> <i>Persea americana</i>	MH553986 MH554152	–	–	MH554410 MH554587	MH554652 MH554625
<i>Pes. disseminata</i>	MEAN 1165 MEAN 1166		Portugal Portugal	<i>Pinus pinea</i> , blighted shoot <i>Pinus pinea</i> , blighted shoot	MT374687 MT374688	–	–	MT374712 MT374700	MT374713 MT374700
<i>Pes. distincta</i>	LC3232 LC8184	T	China China	<i>Camellia sinensis</i> <i>Camellia sinensis</i>	KX895197 KY464138	–	–	KX895293 KY464148	KY464158 Silva et al. (2020)
<i>Pes. diversiseta</i>	MFLUCC 12-0287	T	China	<i>Rhododendron</i> sp. <i>Dendrobium</i> sp.	JX399009	–	–	JX399073 MK975832	JX399040 MK975837
<i>Pes. doftungensis</i>	MFLUCC 14-0115	T	Thailand	<i>Draeacaena</i> sp.	MN962731	–	–	MN962733	Chaiwan et al. (2020)
<i>Pes. dracaenicola</i>	MFLUCC 18-0913	T	Thailand	<i>Dracontomelon</i> <i>daeo</i>	KP781877	–	–	KP781880	Liu et al. (2015)
<i>Pes. draconitomelonis</i>	MFLUCC 10-0149	T	Thailand	<i>Rhododendron</i> <i>delavayi</i>	KC537807	–	–	KC537814	Zhang et al. (2013b)
<i>Pes. ericacearum</i>	IFRDCC 2439	T	China	<i>Sporobolus jacquemontii</i>	MK966339	–	–	MK977635	Crous et al. (2020)
<i>Pes. elatensis</i>	BRIP 66615	T	Australia	On dead grass	MH809381	–	–	MH809389	Ariyawansa & Hyde (2018)
<i>Pes. formosana</i>	NTUCC 17-009	T	Taiwan, China	<i>Camellia sinensis</i>	JO683724	–	–	JQ683740	Maharachchikumburabeta (2013a)
<i>Pes. furcata</i>	MFLUCC 12-0054	T	Thailand	<i>Gautheria forestii</i>	KC537805	–	–	KC537812	Zhang et al. (2013)
<i>Pes. gauthierae</i>	IFRD 41-014	T	China	<i>Gautheria stallon</i>	LC311589	–	–	LC311591	Watanebe et al. (2018)
<i>Pes. gibbosa</i>	NOF 3175	T	Canada	<i>Grevillea</i> sp.	KM199300	KM116212	MH554868	KM199504	Maharachchikumbura et al. (2014)
<i>Pes. grevilleae</i>	CBS 114127	T	Australia	<i>Leucospermum</i> cv. 'Coral'	KM199339	–	–	KM199407	Maharachchikumbura et al. (2014)
<i>Pes. hawaiiensis</i>	CBS 115.391	T	USA	'Protea' cv. 'Susara'	MH553981	–	MH554399	KM199514	Liu et al. (2019)
<i>Pes. hispanica</i>	CBS 265.33	T	Spain	<i>Sciadopitys verticillata</i>	KM199328	KM116228	MH554936	KM199481	Maharachchikumbura et al. (2014)
<i>Pes. hollandica</i>	MEAN 1091 = CPC 36745 = CBS 146839	T	Netherlands	<i>Pinus pinea</i> , blighted shoot	MT374678	–	–	MT374691	Maharachchikumbura et al. (2014)
<i>Pes. humicola</i>	CBS 115450	T	Hong Kong, China	<i>Ilex cinerea</i>	KM199319	KM116208	MH554881	KM199418	Maharachchikumbura et al. (2014)
<i>Pes. humicola</i>	CBS 336.97	T	Papua New Guinea	Soil	KM199317	–	–	KM199420	Maharachchikumbura et al. (2014)
<i>Pes. humanensis</i>	CSUFTCC15	T	China	<i>Camellia oleifera</i>	OK493599	–	–	OK507969	Li et al. (2021)
<i>Pes. hydei</i>	CSUFTCC18	T	China	<i>Camellia oleifera</i>	OK493600	–	–	OK507970	Li et al. (2021)
<i>Pes. inflexa</i>	CSUFTCC19	T	China	<i>Camellia oleifera</i>	OK493601	–	–	OK507971	Li et al. (2021)
<i>Pes. intermedia</i>	MFLUCC 20-0-35	T	Thailand	<i>Litssea petiolata</i>	NR_172003	–	–	OK507972	Li et al. (2021)
<i>Pes. intermedia</i>	MFLUCC 12-0270	T	China	Unidentified tree	JX399008	–	–	OK507973	Li et al. (2021)
<i>Pes. intermedia</i>	MFLUCC 12-0259	T	China	Unidentified tree	JX398993	–	–	OK507974	Li et al. (2021)
<i>Pes. italiana</i>	MFLUCC 12-0657	T	Italy	<i>Cupressus glabra</i>	KP781878	–	–	OK562376	Li et al. (2021)
<i>Pes. jesteri</i>	CBS 109350	T	Papua New Guinea	<i>Fragreae bodenii</i>	KM199380	–	–	MW251113	Maharachchikumbura et al. (2012)
<i>Pes. jiangxiensis</i>	LC4399	T	China	<i>Camellia</i> sp.	KX895009	–	–	JX399072	JX399039
<i>Pes. jinchanghensis</i>	LC8636	T	China	<i>Camellia sinensis</i>	KX895028	–	–	KX399059	Maharachchikumbura et al. (2012)
<i>Pes. kandeliola</i>	NCYUCC 19-0355	T	Taiwan, China	<i>Kandelia candel</i>	MT560722	–	–	KP781882	Liu et al. (2015)
<i>Pes. kenyana</i>	CBS 499354	T	Taiwan, China	<i>Coffea</i> sp.	MT560723	–	MH554958	KM199421	Maharachchikumbura et al. (2014)
<i>Pes. knightae</i>	CBS 442.67	T	Kenya	<i>Knightia</i> sp.	KM199302	KM116234	MH554958	KM199427	Maharachchikumbura et al. (2014)
<i>Pes. leucadendri</i>	CBS 114138	T	New Zealand	<i>Leucadendron</i> sp.	KM199310	KM116227	MH554870	KM199427	Maharachchikumbura et al. (2014)
<i>Pes. liguicola</i>	CBS 121417	T	South Africa	<i>Licuala grandis</i>	MH553987	–	–	MH554412	MH554654
<i>Pes. linearis</i>	HGUP 4057	T	China	<i>Trachelospermum</i> sp.	KC492509	–	–	KC481684	KC481683
<i>Pes. longijappondulata</i>	MFLUCC 12-0271	T	China	<i>Camellia sinensis</i>	JX398992	–	–	JX399058	JX399027
<i>Pes. lusitanensis</i>	LC3013	T	China	<i>Camellia</i> sp.	KX894939	–	–	KX895156	KX895271
<i>Pes. macedamiae</i>	LC344	T	China	<i>Macadamia integrifolia</i>	KX895005	–	–	KX895223	KX895337
<i>Pes. malayana</i>	BRIP 63738b	T	Australia	<i>Macaranga triloba</i>	KX186588	–	–	KX186621	KX186680
<i>Pes. monochaeta</i>	CBS 102220	T	Malaysia	<i>Quercus robur</i>	KM199306	–	–	KM199422	KM199411
<i>Pes. nanningensis</i>	CBS 144.97	T	Netherlands	<i>Camellia oleifera</i>	KM199327	–	–	KM199479	KM199386
<i>Pes. nanningensis</i>	CSUFTCC16	T	China	<i>Camellia oleifera</i>	OK493602	–	–	OK507972	OK562377
<i>Pes. nanningensis</i>	CSUFTCC20	T	China	<i>Camellia oleifera</i>	OK493603	–	–	OK507973	OK562378
<i>Pes. nanningensis</i>	CSUFTCC04	T	China	<i>Camellia oleifera</i>	OK493604	–	–	OK507974	OK562379
<i>Pes. nanningensis</i>	CSUFTCC10	T	China	<i>Camellia oleifera</i>	OK562237	–	–	OK507967	OK562371
<i>Pes. nanningensis</i>	CSUFTCC11	T	China	<i>Camellia oleifera</i>	OK5622372	–	–	OK507968	OK562373
<i>Pes. nanningensis</i>	CSUFTCC12	T	China	<i>Camellia oleifera</i>	OK5622373	–	–	OK507968	OK562373

Table 3 (cont.)

Species	Strain number ¹	Status ²	Country	Substrate	GenBank accession no.				References
					ITS	LSU	RPB2	TEF	
<i>Pes. neofilisea</i>	NTUCC 17-0111	T	Taiwan, China	<i>Neolitsea villosa</i>	MH809383	—	—	MH809391	MH809387
<i>Pes. nova-hollandiae</i>	CBS 130973	T	Australia	<i>Banksia grandis</i>	KM199337	—	—	KM199511	KM199425
<i>Pes. oryzae</i>	CBS 353.69	T	Denmark	<i>Oryza sativa</i>	KM199298	KM116221	MH554947	KM199496	Maharachchikumbura et al. (2014)
<i>Pes. palliolitheae</i>	MAFF 240993	T	Japan	<i>Pieris japonica</i>	NR111022	—	—	LC311585	LC311584
<i>Pes. pandanicola</i>	MFLUCC 16-0255	T	Thailand	<i>Pandanus</i> sp.	MH388361	—	—	MH388366	MH412723
<i>Pes. papuana</i>	CBS 331.96	T	Papua New Guinea	Soil	KM199321	—	—	KM199491	KM199413
<i>Pes. papuana</i>	CBS 114972	T	Hong Kong, China	Leaf	MH553980	—	MH554397	MH704627	Maharachchikumbura et al. (2014)
<i>Pes. papuana</i>	CBS 278.35	T	—	<i>Leucothoe fontanesiana</i>	KM199313	KM116205	MH554939	KM199509	Maharachchikumbura et al. (2014)
<i>Pes. photincola</i>	GZCC 16-0028	T	China	<i>Photinia serrulata</i>	KY072404	—	KY047662	KY047663	Chen et al. (2017)
<i>Pes. pini</i>	MEAN 1092 = CPC 36746 = CBS 146840	T	Portugal	<i>Pinus pinea</i>	MT374680	—	—	MT374693	MT374705
<i>Pes. pinicola</i>	MEAN 1094 = CPC 36748 = CBS 146841	T	Portugal	<i>Pinus pinea</i>	MT374681	—	—	MT374694	MT374706
<i>Pes. portugalica</i>	MEAN 1095 = CPC 36749 = CBS 146842	T	Portugal	<i>Pinus pinea</i>	MT374682	—	—	MT374695	MT374707
<i>Pes. rhizoporae</i>	MEAN 1167	T	China	<i>Pinus pinaster</i>	MT374689	—	—	MT374714	Silva et al. (2020)
<i>Pes. rhododendri</i>	KUMCC 19-0183	T	New Zealand	<i>Pinus armandii</i>	MN412636	—	—	MN417509	Tibpromma et al. (2019)
<i>Pes. rhododendri</i>	CBS 684.85	T	Portugal	<i>Camellia japonica</i>	MH554065	—	—	MH554501	Maharachchikumbura et al. (2014)
<i>Pes. rhododendri</i>	CBS 393.48	T	Thailand	—	KM199335	KM116233	MH554951	KM199510	MH554741
<i>Pes. rhodomitus</i>	MFLUCC 17-0416	T	China	<i>Rhizophora apiculata</i>	MK764283	—	—	MK764327	Norphanphon et al. (2019)
<i>Pes. rosea</i>	I RDCC 2399	T	Zimbabwe	<i>Rhizophora apiculata</i>	KC537804	—	—	KC537811	Norphanphon et al. (2019)
<i>Pes. rosea</i>	CBS 144024	T	China	<i>Pinus</i> sp.	MH554109	—	—	MH554533	Norphanphon et al. (2019)
<i>Pes. rosea</i>	HGUP 4230	T	China	<i>Rhodomyrtus tomentosa</i>	KF412648	—	—	KF412642	Norphanphon et al. (2019)
<i>Pes. rosea</i>	LC3413	T	China	<i>Camellia sinensis</i>	KX894981	—	—	KX895313	Norphanphon et al. (2019)
<i>Pes. rosea</i>	MFLUCC 12-0258	T	China	<i>Pinus</i> sp.	JX399005	—	—	JX399036	Maharachchikumbura et al. (2012)
<i>Pes. scopiae</i>	CBS 176.25	T	—	<i>Chamaecyparis</i> sp.	KM199330	—	—	KM199393	Maharachchikumbura et al. (2014)
<i>Pes. sequoiae</i>	MFLUCC 13-0399	T	Italy	<i>Sequoia sempervirens</i>	KX572339	—	—	—	Maharachchikumbura et al. (2014)
<i>Pes. shorea</i>	MFLUCC 12-0314	T	Thailand	<i>Shorea obtusa</i>	KJ03811	—	—	KJ038117	Song et al. (2013)
<i>Pestalotiopsis 7 FL_2019</i>	CBS 110326	T	USA	<i>Pinus</i> sp.	MH553957	—	—	MH554375	MH554616
<i>Pestalotiopsis 7 FL_2019</i>	CBS 127.80	T	Chile	<i>Pinus radiata</i>	MH553995	—	—	MH554422	MH554664
<i>Pes. spathulata</i>	CBS 356.86	T	Chile	<i>Guettarda avellana</i>	KM199338	—	—	KM199513	KM199423
<i>Pes. spathulata</i>	CBS 144035	T	Australia	<i>Phoenix canariensis</i>	MH554172	MH554366	—	MH554607	MH554845
<i>Pes. spathulata</i>	CBS 114137	T	Australia	<i>Protea</i> cv. 'Pink Ice'	KM199301	—	—	KM199559	KM199469
<i>Pes. spathulata</i>	CBS 114161	T	Australia	<i>Tetrapanax</i> sp.	KM199296	—	—	KM199403	Maharachchikumbura et al. (2014)
<i>Pes. spathulata</i>	CBS 141.69	T	Pacific Islands	Soil	MH554004	—	—	MH554438	MH554680
<i>Pes. spathulata</i>	MFLUCC 17-1616	T	Thailand	<i>Rhizophora apiculata</i>	MK764285	—	—	MK764329	Maharachchikumbura et al. (2014)
<i>Pes. spathulata</i>	IFRDCC 2440	T	China	<i>Trachycarpus fortunei</i>	JQ845947	—	—	JQ845946	JQ845945
<i>Pes. spathulata</i>	MFLUCC 12-0275	T	China	Unidentified tree	JX398998	—	—	JX399063	Zhang et al. (2012a)
<i>Pes. spathulata</i>	MFLUCC 12-0276	T	China	<i>Rhododendron</i> sp.	JX398999	—	—	JX399029	Maharachchikumbura et al. (2012)
<i>Pes. terricola</i>	MFLUCC 12-0274	T	China	<i>Rhododendron</i> sp.	MH554004	—	—	JX399030	Maharachchikumbura et al. (2012)
<i>Pes. thailandica</i>	CBS 365.54	T	Netherlands	<i>Chamaecyparis lawsoniana</i>	MH554037	—	—	MH554432	MH554713
<i>Pes. trachycarpicola</i>	LC3412	T	China	<i>Camellia sinensis</i>	KX894980	—	—	KX895312	Liu et al. (2017)
<i>Pes. unicolor</i>	LC4553	T	China	<i>Podocarpus macrophyllus</i>	KX895012	—	—	KX895231	KX895345
<i>Pes. yunnanensis</i>	HMAS 96359	T	China	<i>Eucalyptus globulus</i>	AY373375	—	—	—	Wei et al. (2013)
<i>Phlogiellinidium eucalypti</i>	CBS 120080	T	Australia	<i>Eucalyptus globulus</i>	NR_132813	DQ923534	—	—	Liu et al. (2019)
<i>Phlogiellinidium eucalyptorum</i>	CBS 120221	T	Australia	<i>Eucalyptus globulus</i>	EU040223	MH554204	—	—	Liu et al. (2019)
<i>Phlogiellinidium uniforme</i>	CBS 131312	T	Australia	<i>Eucalyptus globulus</i>	JQ044426	JQ044445	—	—	Crouse et al. (2011a)
<i>Pseudopeltostictotopsis cocos</i>	CBS 272.29	T	Indonesia	<i>Cocos nucifera</i>	KM199378	KM116276	MH554938	—	Maharachchikumbura et al. (2014)
<i>Pse. elaeidis</i>	CBS 413.62	T	Nigeria	<i>Elaeis guineensis</i>	MH554044	MH554257	MH554955	—	Liu et al. (2019)
<i>Pse. indica</i>	CBS 459.78	T	India	<i>Rosa sinensis</i>	KM199381	MH554263	MH554963	—	Maharachchikumbura et al. (2014)
<i>Pseudosarcostroma osyridicola</i>	CBS 103.76	T	France	<i>Osyris alba</i>	MH553954	MH554177	MH554851	—	Liu et al. (2019)

Table 3 (cont.)

Species	Strain number ¹	Status ²	Country	Substrate	GenBank accession no.				References
					ITS	LSU	RPB2	TEF	
<i>Robillarda africana</i>	CBS 122.75	T	South Africa	–	KR873263	KR873281	MH554896	–	Crous et al. (2015a)
<i>Rob. austriana</i>	CBS 143882	T	Australia	–	MH554091	MH555005	–	–	Liu et al. (2019)
<i>Rob. roystoneae</i>	CBS 115445	T	Hong Kong, China	<i>Roystonea regia</i>	KR873254	KR873282	MH554880	–	Crous et al. (2015a)
<i>Rob. sessilis</i>	CBS 114312	ET	Germany	Dust	KR873256	KR873284	MH554877	–	Liu et al. (2019)
<i>Rob. terra</i>	CBS 58771	T	India	Soil	KJ710484	KJ710459	MH554971	–	Crous et al. (2015a)
<i>Sarcostroma austrolienense</i>	CBS 144160	T	Australia	<i>Daviesia latifolia</i>	MH554138	MH554340	MH555044	–	Liu et al. (2019)
<i>Sar. diversispicatum</i>	CBS 189.81	T	Australia	<i>Correa reflexa</i>	MH554016	MH554236	MH554929	–	Liu et al. (2019)
<i>Sar. grevilleae</i>	CBS 143418	T	Australia	<i>Grevillea</i> sp.	MH554006	MH554227	MH554922	–	Liu et al. (2019)
<i>Sar. leucospermi</i>	CBS 111290	T	South Africa	<i>Leucospermum</i> cv. 'High Gold'	MH554081	MH554292	MH554993	–	Liu et al. (2019)
<i>Sar. longiapendiculatum</i>	CBS 111309	T	South Africa	<i>Leucospermum</i> cv. 'High Gold'	MH554079	MH554290	MH554991	–	Liu et al. (2019)
<i>Sar. paragrevilleae</i>	CBS 111308	T	South Africa	<i>Leucospermum</i> cv. 'High Gold'	MH554080	MH554291	MH554992	–	Liu et al. (2019)
<i>Sar. proteae</i>	CBS 114142	T	Australia	<i>Grevillea</i> sp.	MH553974	MH554193	MH554871	–	Liu et al. (2019)
<i>Sar. proteae</i>	CBS 113610	T	Australia	<i>Protea magnifica</i>	MH553968	MH554187	MH554862	–	Liu et al. (2019)
<i>Sar. leucospermi</i>	CBS 114189	T	Australia	<i>Protea magnifica</i>	MH553976	MH554195	MH554874	–	Liu et al. (2019)
<i>Sar. restionis</i>	CBS 118153	T	South Africa	<i>Ischyrolepis</i> cf. <i>sieberi</i>	DQ278923	DQ278925	MH554890	–	Liu et al. (2019)
	CBS 282.65	UK	UK	<i>Pteridium aquilinum</i>	AB594804	AB593736	MH554940	–	Liu et al. (2019)
	CBS 118154	T	South Africa	<i>Restio filiformis</i>	DQ278924	DQ278924	MH554891	–	Liu et al. (2019)
	CBS 111311	T	New Zealand	<i>Leucospermum</i> sp.	MH553958	MH554180	MH554854	–	Liu et al. (2019)
	CBS 114130	T	South Africa	<i>Vitis vinifera</i>	MH553973	MH554192	MH554869	–	Liu et al. (2019)
<i>Seimatosporium botan</i>	HMC-sei-302PD	T	Chile	<i>Vitis vinifera</i>	JN088482	–	–	–	Hatakeyama & Harada (2004)
<i>Seim. discosporoides</i>	NBRC 104200 = H4619	T	Japan	<i>Peonia suffruticosa</i>	AB594799	AB593731	–	–	Tanaka et al. (2011)
<i>Seim. elegans</i>	NBRC 104201	T	Canada	<i>Punica granatum</i>	AB594800	AB593732	–	–	Wijayawardene et al. (2016a)
<i>Seim. eucalypti</i>	NBRC 322674	T	Japan	<i>Melaleuca ericifolia</i>	AB594801	AB593733	–	–	Wijayawardene et al. (2016a)
<i>Seim. faciatum</i>	CPC 156	T	South Africa	<i>Eucalyptus smithii</i>	JN871200	JN871209	–	–	Wijayawardene et al. (2016a)
<i>Seim. faciatum</i>	CPC 13578	T	Australia	<i>Eucalyptus</i> sp.	JN871204	JN871213	–	–	Wijayawardene et al. (2016a)
<i>Seim. ficeae</i>	MFLUCC 15-0519	T	Italy	<i>Rubus</i> sp.	KR092800	KR092806	–	–	Wijayawardene et al. (2016a)
<i>Seim. folicola</i>	NBRC 32676	T	Japan	<i>Juniperus phoenicea</i>	AB594802	AB593732	–	–	Wijayawardene et al. (2016a)
<i>Seim. glandigenum</i>	CBS 437.87	T	Germany	<i>Fagus sylvatica</i>	MH554047	MH554957	MH554482	MH554723	Liu et al. (2019)
<i>Seim. glandigenum</i>	NBRC 32677	T	Japan	<i>Protea</i> sp.	AB594803	AB593735	–	–	Wijayawardene et al. (2016a)
<i>Seim. grevilleae</i>	ICMP 10981	T	South Africa	<i>Pteridium aquilinum</i>	AF405304	AF382372	–	–	Wijayawardene et al. (2016a)
<i>Seim. hakeae</i>	NBRC 32678	T	Japan	<i>Hypericum</i> sp.	AB594804	AB593736	–	–	Wijayawardene et al. (2016a)
<i>Seim. hypericinum</i>	NBRC 32647	T	USA	<i>Prunus persica</i>	AB594805	AB593737	–	–	Wijayawardene et al. (2016a)
<i>Seim. luteoporum</i>	Napa754	T	USA	<i>Vitis vinifera</i>	KY706283	KY706308	KY706333	KY706258	Liu et al. (2019)
<i>Seim. mariae</i>	CBS 142599	T	Japan	<i>Correa reflexa</i>	KY706284	KY706309	KY706334	KY706259	Liu et al. (2019)
<i>Seim. marianicum</i>	NBRC 32681	T	Iran	<i>Vitis vinifera</i>	AB594807	AB593740	–	–	Wijayawardene et al. (2016a)
<i>Seim. obtusum</i>	IRAN 2310CT = CBS 143781	T	Iran	<i>Vitis vinifera</i>	MW361952	MW361960	MW375356	MW375352	Moghadam et al. (2022)
<i>Seim. parasiticum</i>	IRAN 2300C = CBS 143780	T	Australia	<i>Corymbia henryi</i>	MW361951	MW361959	MW375357	MW375351	Moghadam et al. (2022)
<i>Seim. pezzoides</i>	CPC 12935	T	Japan	<i>Physoscarpus amurensis</i>	JN871206	JN871215	–	–	Barber et al. (2011)
<i>Seim. physocarpae</i>	NBRC 32682	T	Unknown	<i>Physoscarpus opulifolius</i>	AB594808	AB593741	–	–	Wijayawardene et al. (2016a)
<i>Seim. physocarpae</i>	71-TB	T	Russia	<i>Physoscarpus opulifolius</i>	KF573981	KT198722	KT198723	MH554917	Lawrence et al. (2018)
<i>Seim. physocarpae</i>	CBS 139968 = MFLUCC 14-0625	T	Russia	<i>Physoscarpus amurensis</i>	MH554278	MH554979	MH554502	MH554742	Liu et al. (2019)
<i>Seim. physocarpae</i>	MFLUCC 14-0625	T	Netherlands	<i>Pistacia vera</i>	KP04463	MH554915	MH554432	MH554747	Crous et al. (2014b)
<i>Seim. pseudorosae</i>	CBS 138865 = CPC 24455	T	Iran	<i>Pistacia vera</i>	MH554126	MH554331	MH555035	MH554561	Crous et al. (2014b)
<i>Seim. querincum</i>	MFLUCC 14-0468	T	Iran	<i>Rosa villosa</i>	–	KU359035	–	KU359035	Li et al. (2016)
<i>Seim. restionis</i>	MFLUCC 14-1198	T	Italy	<i>Quercus robur</i>	KU974965	KU974964	–	–	Goonasekara et al. (2016)
<i>Seim. rhombisporum</i>	CBS 118154	T	Germany	<i>Restio filiformis</i>	DQ278922	DQ278924	–	–	Lawrence et al. (2018)
<i>Seim. roseae</i>	MFLUCC 15-0727	ET	South Africa	<i>Vaccinium myrtillus</i>	KR092780	KR092782	–	–	Wijayawardene et al. (2016a)
<i>Seim. roseae</i>	CBS 139823 = MFLUCC 14-0621	T	Italy	<i>Rosa kalmussica</i>	KT198727	LT853203	LT853203	LT853203	Liu et al. (2019)

Table 3 (cont.)

Species	Strain number ¹	Status ²	Country	Substrate	GenBank accession no.				References
					ITS	LSU	RPB2	TEF	
<i>Seim. soli</i>	CBS 941.69	T	Denmark	Soil	MH554222	MH554983	MH554507	-	Liu et al. (2019)
<i>Seim. vitifoliae</i>	CBS 142600	T	USA	<i>Vitis vinifera</i>	KY706296	KY706321	KY706346	KY706271	Lawrence et al. (2018)
<i>Seim. vitis</i>	Napa751	T	USA	<i>Vitis vinifera</i>	KY706289	KY706314	-	KY706339	Lawrence et al. (2018)
<i>Seim. vitis-viniferae</i>	MFLUCC 14-0051	T	Italy	<i>Vitis vinifera</i>	KR920363	KR920362	-	KY706264	Senanayake et al. (2015)
<i>Seim. vitis-viniferae</i>	CBS 123004	T	Spain	<i>Vitis vinifera</i>	MH539922	MH554211	MH554901	-	Liu et al. (2019)
<i>Seim. vitis-viniferae</i>	CBS 116499	T	Iran	<i>Vitis vinifera</i>	MH553984	MH554201	MH554884	MH554402	MH554660
<i>Seim. walkeri</i>	CPC 17644	T	Australia	<i>Eucalyptus</i> sp.	JN871207	JN871216	-	-	MH554643
<i>Seridium aquaticum</i>	MFLUCC 17-0474	T	China	Decaying wood	MK828605	-	-	-	Barber et al. (2011)
<i>S-136</i>	S-136	T	China	Decaying wood	MK828606	-	-	-	Luo et al. (2019)
<i>Seir. camelliae</i>	MFLUCC 12-0647	T	China	<i>Camellia reticula</i>	JQ683725	-	-	-	Luo et al. (2019)
<i>Seir. cancerinum</i>	CBS 226.35 = IMI 052256	T	Kenya	<i>Cupressus macrocarpa</i>	LT853089	MH554241	LT853137	JQ683741	Maharachikumbura et al. (2015)
<i>Seir. cancerinum</i>	CBS 907.85	T	South Africa	<i>Cupressus lusitanica</i>	LT853090	-	LT853138	LT853186	Bonthond et al. (2018)
<i>Seir. cardinale</i>	CBS 909.85	T	South Africa	<i>Cupressus lusitanica</i>	LT853064	-	LT853113	LT853161	Marin-Felix et al. (2019)
<i>Seir. cardinale</i>	CBS 910.85	T	South Africa	<i>Cupressus sempervirens</i>	LT853065	-	LT853114	LT853162	Marin-Felix et al. (2019)
<i>Seir. cardinale</i>	CBS 523.82	T	New Zealand	<i>Cupressocyparis sp.</i>	LT853062	-	LT853111	LT853159	Marin-Felix et al. (2019)
<i>Seir. ceratosporum</i>	PHS12001Pathow07	T	China	<i>Vitis vinifera</i>	AV687314	-	-	-	Jiang et al. (2019)
<i>Seir. chinense</i>	CFCC 53031	T	China	<i>Trachycarpus fortunei</i>	MK353158	-	MK351796	MK351799	Jiang et al. (2019)
<i>Seir. chinense</i>	CFCC 53032	T	China	<i>Trachycarpus fortunei</i>	MK353159	-	MK351797	MK351800	Jiang et al. (2019)
<i>Seir. cypressi</i>	CFCC 53033	T	China	<i>Trachycarpus fortunei</i>	MK353160	-	MK351798	MK351801	Jiang et al. (2019)
<i>Seir. cypressi</i>	CBS 122616	ET	Greece	<i>Cupressus sp.</i>	LT853082	-	LT853130	LT853179	Jiang et al. (2019)
<i>Seir. eucaalypti</i>	CBS 224.55 = IMI 052254	ET	Kenya	<i>Cupressus macrocarpa</i>	LT853083	MH554251	LT853131	LT853199	Jiang et al. (2019)
<i>Seir. kartense</i>	CBS 343.97	ET	Australia	<i>Eucalyptus delegatensis</i>	LT853099	-	LT853146	LT853196	Jiang et al. (2019)
<i>Seir. kenyanium</i>	CBS 142629 = CPC 20183	T	Australia	<i>Eucalyptus cladocalyx</i>	LT853100	-	LT853147	LT853197	Bonthond et al. (2018)
<i>Seir. marginatum</i>	CBS 228.55 = IMI 052257	T	Kenya	<i>Juniperus procera</i>	LT853098	MH554242	LT853145	LT853195	Jiang et al. (2019)
<i>Seir. neocupressi</i>	CBS 140403	ET	France	<i>Rosa canina</i>	KT949914	MH554223	LT853149	LT853199	Jakitsch et al. (2016)
<i>Seir. papillatum</i>	CBS 142625 = CPC 23786	T	Italy	<i>Cupressus sempervirens</i>	LT853079	MH554329	LT853127	LT853176	Bonthond et al. (2018)
<i>Seir. pezizoides</i>	CBS 142626	T	Italy	<i>Cupressus sempervirens</i>	LT853080	-	LT853128	LT853177	Bonthond et al. (2018)
<i>Seir. phylloxae</i>	CBS 340.97 = VPRI 20827	T	Australia	<i>Eucalyptus delegatensis</i>	LT853102	DQ414531	LT853150	LT853200	Jiang et al. (2019)
<i>Seir. podocarpi</i>	CBS 145115	T	Italy	<i>Vitis vinifera</i>	MK079342	-	MK058475	MK058480	MK058485
<i>Seir. pseudocardinale</i>	CBS 133587 = CPC 19964	T	Italy	<i>Phyllica arborea</i>	LT853091	-	LT853139	LT853183	Crous et al. (2012)
<i>Seir. pseudocardinale</i>	CPC 19962	T	Tristan da Cunha	<i>Phyllica arborea</i>	LT853092	-	LT853140	LT853189	Crous et al. (2012)
<i>Seir. pseudocardinale</i>	CBS 137995	T	South Africa	<i>Podocarpus latifolius</i>	LT853101	-	LT853148	LT853198	Crous et al. (2014a)
<i>Seir. pseudocardinale</i>	MFLUCC 13-0525	T	Italy	<i>Cupressus arizonica</i>	KU848210	-	-	-	Wijawardene et al. (2016b)
<i>Seir. rosarium</i>	CBS 122613 = CMW 1648	T	Portugal	<i>Cupressus sp.</i>	LT853096	MH554206	LT853143	LT853193	Wijawardene et al. (2018)
<i>Seir. spyradicola</i>	MFLUCC 17-0054	T	Italy	<i>Rosa sp.</i>	MG829061	-	LT853142	LT853192	Bonthond et al. (2018)
<i>Seir. unicorne</i>	CBS 142628	T	Australia	<i>Spiraea globosum</i>	LT853095	-	LT853135	LT853184	Bonthond et al. (2018)
<i>Seir. venetum</i>	CBS 120306	T	South Africa	<i>Cupressus sempervirens</i>	LT853087	-	LT853136	LT853185	Bonthond et al. (2018)
<i>Sporocadus bisepatus</i>	CBS 538.82 = NBRC 32684	T	New Zealand	<i>Cryptomeria japonica</i>	KT438836	-	-	KT438837	Maharachikumbura et al. (2015)
<i>Spo. cornicola</i>	MFLUCC 14-0265	T	Italy	<i>Cornus mas</i>	-	MH53956	MH554779	MH554853	MH554374
<i>Spo. cornicola</i>	CBS 110324 = MYC 754	T	Germany	<i>Cornus sanguinea</i>	MH554121	MH554326	MH555029	MH554555	MH554615
<i>Spo. cornicola</i>	CBS 143889 = CPC 23235	T	Italy	<i>Cornus sanguinea</i>	KU974967	-	-	-	MH554794
<i>Spo. cornicola</i>	MFLUCC 14-0448	T	Russia	<i>Cornus sp.</i>	KT162918	KR59739	-	-	Liu et al. (2019)
<i>Spo. cornicola</i>	MFLUCC 14-0467	T	Russia	<i>Cotinus coggygria</i>	MH554003	MH554222	MH554916	MH554433	Moghadam et al. (2022)
<i>Spo. incanum</i>	CBS 139966 =	T	Spain	<i>Prunus dulcis</i>	MH53991	MH554210	MH554417	MH554659	Liu et al. (2019)
<i>Spo. italicus</i>	MFLUCC 14-1196	T	Italy	<i>Crateagus sp.</i>	MF614829	-	-	-	Moghadam et al. (2022)
<i>Spo. kurdistanicus</i>	IRAN 2356C = CBS 143778	T	Iran	<i>Vitis vinifera</i>	MW361950	MW361958	-	MW375356	Moghadam et al. (2022)
<i>Spo. kurdistanicus</i>	IRAN 2355C	T	Iran	<i>Vitis vinifera</i>	MW361948	MW361957	-	MW375355	Moghadam et al. (2022)
<i>Spo. kurdistanicus</i>	IRAN 2313C = CBS 143777	T	Iran	<i>Vitis vinifera</i>	MW361947	MW361956	-	MW375354	Moghadam et al. (2022)

Table 3 (cont.)

Species	Strain number ¹	Status ²	Country	Substrate	GenBank accession no.				References
					ITS	LSU	RPB2	TEF	
<i>Spo. lichenicola</i>	CBS 354.90 = NBRC 32677	Germany	Germany	<i>Fagus sylvatica</i>	MH554035	MH554252	MH554948	MH554470	MH554711 Liu et al. (2019)
	CPC 24528	UK	UK	<i>Juniperus communis</i>	MH554127	MH554332	MH555036	MH554562	MH554800 Liu et al. (2019)
<i>Spo. malii</i>	NBRC 32625 = IMI 079706	ET	Netherlands	<i>Rosa canina</i>	MH883643	MH883646	MH883647	MH883644	MH883445 Liu et al. (2019)
<i>Spo. microcyclus</i>	CBS 446.70	T	Germany	<i>Malus sylvestris</i>	MH554049	MH554261	MH554960	MH554484	MH554725 Liu et al. (2019)
<i>Spo. multisepultatus</i>	CBS 424.95	T	Netherlands	<i>Sorbus aria</i>	MH554045	MH554258	MH554956	MH554480	MH554721 Liu et al. (2019)
<i>Spo. pseudocomi</i>	CBS 887.68 = NBRC 32680	T	Netherlands	<i>Ribes sp.</i>	MH554068	MH554283	MH554981	MH554504	MH554744 Liu et al. (2019)
<i>Spo. pseudocomi</i>	CBS 143899 = CPC 26606	T	Serbia	<i>Viburnum sp.</i>	MH554141	MH554343	MH555047	MH554576	MH554814 Liu et al. (2019)
<i>Spo. rosarum</i>	MFLUCC 13-0529	T	Italy	<i>Cornus sp.</i>	–	KU359033	–	–	Moghadam et al. (2022)
	CBS 113832 = UPSC 2172	T	Sweden	<i>Rosa canina</i>	MH553970	MH554189	MH554864	MH554388	MH554629 Liu et al. (2019)
	MFLUCC 15-0563	T	Italy	<i>Rosa canina</i>	MG828960	MG829071	–	–	Liu et al. (2019)
<i>Spo. rosigena</i>	MFLUCC 14-0466	T	Italy	<i>Rosa canina</i>	KT284775	KT281912	–	–	Liu et al. (2019)
	CBS 116498	Iran	Latvia	<i>Vitis vinifera</i>	MH553983	MH554200	MH554883	MH554401	MH554642 Liu et al. (2019)
	CBS 129166 = MSCL 860	T	Netherlands	<i>Rhododendron</i>	MH553996	MH554215	MH554905	MH554423	MH554685 Liu et al. (2019)
	CBS 182.50	T	Netherlands	<i>Pyrus communis</i>	MH554013	MH554233	MH554923	MH554457	MH554889 Liu et al. (2019)
	CBS 250.49	T	Netherlands	<i>Rubus fruticosus</i>	MH554023	MH554245	MH554934	MH554457	MH554899 Liu et al. (2019)
	CBS 466.96	T	Italy	<i>Rubus sp.</i>	MH554052	MH554265	MH554965	MH554487	MH554728 Liu et al. (2019)
	MFLU 16-0239	T	Canada	<i>Rosa canina</i>	MG828958	MGB29069	–	–	Liu et al. (2019)
	CBS 616.83	T	–	<i>Arceuthobium pusillum</i>	MH554060	MH554273	MH554974	MH554496	MH554737 Liu et al. (2019)
	CBS 160.25	T	Italy	<i>Sorbus terminalis</i>	MH554008	MH554229	MH554924	MH554442	MH554684 Liu et al. (2019)
	MFLUCC 14-0469	T	Italy	<i>Euphorbia sp.</i>	KT284774	KT281911	–	–	Liu et al. (2019)
	CBS 506.71	T	Sweden	<i>Rosa canina</i>	MH554055	MH554288	MH554968	MH554490	MH554731 Liu et al. (2019)
	CBS 114203 = UPSC 2430	T	Austria	<i>Robinia pseudoacacia</i>	MH553977	MH554196	MH554876	MH554395	MH554636 Liu et al. (2019)
	CBS 140411	ET	France	<i>Juniperus phoenicea</i>	NR_154423	KT949918	MH554920	–	Liu et al. (2019)
	CBS 477.77	T	Japan	<i>Rhododendron brachycarpum</i>	MH554053	MH554216	MH554966	–	Liu et al. (2019)
	MAFF 239201	T	Turkey	<i>Rhododendron brachycarpum</i>	LC047753	LC047744	–	–	Liu et al. (2019)
	MAFF 243052	T	Japan	<i>Soil</i>	MH554042	MH554255	MH554953	–	Liu et al. (2019)
	CBS 398.71	T	Turkey	<i>Gossypium sp.</i>	MH554021	MH554243	MH554932	–	Liu et al. (2019)
	CBS 231.77	T	France	<i>Vitis vinifera</i> cv. 'Prunelard'	MH554111	MH554317	MH555020	–	Liu et al. (2019)
	CPC 21354	T	Switzerland	<i>Heterodera carotae</i>	MH554061	MH554274	MH554975	–	Liu et al. (2019)
	CBS 642.97	T	Chile	<i>Gevuina avellana</i>	MH554041	MH554254	MH554952	–	Liu et al. (2019)
	CBS 393.80	T	Netherlands	<i>Prunus laurocerasus</i>	MH554070	MH554281	MH554982	–	Liu et al. (2019)
	CBS 938.70	T	–	<i>Prunus sp.</i>	MH554036	MH554253	MH554949	–	Liu et al. (2019)
	CBS 356.33	NT	France	<i>Vitis vinifera</i> cv. 'Prunelard'	MH554112	MH554318	MH555021	–	Liu et al. (2019)
	CBS 144025	T	Netherlands	<i>Lupinus sp.</i>	MH554033	MH554250	MH554945	–	Liu et al. (2019)
	CBS 338.32	T	–	<i>Prunus armeniaca</i>	MH554010	MH554231	–	–	Liu et al. (2019)
	CBS 165.25	T	Sweden	<i>Salix caprea</i>	MH553971	MH554190	MH554865	–	Liu et al. (2019)
	CBS 113991	T	Finland	<i>Skin of man</i>	NR_155804	NG_05681	MH554950	–	Liu et al. (2019)
	CBS 387.77	T	Germany	<i>Quercus robur</i>	MH553997	MH554216	MH554906	–	Liu et al. (2029)
	MFLUCC 14-1198	T	–	<i>Rhododendron</i> sp.	–	–	–	–	–
	CBS 129171	T	–	–	–	–	–	–	–

¹ BRIP: Queensland Plant Pathology Herbarium, Australia; CBS: Culture collection of the Westerdijk Fungal Biodiversity Institute, Utrecht, The Netherlands; CFC: China Forestry Culture Collection Center, China; CMW: Culture Collection of the Forestry and Agricultural Biotechnology Institute (FABI), University of Pretoria, Pretoria, South Africa; CPC: Culture collection of Pedro Crous, housed at the Westerdijk Institute; HGUP: Plant Pathology Herbarium of Guizhou University; HHUF: herbarium of Hiroshima University; HKUCC: The University of Hong Kong Culture Collection; HPC: Herbarium of Pedro Crous, housed at the Westerdijk Institute; ICMP: International Collection of Micro-organisms from Plants, Landcare Research, Private Bag 9210, Auckland, New Zealand; IFRDCC: International Fungal Research and Development Culture Collection; IMI: International Mycological Institute, CABI-Bioscience, Egham, Berkshire Lane, United Kingdom; LC: working collection of Lei Cai, housed at the Institute of Microbiology, Chinese Academy of Sciences, Beijing, China; MAFF: Ministry of Agriculture, Forestry and Fisheries, Tsukuba, Ibaraki, Japan; MEAN: culture collection of INIAV Institute, Oeiras, Portugal; MFLUCC: Mae Fah Luang University Culture Collection; NOF: The Fungi Culture Collection of the Northern Foresty Centre, Alberta, Canada; MSCL: Microbial Strain Collection of Latvia; NBRC: Biological Resource Center, NTU: National Taiwan University Culture Collection, Taiwan; UPSC: Uppsala University Culture Collection of Fungi, Sweden; VPR: Victorian Plant Disease Herbarium, Australia.

² Status: status of the strains. ET: ex-epitype; IT: ex-isotype; NT: ex-neotype; R: reference strain; ST: ex-synonym. T: ex-type.

³ MFLUCC 15-0563: Type of *Seimatosporium rosgenii*; MFLUCC 14-0466: Type of *Seimatosporium pseudosorosum*.

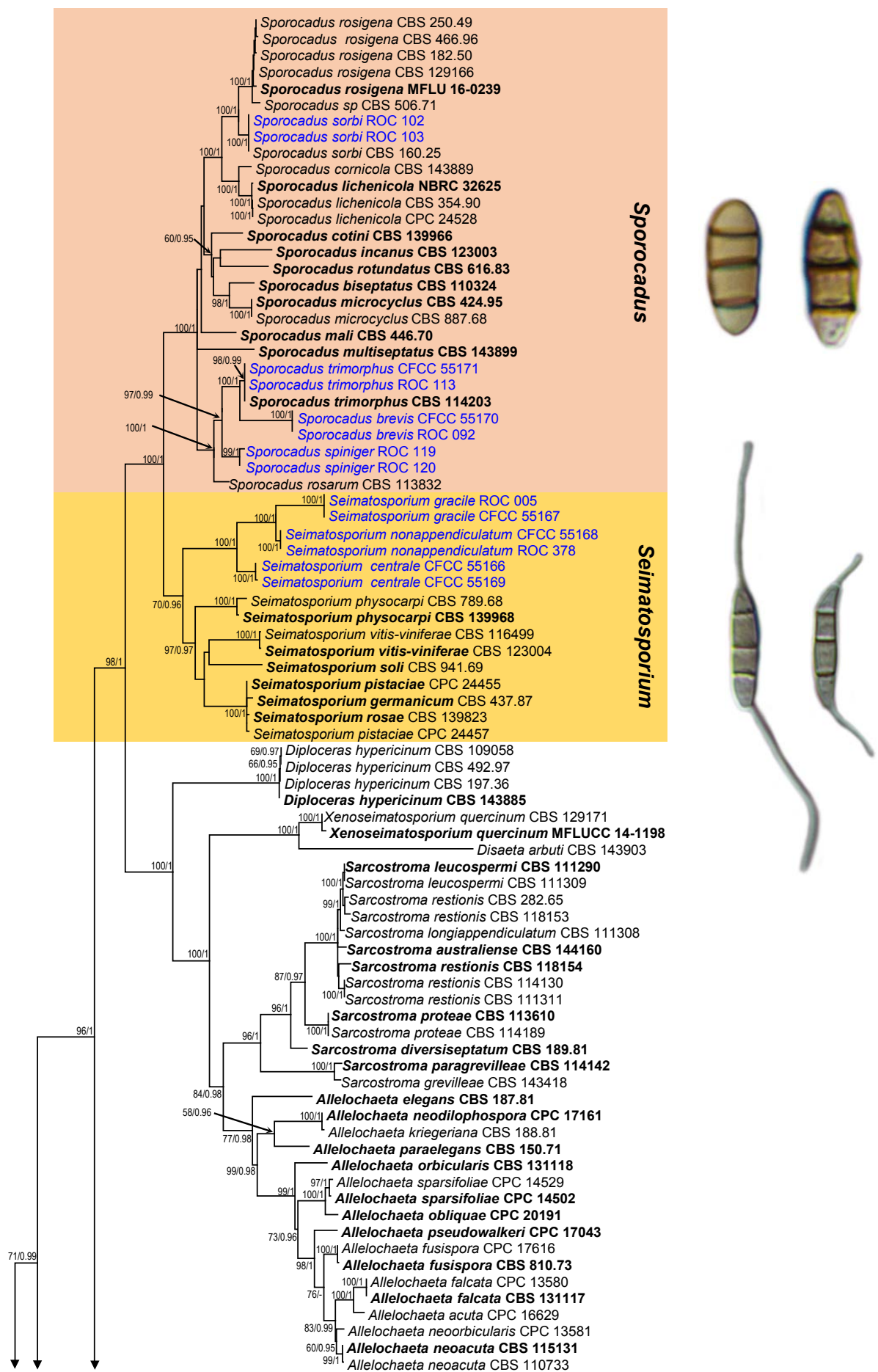


Fig. 2 Phylogenetic tree of Sporocadaceae (50 % majority rule consensus) based on maximum likelihood (ML) analysis of the combined LSU, ITS and RPB2 sequence alignment. Nodes are labelled with bootstrap values from RAxML/Bayesian posterior probabilities. Nodes receiving below 50 bootstrap values and 0.5 probability values are not labelled. The scale bar represents the expected number of changes per site. Genera in this study are delimited in coloured boxes and isolates collected in this study are in **bold**. Ex-type strains are represented in **bold**.

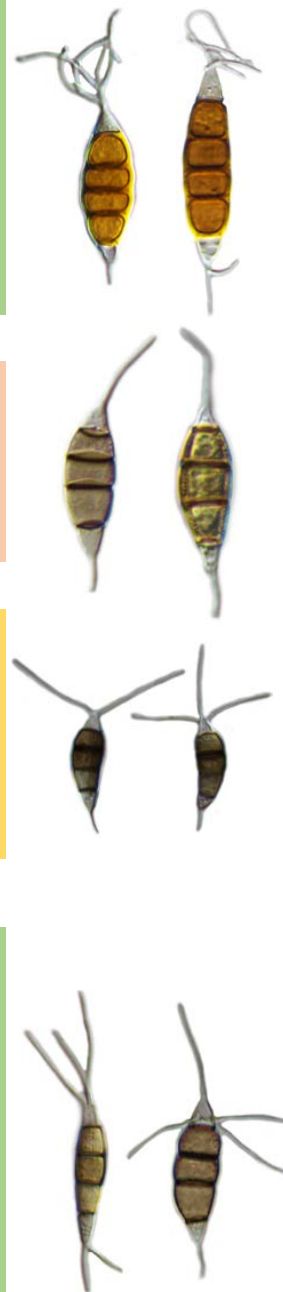
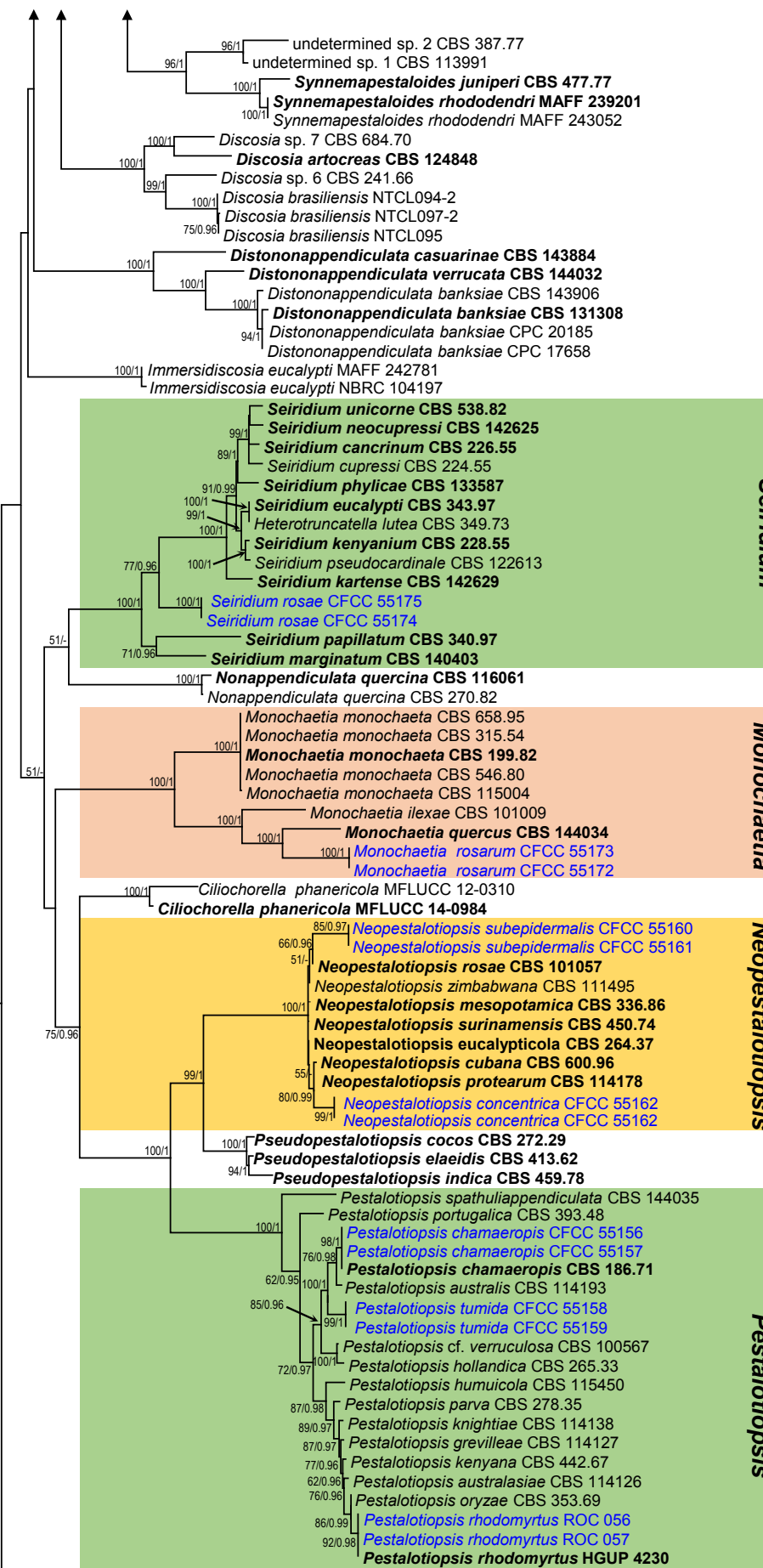
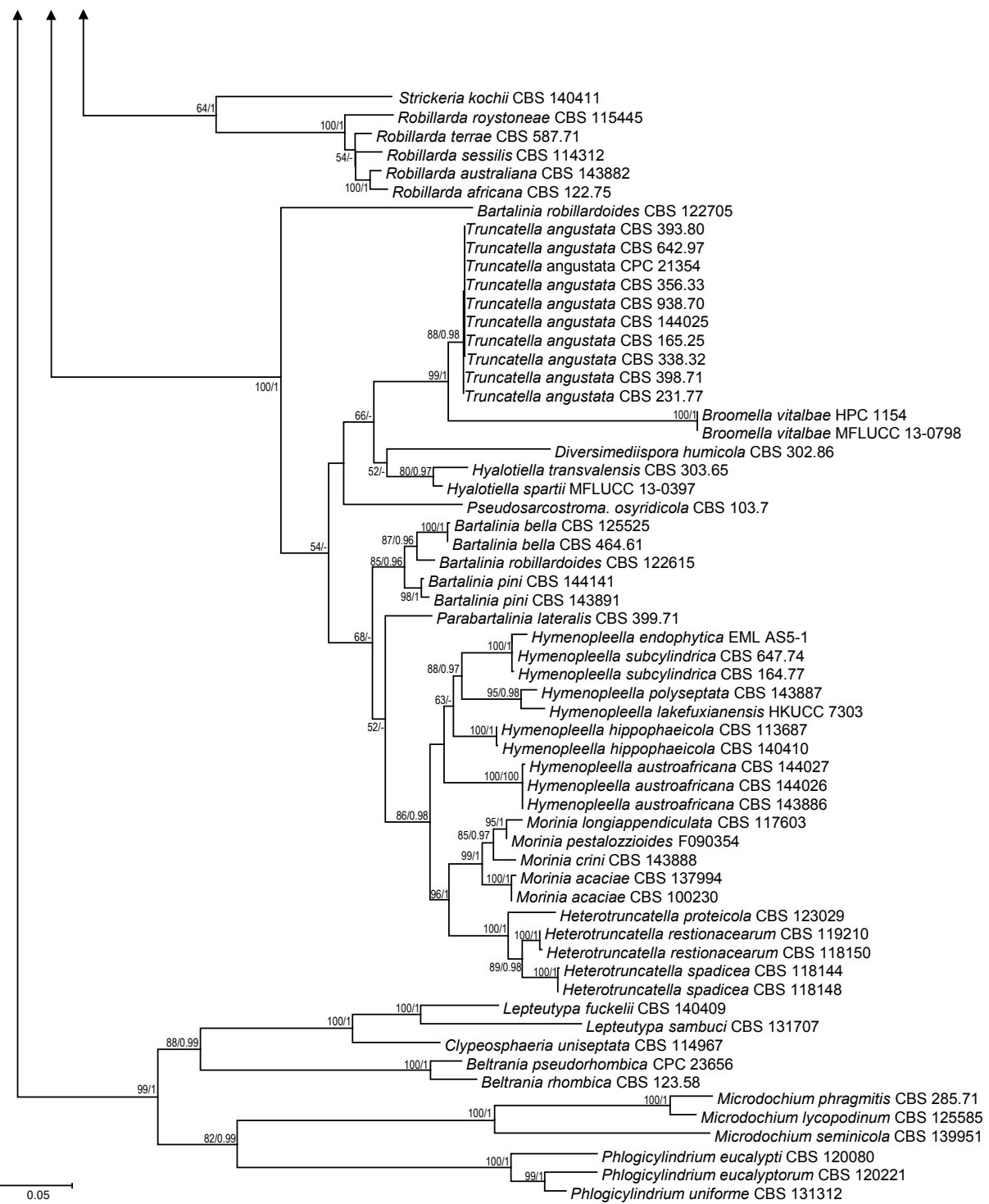


Fig. 2 (cont.)

**Fig. 2** (cont.)

and Maximum-parsimony bootstrap values (MPBP) equal or greater than 50 % are provided for each tree. Bayesian posterior probabilities (BYPP) > 0.90 are indicated as thickened lines.

Prevalence

To determine the prevalence of Sporocadaceae genera and species on *Rosa* spp. and plant parts (branches, fruits, leaves or spines), the Isolation Rate (RI) was calculated for each species with the formula: RI % = (NS / NI) × 100, where NS was the number of isolates from the same genera or species, and NI was the total number of isolates from each *Rosa* sp. or plant part. The overall RI was calculated using the NI value equal to the total number of isolates obtained from *Rosa* plants (Vieira et al. 2014, Fu et al. 2019, Guo et al. 2020).

RESULTS

Phylogenetic analyses

The concatenated DNA sequence dataset (ITS, LSU and RPB2) was used to infer delimitation at the family level. The concatenated alignment had a total length of 2419 characters including alignment gaps (659 for ITS, 890 for LSU and 832 for RPB2). Of these, 1401 characters were constant, 144 variable characters were parsimony-uninformative and 874 characters were parsimony informative. The ML search resolved a best tree with an lnL of -36418.696700. The BA lasted for 1855 000 generations and the 50 % consensus tree and posterior probabilities were calculated from 2784 trees from two runs. The ML tree confirmed the same tree topology and the clades as those presented in the Bayesian phylogeny (Fig. 2).

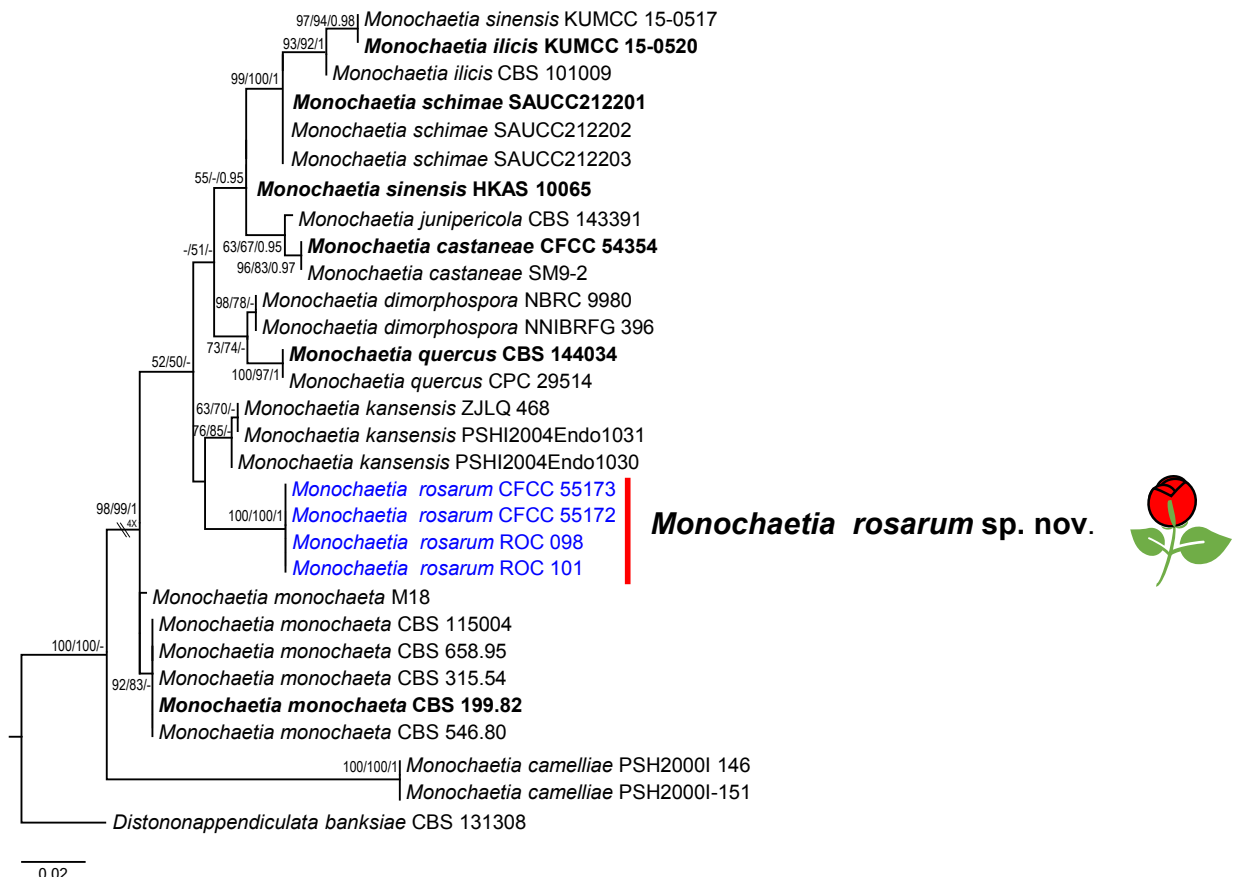


Fig. 3 Phylogenetic tree of *Monochaetia* resulting from maximum likelihood (ML) analysis of the ITS sequence alignment. Nodes are labelled with bootstrap values from RAxML/Parsimony bootstrap/Bayesian posterior probabilities values. Nodes receiving below 50 bootstrap values and 0.5 probability values are not labelled. The scale bar represents the expected number of changes per site. Ex-type strains are represented in **bold**; strains obtained in the current study in blue. The flower symbol represents species that have been recorded from *Rosa*.

Following alignment of *Monochaetia*, the ITS sequence data with a total of 599 characters including gaps, of which 496 characters were constant, 15 variable characters were parsimony uninformative, and 88 characters were variable and parsimony informative. The parsimony analysis resulted in 1000 equally parsimonious trees, one of which is in Fig. 3 (CI = 0.780, RI = 0.887, RC = 0.692, HI = 0.220). The topology of the phylogenetic trees generated from the MP, ML and BA methods were congruent.

In the phylogenetic tree constructed for *Neopestalotiopsis* and *Pestalotiopsis*, sequences of the combined ITS, TEF and TUB were aligned. In *Neopestalotiopsis*, the alignment comprises 2263 characters including alignment gaps after alignment (580 for ITS, 592 for TEF and 787 for TUB). Of these, 1647 characters were constant, 383 variable characters were parsimony-uninformative and 233 characters were parsimony informative. The MP analysis resulted in a single equally most parsimonious tree (CI = 0.672, RI = 0.659, RC = 0.442, HI = 0.328). In *Pestalotiopsis*, the alignment comprises 2183 characters including alignment gaps after alignment (590 for ITS, 670 for TEF and 909 for TUB), of which 1165 characters were constant, 384 variable characters were parsimony-uninformative and 634 characters were parsimony informative. The MP analysis resulted in a single equally most parsimonious tree (CI = 0.565, RI = 0.845, RC = 0.478, HI = 0.435). MP was similar to the topology from ML and BA (Fig. 4, 5).

In *Seimatosporium*, the combined ITS + LSU dataset had an aligned length of 1495 characters in the dataset (601 for ITS and 887 for LSU), of which 1181 characters are constant, 118 are variable and parsimony-uninformative, and 196 are parsimony informative. Maximum Parsimony analysis yielded 750 equally parsimonious trees (CI = 0.674, RI = 0.738, RC = 0.497, HI = 0.326), and a strict consensus tree is shown in Fig. 6.

In *Seiridium*, the combined ITS, RPB2, TEF and TUB dataset consists of 2897 characters including alignment gaps (598 for ITS, 818 for RPB2, 606 for TEF and 829 for TUB), of which 1637 are constant, 454 are variable parsimony uninformative characters and 806 are parsimony-informative characters. The MP analysis resulted in a single equally most parsimonious tree (CI = 0.664, RI = 0.689, RC = 0.457, HI = 0.336) (Fig. 7).

In *Sporocadus*, the combined sequences of ITS, LSU, RPB2, TEF and TUB were aligned. The combined data comprises 3619 characters including alignment gaps (566 for ITS, 900 for LSU, 869 for RPB2, 496 for TEF and 760 for TUB). Of these, 2671 characters were constant, 263 variable characters were parsimony-uninformative and 685 characters were parsimony informative. The MP analysis resulted in a single equally most parsimonious tree (CI = 0.657, RI = 0.808, RC = 0.531, HI = 0.343) (Fig. 8).

All the MP analyses resulted in a tree with the same topology and terminal clades as the ML and BA trees. The new species from the present study appeared in distinct clades with high bootstrap support.

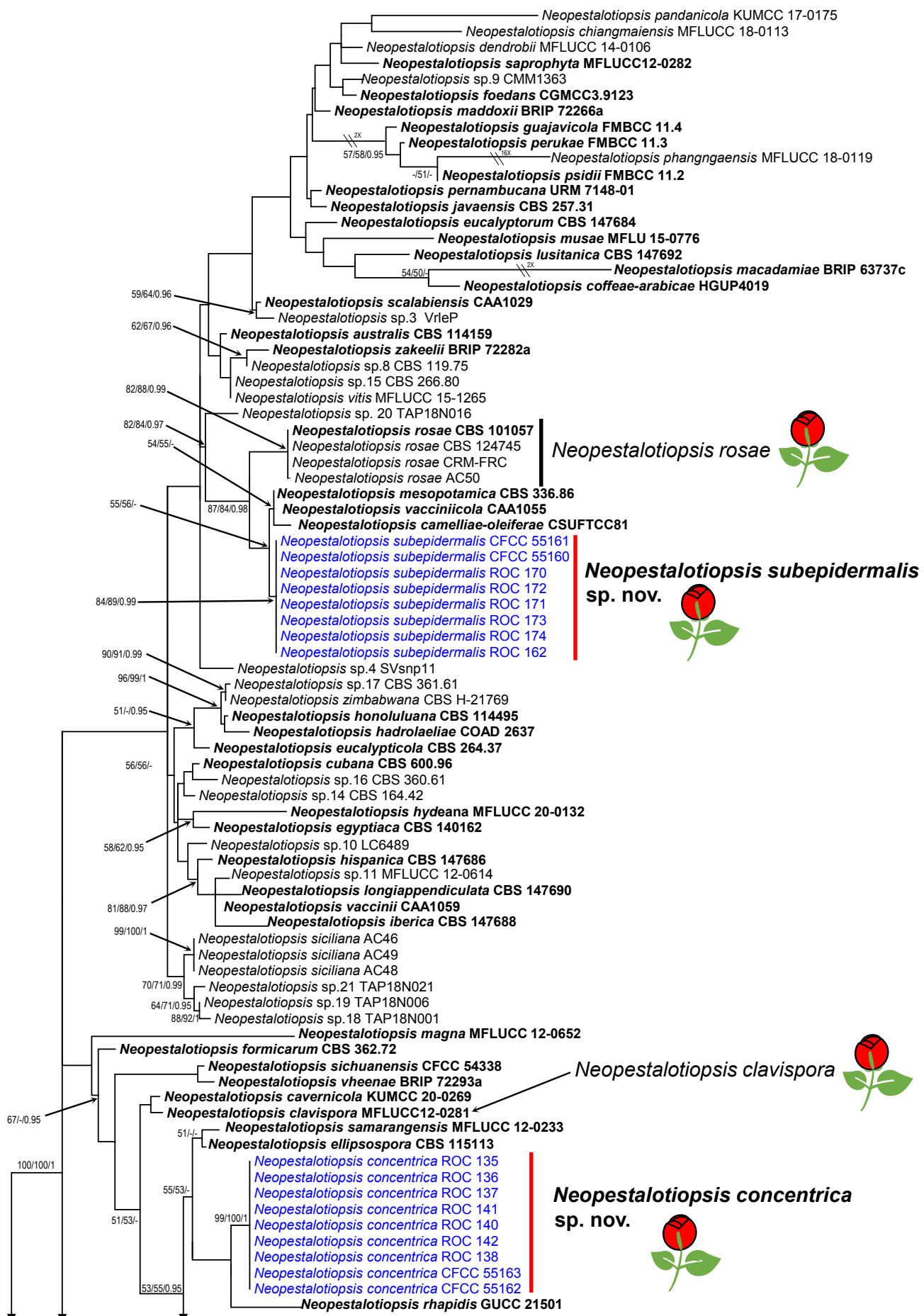


Fig. 4 The best Maximum Likelihood tree from the multi-gene alignment (ITS, TUB and TEF) for the *Neopestalotiopsis*. Nodes are labelled with bootstrap values from RAxML/Parsimony/bootstrap/Bayesian posterior probabilities values. Nodes receiving below 50 bootstrap values and 0.5 probability values are not labelled. The scale bar represents the expected number of changes per site. Ex-type strains are represented in **bold**; strains obtained in the current study in blue. The flower symbol represents species that have been recorded from *Rosa*.

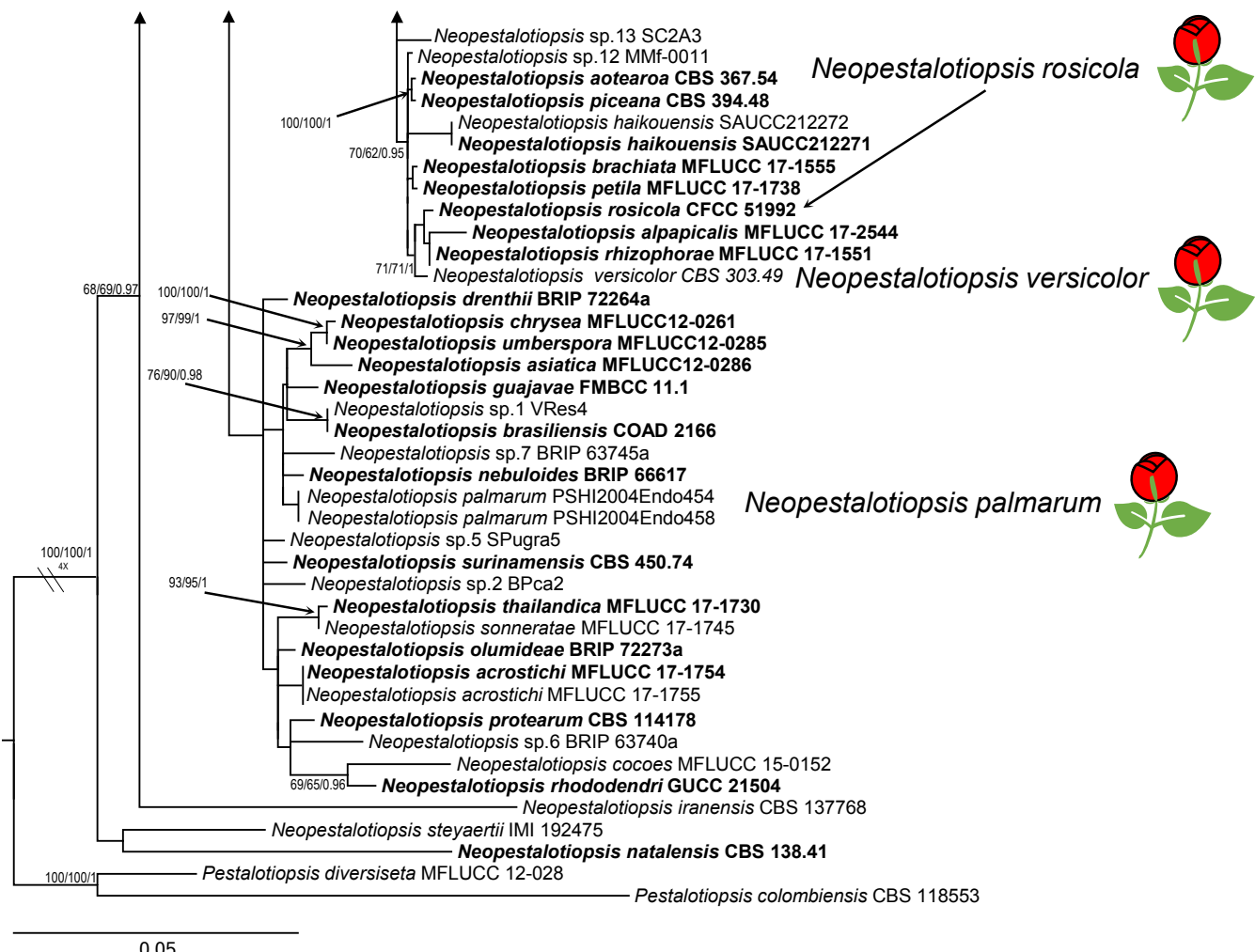


Fig. 4 (cont.)

Taxonomy

Based on the morphology and multi-locus phylogeny, 126 isolates were assigned to 15 species belonging to six genera in Sporocadaceae, including 11 species newly described below.

Monochaetia rosarum C. Peng & C.M. Tian, sp. nov. — MycoBank MB 843811; Fig. 9

Etymology. The species epithet reflects the name of the host plant genus *Rosa*.

Typus. CHINA, Henan Province, Nanyang City, Neixiang county, Baotianman Nature Reserve, N33°29'29" E111°55'50", alt. 1311 m, on branches of *R. chinensis*, 7 Aug. 2020, C.M. Tian, Y.M. Liang & C. Peng (holotype BJFC-S1877, ex-type culture CFCC 55172 = ROC 099).

Symptoms appeared as circular to irregular, red or dark brown and raised, dehiscent lesions on twigs and branches (Fig. 9b–c). Sexual morph not observed. Asexual morph: *Acervular conidiomata* visible on the host, globose or irregular, superficial to semi-immersed, scattered or aggregated, black or red, 76–118 µm diam. *Conidiophores* septate and branched, hyaline, smooth-walled or verruculose. *Conidiogenous cells* annellidic, discrete or integrated, cylindrical, subcylindrical, hyaline or pale brown, smooth, 6.5–14(–15) × (1–)1.5–2 µm (av. = 10.7 ± 2.84 × 1.7 ± 0.26 µm). *Conidia* fusoid, straight or slightly curved, 4-septate, wall smooth, not constricted at the septa, (17.5–)18–20(–21) × 5–6(–7) µm (av. = 19.5 ± 0.95 × 5.4 ± 0.37 µm); basal cell obconic with or without truncate base, thin-walled, hyaline, 2.5–3(–3.5) µm (av. = 2.6 ± 0.27 µm) long; three median cells,

doliiform or subcylindrical, mid-brown, thick-walled, the first median cell from base (3–)3.5–5 µm (av. = 4.2 ± 0.42 µm) long, the second cell (2.5–)3–3.5(–4.5) µm (av. = 3.4 ± 0.27 µm) long, the third cell (3–)3.5–4(–5) µm (av. = 3.7 ± 0.36 µm) long, together (10.5–)11.5–12.5(–13) µm (av. = 12.1 ± 0.47 µm) long; apical cell conic with an acute apex, thin-walled, hyaline, 2–2.5(–3) µm (av. = 2.4 ± 0.31 µm) long; apical appendage single, tubular, attenuated, unbranched, variously bent; (8–)9–12(–12.5) µm (av. = 10.8 ± 1.36 µm) long; basal appendage single, unbranched, centric, 4.5–6(–6.5) µm (av. = 5.5 ± 0.48 µm); mean conidium length/width ratio = 3.25 : 1.

Culture characteristics — On PDA, colonies slowly growing, up to 10 mm diam after 3 d and reaching 38–40 mm after 15 d, white to pale grey with a uniform texture, with an irregular margin, lacking aerial mycelium, becoming greyish and yellowish after 30 d, reverse yellowish brown. Conidiomata globose, distributed irregularly on the medium surface, exuding globose, dark brown to black conidial masses.

Additional materials examined. CHINA, Henan Province, Nanyang City, Neixiang county, Baotianman Nature Reserve, N33°29'68" E111°55'16", alt. 1329 m, on branches of *R. chinensis*, 7 Aug. 2020, C.M. Tian, Y.M. Liang & C. Peng (BJFC-S1878, cultures CFCC 55173 = ROC 100, ROC 98, ROC 101).

Notes — *Monochaetia rosarum* forms an independent clade and is phylogenetically distinct from *M. kansensis* (Fig. 3). *Monochaetia rosarum* can be distinguished from *M. kansensis* in ITS loci by 13 bp differences (from 561 characters, with 97.6 % sequence identity, including 3 bp gaps). In addition, *M. rosarum* differs from *M. kansensis* in producing thinner conidia (5–6 µm

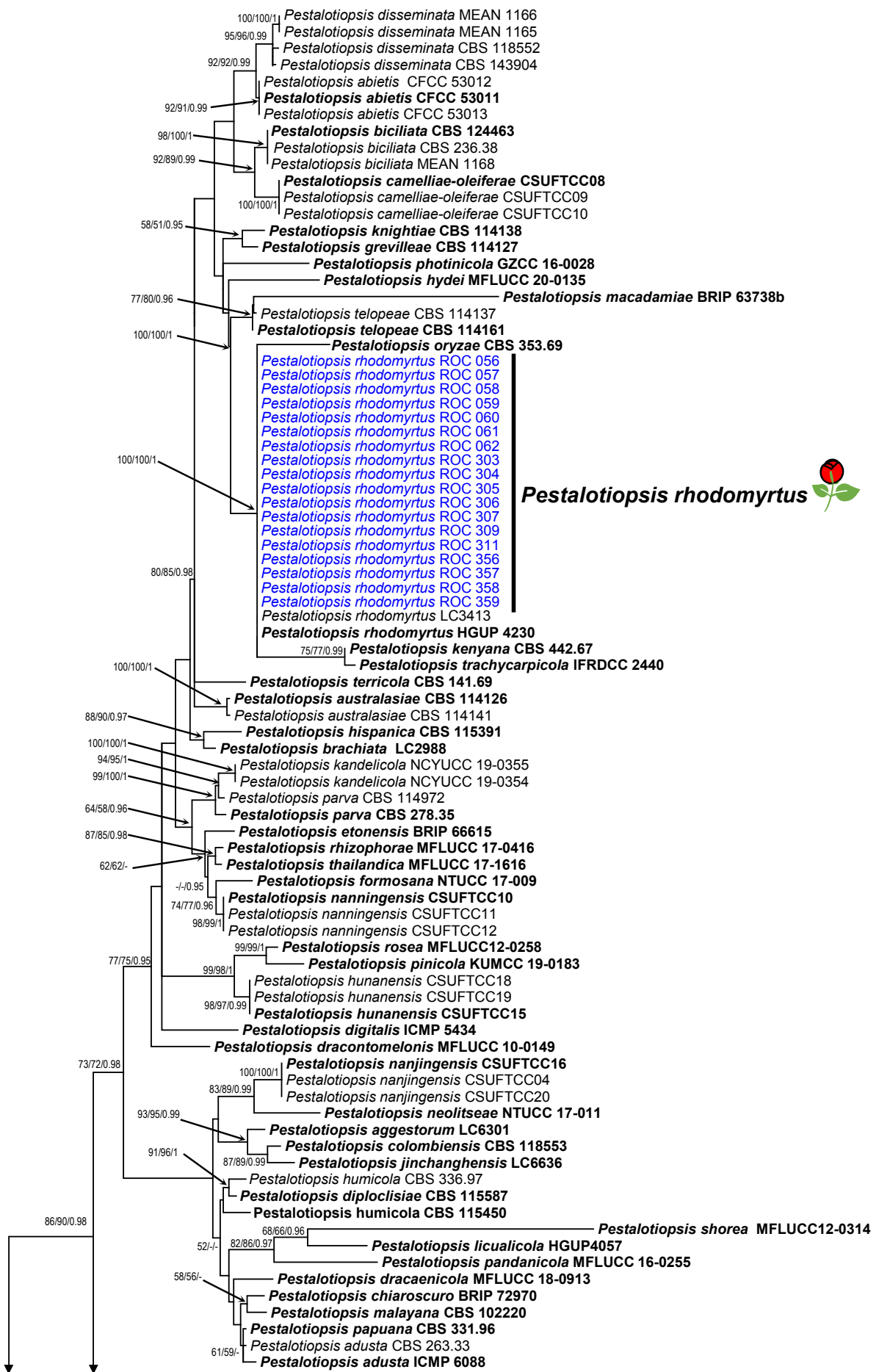


Fig. 5 The best Maximum Likelihood tree from the multi-gene alignment (ITS, TUB and TEF) for the Pestalotiopsis. Nodes are labelled with bootstrap values from RAxML/Parsimony bootstrap/Bayesian posterior probabilities values. Nodes receiving below 50 bootstrap values and 0.5 probability values are not labelled. The scale bar represents the expected number of changes per site. Ex-type strains are represented in bold; strains obtained in the current study in blue. The flower symbol represents species that have been recorded from Rosa.

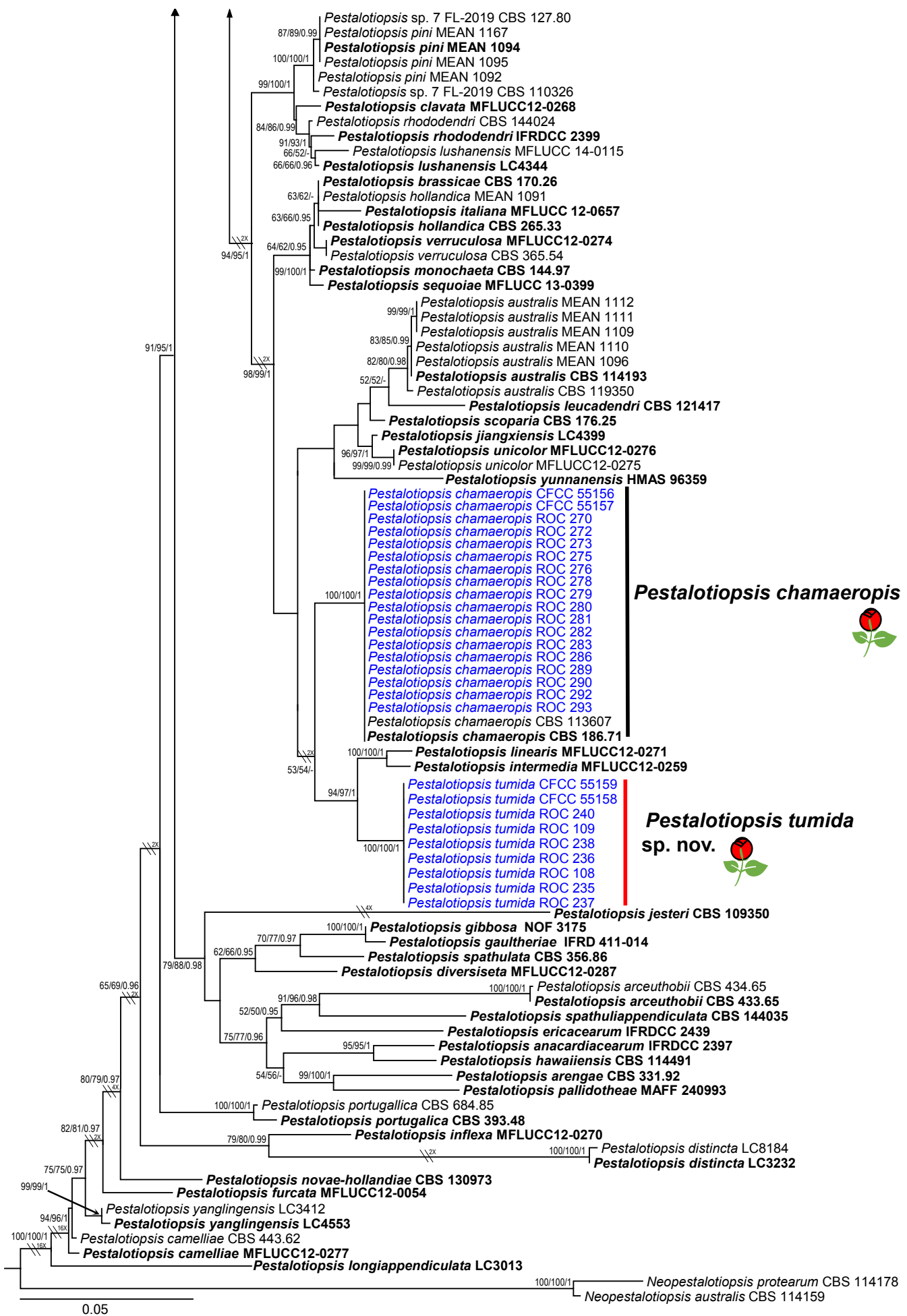


Fig. 5 (cont.)

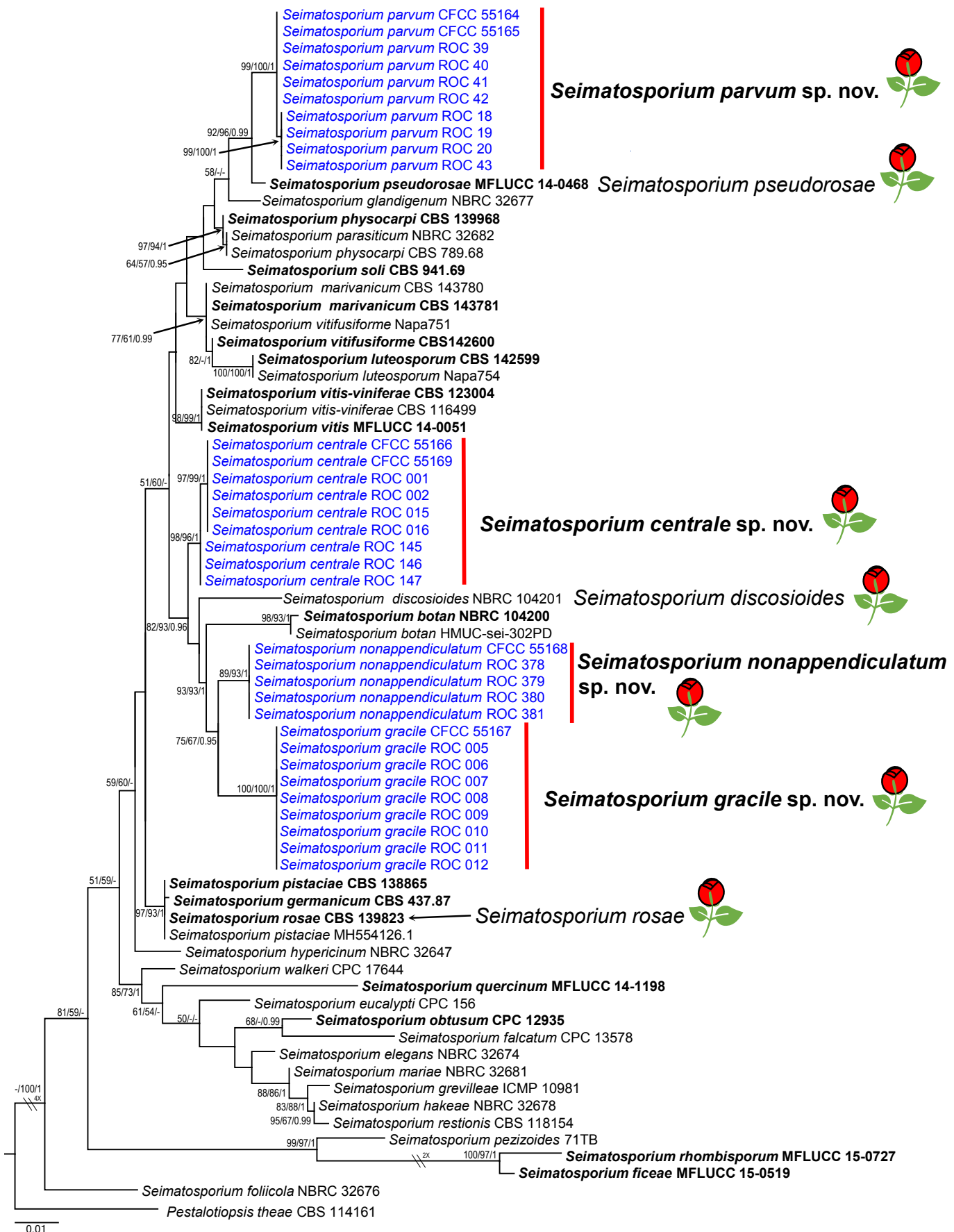


Fig. 6 The best Maximum Likelihood tree from the multi-gene alignment (ITS and LSU) for the *Seimatosporium*. Nodes are labelled with bootstrap values from RAxML/Parsimony/bootstrap/Bayesian posterior probabilities values. Nodes receiving below 50 bootstrap values and 0.5 probability values are not labelled. The scale bar represents the expected number of changes per site. Ex-type strains are represented in **bold**; strains obtained in the current study in blue. The flower symbol represents species that have been recorded from *Rosa*.

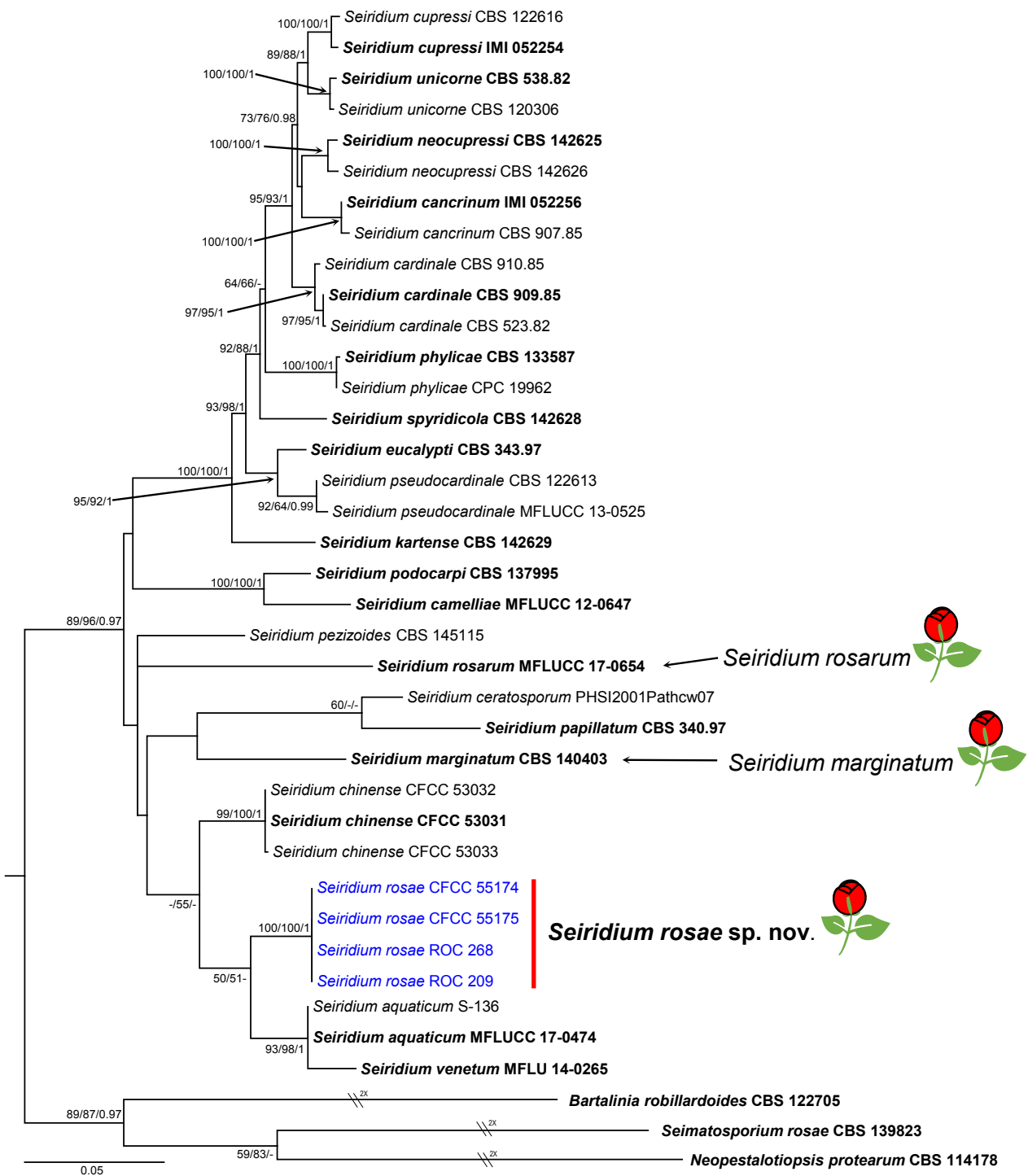


Fig. 7 The best Maximum Likelihood tree from the multi-gene alignment (ITS, *RPB2*, *TEF* and *TUB*) for the *Seiridium*. Nodes are labelled with bootstrap values from RAxML/Parsimony/bootstrap/Bayesian posterior probabilities values. Nodes receiving below 50 bootstrap values and 0.5 probability values are not labelled. The scale bar represents the expected number of changes per site. Ex-type strains are represented in **bold**; strains obtained in the current study in blue. The flower symbol represents species that have been recorded from *Rosa*.

vs 6–8 µm). Furthermore, the apical and basal appendages of *M. rosarium* are significantly shorter than those of *M. kansensis* (9–12 µm vs 15–26 µm and 4.5–6 µm vs 10–38 µm).

Four *Monochaetia* species have been reported from *Rosa* spp., i.e., *M. concentrica*, *M. rosae-caninae*, *M. seiridioides* and *M. turgida* (Guba 1961, Tai 1979, Nag Raj 1993, Chen 2003). These four species are easily distinguishable from our new species based on conidial dimensions. *Monochaetia concentrica* and *M. seiridioides* have longer conidia than *M. rosarium* (20–26 µm vs 18–20 µm and 26–28 µm vs 18–20 µm). *Monochaetia turgida* has wider conidia than *M. rosarium* (7.6–8.3 µm vs 5–6 µm).

Although *M. rosarium* and *M. rosae-caninae* have similar conidial width (5–6 µm vs 5–7 µm), the conidia of *M. rosarium* is significantly longer than those of *M. rosae-caninae* (18–20 µm vs 16–18 µm). In addition, *M. rosarium* is similar to *M. camelliae* in conidial dimensions (18–20 × 5–6 µm vs 18–20 × 4–7 µm), the latter having been previously reported from *Camellia*, *Eucalyptus* and *Peltophorum*. However, based on the combined gene phylogenetic analysis, *M. rosarium* is separated from *M. camelliae* and the apical appendages of *M. rosarium* are shorter than those of *M. camelliae* (9–12 µm vs 12–14 µm).

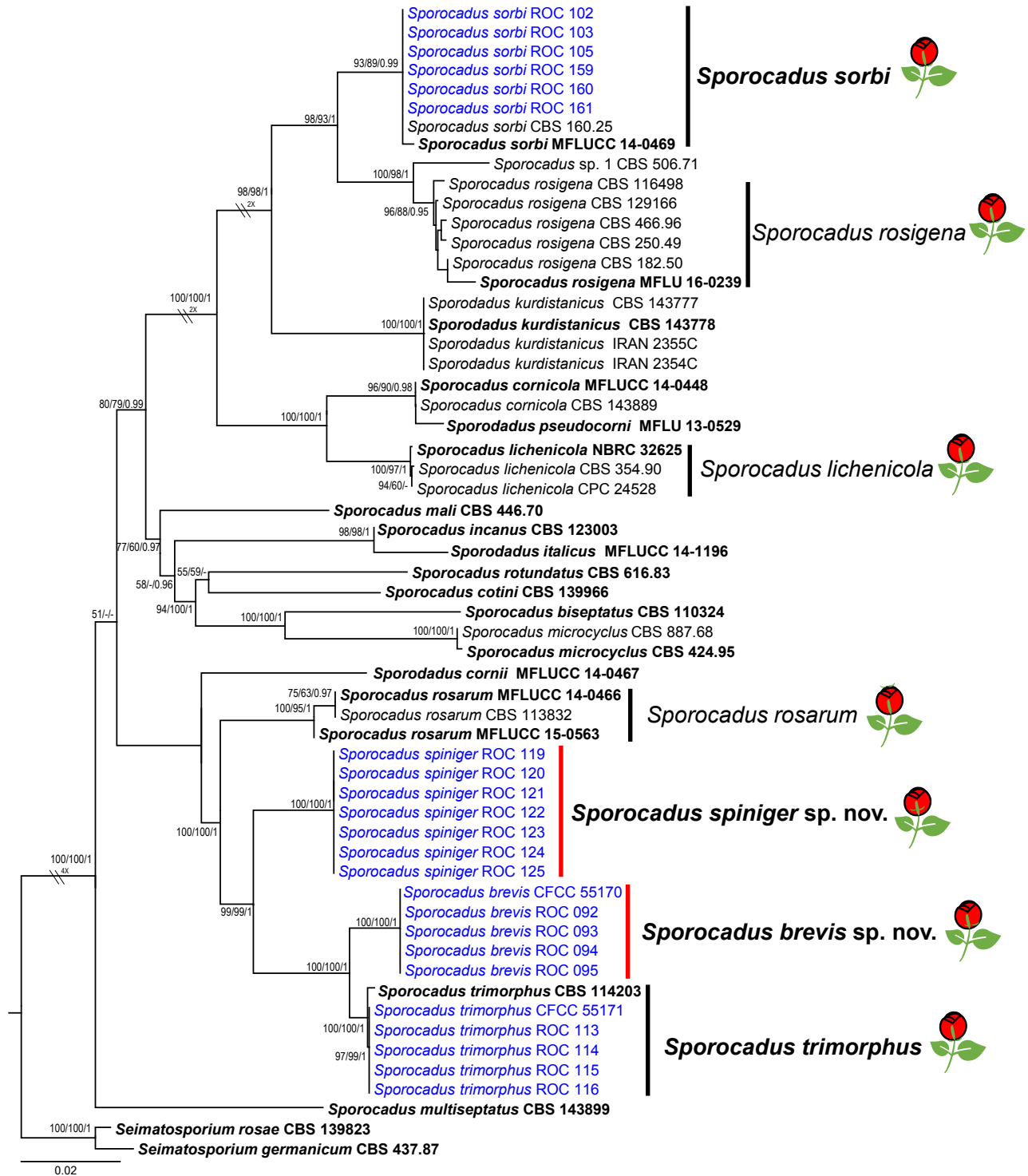


Fig. 8 The best Maximum Likelihood tree from the multi-gene alignment (ITS, LSU, RPB2, TEF and TUB) for the *Sporocadus*. Nodes are labelled with bootstrap values from RAxML/Parsimony bootstrap/Bayesian posterior probabilities values. Nodes receiving below 50 bootstrap values and 0.5 probability values are not labelled. The scale bar represents the expected number of changes per site. Ex-type strains are represented in bold; strains obtained in the current study in blue. The flower symbol represents species that have been recorded from *Rosa*.

Key to *Monochaetia* species on *Rosa* spp.

- Conidial length more than 20 µm 2
- Conidial length less than 20 µm 3
- Conidia 20–26 × 6.5–8.5 µm, apical appendage 15 µm long *M. concentrica*
- Conidia 26–28 × 6–7 µm, apical appendage 12 µm long *M. seiridioides*
- Conidial width more than 8 µm *M. turgida*
- Conidial width less than 8 µm 4
- Conidia 16–18 × 5–7 µm *M. rosae-caninae*
- Conidia 18–20 × 5–6 µm *M. rosarum*

***Neopestalotiopsis concentrica* C. Peng & C.M. Tian, sp. nov.**
— MycoBank MB 843813; Fig. 10

Etymology. Name refers to the concentric circles formed by colonies on PDA.

Typus. CHINA, Henan Province, Xinyang City, Jigong Mountain, N31°49'3" E114°4'33", alt. 717 m, on spines of *R. rugosa*, 6 Aug. 2020, C. Peng & S. Jia (holotype BJFC-S1882, ex-type culture CFCC 55162 = ROC 053).

Sexual morph not observed. Asexual morph: *Acervular conidiomata* globose or irregular, superficial to semi-immersed, scattered or aggregated, visible as black acervuli on the host, 93–117 µm diam. *Conidiophores* often reduced to conidiogenous



Fig. 9 *Monochaetia rosarum* (BJFC-S1877, holotype). a. Disease symptoms; b–c. habit of conidiomata on branch; d. colonies on PDA at 3 d (left) and 15 d (right); e. longitudinal section through conidioma; f. conidiomata on PDA; g–i. conidiogenous cells with attached conidia; k. conidia. — Scale bars: b–c, e = 50 µm; f = 200 µm; g–k = 10 µm.

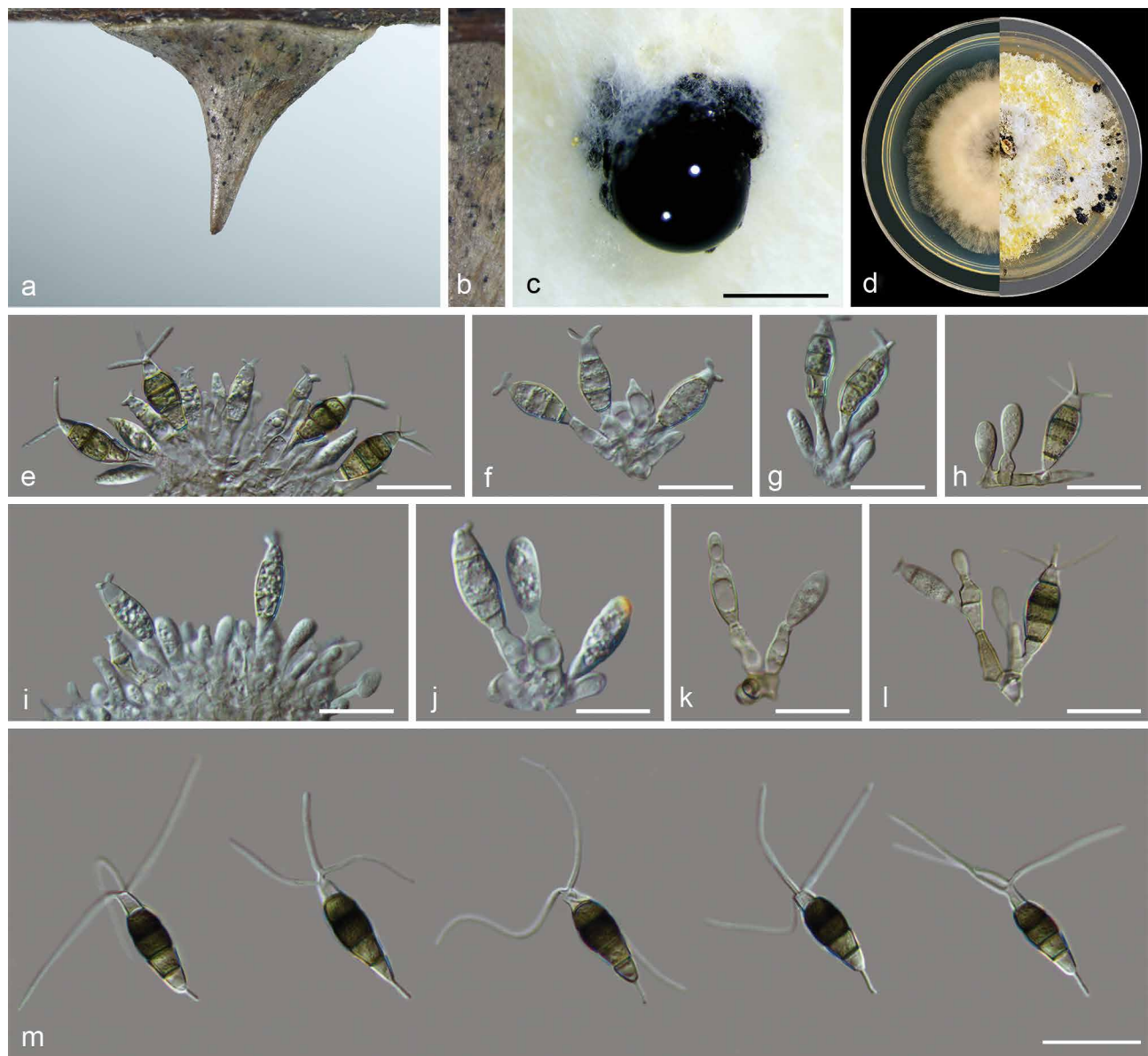


Fig. 10 *Neopestalotiopsis concentrica* (BJFC-S1882, holotype). a–b. Appearance of conidiomata on host substrate; c. conidioma on PDA; d. colonies on PDA at 3 d (left) and 15 d (right); e–l. conidiogenous cells with attached conidia; m. conidia. — Scale bars: c = 200 µm; e–l = 10 µm.

cells. *Conidiogenous cells* discrete, ampulliform or irregular, variable in size, (3–)3.5–14.5(–15) × 3–5(–5.5) µm (av. = 7.8 ± 4.96 × 4.0 ± 1.21 µm), hyaline to subhyaline. *Conidia* fusoid, ellipsoid, straight to slightly curved, 4-septate, 14–18.5(–19) × 4.5–5(–6) µm (av. = 15.7 ± 1.06 × 4.9 ± 0.69 µm); basal cell conic to obconic with a truncate base, hyaline and thin-walled, 3–3.5(–4.0) µm (av. = 4.3 ± 0.21 µm) long; three median cells doliform, (9–)9.5–10.5(–11) µm (av. = 10.0 ± 0.96 µm) long, wall rugose, versicoloured, septa darker than the rest of the cell, second cell from the base pale brown, 3–3.5 µm (av. = 3.3 ± 0.28 µm) long; third cell honey brown, 3–4 µm (av. = 3.74 ± 0.44 µm) long; fourth cell brown, 3–3.5 µm (av. = 3.1 ± 0.31 µm) long; apical cell (2.5–)3–3.5(–4) µm (av. = 3.4 ± 0.86 µm) long, hyaline, cylindrical, thin- and smooth-walled; with 2–3 tubular apical appendages (mostly three), branched or unbranched, filiform, 19–26(–26.5) µm (av. = 22.6 ± 2.14 µm) long; basal appendage single, tubular, unbranched, centric, (3–)3.5–5.5(–6.0) µm (av. = 4.1 ± 0.95 µm) long.

Culture characteristics — Colony on PDA with flattened mycelium, white, smoke grey in the centre, reverse with smoke grey pigments formed a concentric ring pattern, reaching at 58–62 mm diam in 15 d at 28 °C. Conidiomata globose, irregularly distributed on the medium surface, exuding globose, dark brown to black conidial masses.

Additional materials examined. CHINA, Henan Province, Xinyang City, Jigong Mountain, N31°49'1" E114°4'12", alt. 723 m, on spines of *R. chinensis*, 6 Aug. 2020, C. Peng & S. Jia (BJFC-S1883, living culture CFCC 55163 = ROC 064, ROC 135, ROC 136); Henan Province, Nanyang City, Xinyang City, Shihe District, N31°49'8" E114°3'58", alt. 727 m, on spines of *R. chinensis*, 6 Aug. 2020, C. Peng & S. Jia (BJFC-S1884, cultures ROC 137, ROC 138, ROC 140, ROC 141, ROC 142).

Notes — This species is most closely related to *N. ellipspora*, *N. rhipidis* and *N. samarangensis* (Fig. 4), but distinguished from *N. ellipspora* by 15 bp difference in the concatenated alignment (two in the ITS region (482/484, 99.5 % with no gaps), nine TEF (531/540, 98.3 % with four gaps) and four TUB (436/440, 99.0 % with four gaps)), from *N. rhipidis* by 13 bp difference (six in the ITS region (507/513, 98.8 % with no gaps), three TEF (499/502, 99.4 % with three gaps) and four TUB (743/747, 99.4 % with no gaps)) and from *N. samarangensis* by 12 bp difference (three in the ITS region (481/484, 99.3 % with two gaps), three TEF (537/540, 99.4 % with three gaps) and six TUB (434/440, 98.6 % with no gaps)). Moreover, *N. concentrica* differs from these two species in morphology, namely by having longer apical appendages than *N. ellipspora* (19–26 µm vs 5–12 µm), *N. rhipidis* (19–26 µm vs 11–16 µm) and *N. samarangensis* (19–26 µm vs 12–18 µm). However, its conidia are shorter than those of *N. ellipspora* (14–18.5 µm

vs 19–25 µm), *N. rhipidis* (14–18.5 µm vs 22–25.5 µm) and *N. samarangensis* (14–18.5 µm vs 18–21 µm).

Neopestalotiopsis concentrica is phylogenetically and morphologically distinct from *N. clavispora*, *N. palmarum*, *N. rosae*, *N. rosicola* and *N. versicolor*, which were previously also reported from Rosa (Liu et al. 2010, Feng et al. 2014, Maha-rachchikumbura et al. 2014, Jiang et al. 2018, Vu et al. 2019). Its conidia are smaller than *N. clavispora* (14–18.5 × 4.5–5 µm vs 20–24 × 6.5–8.5 µm), *N. palmarum* (14–18.5 × 4.5–5 µm vs 19–23.6 × 5.6–6.6 µm), *N. rosae* (14–18.5 × 4.5–5 µm vs 22–37 × 7.5–9.5 µm), *N. rosicola* (14–18.5 × 4.5–5 µm vs 20.2–25.5 × 5.5–8 µm) and *N. versicolor* (14–18.5 × 4.5–5 µm vs 21.2–28.3 × 7.1–8.3 µm).

***Neopestalotiopsis subepidermalis* C. Peng & C.M. Tian, sp. nov.** — MycoBank MB 843812; Fig. 11

Etymology. Referring to the conidioma occurring under the epidermis of spines, not breaking through the epidermis.

Typus. CHINA, Henan Province, Xinyang City, Jigong Mountain, N31°49'15" E114°3'31", alt. 163.4 m, on spines of *R. rugosa*, 5 Aug. 2020, C. Peng & S. Jia (holotype BJFC-S1879, ex-type culture CFCC 55160 = ROC 161, ROC 162).

Sexual morph not observed. Asexual morph: *Acervular conidiomata* globose or irregular, superficial to semi-immersed, scattered or aggregated, visible as black acervuli on the host, 80–122 µm diam. *Conidiophores* septate, branched, subcylindrical, hyaline to subhyaline, often reduced to conidiogenous cells. *Conidiogenous cells* discrete, collarette present and not

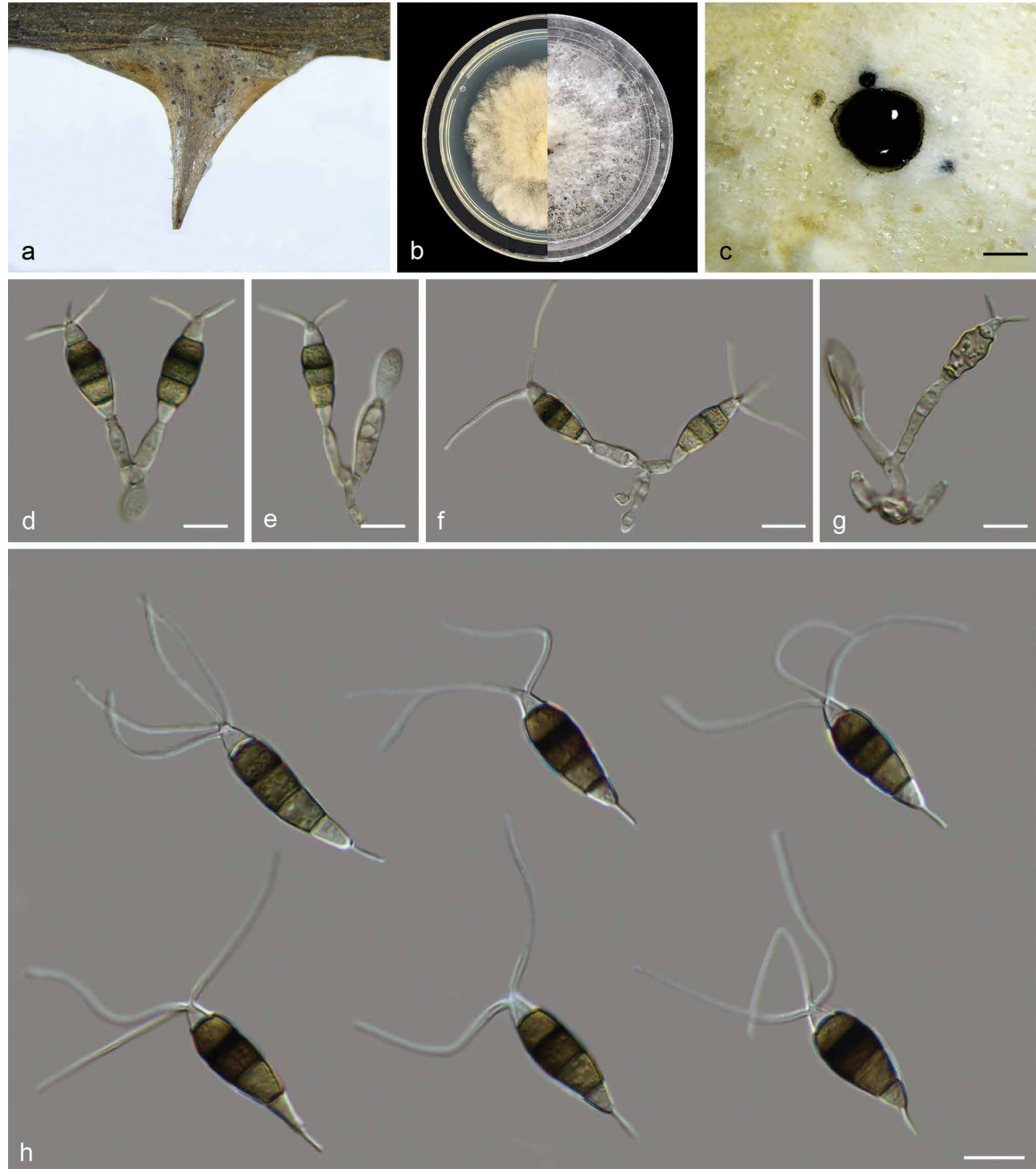


Fig. 11 *Neopestalotiopsis subepidermalis* (BJFC-S1879, holotype). a. Appearance of conidiomata on host substrate; b. colonies on PDA at 3 d (left) and 15 d (right); c. conidiomata on PDA; d–g. conidiogenous cells with attached conidia; h. conidia. — Scale bars: c = 200 µm; d–h = 10 µm.

flared, cylindrical, hyaline to subhyaline, (5.5–)6–18(–18.5) × 3–5 µm (av. = $11.2 \pm 2.90 \times 3.8 \pm 0.60$ µm). Conidia fusoid, ellipsoid, straight to slightly curved, 4-septate, (19.5–)20–25(–26) × 7.5–9(–9.5) µm (av. = $22.6 \pm 2.10 \times 8.4 \pm 0.95$ µm); basal cell conic to obconic with a truncate base, hyaline and thin-walled, 4.0–5.5 µm (av. = 4.6 ± 0.64 µm) long; three median cells doliform, 14–16 µm (av. = 15.0 ± 1.06 µm) long, wall rugose, versicoloured, septa darker than the rest of the cell, second cell from the base pale brown, (4.5–)5–6 µm (av. = 5.7 ± 0.44 µm) long; third cell honey brown, (4.5–)5–6 µm (av. = 5.4 ± 0.36 µm) long; fourth cell brown, (3.5–)4–5 µm (av. = 4.5 ± 0.72 µm) long; apical cell 3–3.5(–4) µm (av. = 3.2 ± 0.27 µm) long, hyaline, cylindrical, thin- and smooth-walled; with 2–4 tubular apical appendages, branched or unbranched, filiform, (26.5–)27–32.5(–33.5) µm (av. = 29.2 ± 1.79 µm) long; basal appendage single, tubular, unbranched, centric, (6.5–)7–7.5(–8) µm (av. = 7.3 ± 0.58 µm) long.

Culture characteristics — Colonies on PDA with aerial mycelium white, fluffy, reverse yellowish pigment accumulation in the centre, surrounded by amber, pure white at the colony margin, reaching at 58–60 mm diam in 15 d at 28 °C. Conidiomata globose, irregularly distributed on the medium surface, exuding globose, dark brown to black conidial masses.

Additional materials examined. CHINA, Henan Province, Xinyang City, Jigong Mounta, N31°49'20" E114°32'6", alt. 220.1 m, on spines of *R. chinensis*, 5 Aug. 2020, C. Peng & S. Jia (BJFC-S1880, cultures CFCC 55161 = ROC 169, ROC 170); Henan Province, Xinyang City, Shihe District, N31°49'23" E114°3'24", alt. 199.6 m, on branches and spines of *R. chinensis*, 5 Aug. 2020, C. Peng & S. Jia (BJFC-S1881, cultures ROC 171, ROC 172, ROC 173, ROC 174).

Notes — The eight strains of *N. subepidermalis* in the present study form a well-supported independent clade distinct from known *Neopestalotiopsis* species (ML/MP/BI = 87/84/0.98). *Neopestalotiopsis subepidermalis* is most closely related to *N. camelliae-oleiferae*, *N. mesopotamica*, *N. rosae* and *N. vacciniicola* (Fig. 4), but differs from them in concatenated alignment. A comparison of the ITS region showed one nucleotide difference (453/454, 99.7 % with two gaps) with *N. camelliae-oleiferae*, three nucleotide differences (526/529, 99.4 % with a single gap) with *N. mesopotamica*, two nucleotide differences (524/526, 99.6 % with no gaps) with *N. rosae*, one nucleotide differences (519/520, 99.8 % with a single gap) with *N. vacciniicola*. Comparison of the TEF region revealed 15 bp differences (520/535, 97.1 % with no gaps) with *N. camelliae-oleiferae*, three bp differences (469/472, 99.5 % with no gaps) with *N. mesopotamica*, two bp differences (479/481, 99.5 % with no gaps) with *N. rosae*, 13 bp differences (462/475, 97.2 % with no gaps) with *N. vacciniicola*. Comparison of the TUB region revealed two bp differences (400/402, 99.5 % with no gaps) with *N. camelliae-oleiferae*, eight bp differences (723/731, 98.9 % with no gaps) with *N. mesopotamica*, 11 bp differences (736/747, 98.5 % with no gaps) with *N. rosae*, seven bp differences (412/419, 98.3 % with no gaps) with *N. vacciniicola*. *Neopestalotiopsis rosae* was also recorded from *Rosa*, but the morphological characteristics of *N. rosae*, in which the apical appendages do not arise from the apical crest are distinct from *N. subepidermalis* and other taxa in this genus (Maharachchikumbura et al. 2014). In addition, *N. subepidermalis* differs from the three other species in the dimensions of its conidia and apical appendages: the conidia of *N. subepidermalis* are shorter than *N. mesopotamica* (20–25 µm vs 26–32 µm), but longer than those of *N. vacciniicola* (20–25 µm vs 14.5–15.2 µm). Furthermore, the apical appendages of *N. subepidermalis* are significantly longer than those of *N. camelliae-oleiferae* (27–32.5 µm vs 15.5–18.5 µm) and *N. vacciniicola* (27–32.5 µm vs 4.3–24.3 µm).

Based on the phylogeny, *N. subepidermalis* is distinct from *N. clavispora*, *N. palmarum*, *N. rosicola* and *N. versicolor*, the four *Neopestalotiopsis* species associated with *Rosa* besides *N. rosae* (Liu et al. 2010, Feng et al. 2014, Jiang et al. 2018, Vu et al. 2019) (Fig. 4). Furthermore, *N. subepidermalis* differs from *N. clavispora* and *N. versicolor* in having the longer basal appendage (7–7.5 µm vs 3–5.5 µm and 7–7.5 µm vs 2.4–6.8 µm), while *N. subepidermalis* has longer apical appendages than *N. rosicola* and *N. palmarum* (27–32.5 µm vs 17–22.8 µm and 27–32.5 µm vs 11.8–18.9 µm).

Key to *Neopestalotiopsis* species on *Rosa* spp.

1. Conidial width less than 6 µm 2
1. Conidial width more than 6 µm 3
2. Conidia 14–18.5 × 4.5–5 µm, apical appendage 19–26 µm long *N. concentrica*
2. Conidia 19–23.6 × 5.6–6.6 µm, apical appendage 11.8–18.9 µm long *N. palmarum*
3. Basal appendages less than 5.5 µm 4
3. Basal appendages more than 5.5 µm 5
4. Conidia 20–24 × 6–8 µm, apical appendages 22–32 µm *N. clavispora*
4. Conidia 21.2–28.3 × 7.1–8.3 µm, apical appendage 18.9–30.7 µm long *N. versicolor*
5. Apical appendages do not arise from the apical crest *N. rosae*
5. Apical appendages arise from the apical crest 6
6. Conidia 20.2–25.5 × 5.5–8.0 µm, apical appendages 17.0–22.8 µm *N. rosicola*
6. Conidia 20–25 × 7.5–9 µm, apical appendages 27–32.5 µm *N. subepidermalis*

Pestalotiopsis chamaeropis Maharachch. et al., Stud. Mycol. 79: 158. 2014 — Fig. 12

Sexual morph not observed. Asexual morph: *Acervular conidiomata* globose or irregular, superficial to semi-immersed, scattered or aggregated, visible as black acervuli on the host. *Conidiophores* septate, branched, subcylindrical, hyaline, verruculose. *Conidiogenous cells* discrete, cylindrical, hyaline, smooth-walled, collarette present and not flared, with prominent periclinal thickening, (5.5–)7–8.5(–10) × 2–4(–4.5) µm (av. = $7.6 \pm 1.32 \times 3.4 \pm 0.66$ µm). Conidia fusoid, ellipsoid, straight to slightly curved, 4-septate, (25–)26–27.5(–28) × 7–8.5(–9) µm (av. = $27 \pm 0.54 \times 7.9 \pm 0.56$ µm); basal cell obconic with a truncate base, hyaline, thin-walled, 4.5–5.5(–6) µm (av. = 5.1 ± 0.36 µm) long; three median cells doliform to subcylindrical, (15–)16.5–17(–18) µm (av. = 16.7 ± 0.52 µm) long, wall verruculose, concolourous, but occasionally the two upper median cells are slightly darker than the lower median cell, brown, second cell from the base 3.5–6(–6.5) µm (av. = 5.2 ± 0.81 µm) long, third cell (3–)5–6(–6.5) µm (av. = 5.4 ± 0.35 µm) long, fourth cell (3.5–)5.5–6(–6.5) µm (av. = 5.7 ± 0.42 µm) long; apical cell 3.5–5(–6) µm (av. = 4.4 ± 0.57 µm) long, hyaline, subcylindrical, thin- and smooth walled; with 2–3 tubular apical appendages (mostly three), arising from the apical crest, unbranched, filiform, variable in size, 6–24(–24.5) µm (av. = 16.4 ± 3.66 µm) long; basal appendage single, tubular, unbranched, centric, 5.5–8(–8.5) µm (av. = 6.7 ± 1.07 µm) long.

Culture characteristics — Colony on PDA with fluffy mycelium, panniform, aerial mycelium white, reverse white or light yellow, being yellow at the centre and white at the edge. Colony 60–66 mm diam in 15 d at 28 °C. Conidiomata globose, irregularly distributed on the medium surface, exuding globose, dark brown to black conidial masses.



Fig. 12 *Pestalotiopsis chamaeropis* (BJFC-S1885). a. Appearance of conidiomata on host substrate; b. colonies on PDA at 3 d (left) and 15 d (right); c. conidiomata on PDA; d–i. conidiogenous cells with attached conidia; j. conidia. — Scale bars: c = 200 µm; d–i = 10 µm.

Materials examined. CHINA, Gansu Province, Tianshui City, Maiji District, Maiji Mountain, N34°20'35" E106°0'22", alt. 1509 m, on spines of *R. chinensis*, 18 Aug. 2020, C. Peng & S. Jia (BJFC-S1885, cultures CFCC 55156 = ROC 23-1, ROC 270, ROC 272, ROC 273, ROC 275); Gansu Province, Tianshui City, Maiji District, Maiji Mountain, N34°20'52" E106°0'16", alt. 1508 m, on spines of *R. chinensis*, 18 Aug. 2020, C. Peng & S. Jia (BJFC-S1886, cultures CFCC 55157 = ROC 23-2, ROC 276, ROC 278, ROC 279, ROC 280); Gansu Province, Tianshui City, Maiji District, Maiji Mountain, N34°20'17" E106°0'36", alt. 1500 m, on spines of *R. chinensis*, 19 Aug. 2020, C. Peng

& S. Jia (BJFC-S1887, cultures ROC 281, ROC 282, ROC 283, ROC 286); ibid. (cultures ROC 289, ROC 290, ROC 292, ROC 293).

Notes — *Pestalotiopsis chamaeropis* was first described from leaves of *Chamaerops humilis* in Italy and subsequently reported on a wide range of hosts (e.g., *Camellia sinensis*, *Pieris japonica*, *Prostanthera rotundifolia*, *Vandopsis* spp. and *Vitis vinifera*) (Maharachchikumbura et al. 2014, Moslemi & Taylor 2015, Liu et al. 2017, Ran et al. 2017, Jayawardena

et al. 2018, Nozawa et al. 2019, Wang et al. 2019b). In this study, 18 isolates clustered together with the ex-type culture of *Pes. chamaeropis* (CBS 186.71) in the multi-locus phylogenetic tree (Fig. 5). This is the first report of this fungus on *R. chinensis*. Compared with the description of the ex-type isolate CBS 186.71, CFCC 55156 has smaller conidiogenous cells ($7\text{--}8.5 \times 2\text{--}4 \mu\text{m}$ vs $20\text{--}50 \times 2\text{--}5 \mu\text{m}$).

Pestalotiopsis rhodomyrtus Y. Song et al., Phytotaxa 126: 27. 2013 — Fig. 13

Sexual morph not observed. Asexual morph: *Acervular conidiomata* globose or irregular, superficial to semi-immersed, scattered or aggregated, visible as black acervuli on the host, $86\text{--}99 \mu\text{m}$. *Conidiophores* branched, subcylindrical, hyaline. *Conidiogenous cells* discrete, cylindrical or ampulliform, hyaline, smooth-walled, collarette present and not flared, with prominent periclinal thickening, $(5\text{--})6.5\text{--}10(11.5) \times (1.5\text{--})2\text{--}3 \mu\text{m}$ (av. = $8.4 \pm 1.35 \times 2.7 \pm 0.67 \mu\text{m}$). *Conidia* fusoid, ellipsoid,

straight to slightly curved, 4-septate, $(17.5\text{--})19\text{--}26 \times (5\text{--})5.5\text{--}6.5(7) \mu\text{m}$ (av. = $22.7 \pm 1.21 \times 5.9 \pm 0.52 \mu\text{m}$); basal cell obconic with a truncate base, hyaline, minutely verruculose and thin-walled, $3\text{--}5(5.5) \mu\text{m}$ (av. = $4.2 \pm 0.52 \mu\text{m}$) long; three median cells doliform to subcylindrical, $(11\text{--})12\text{--}18.5(19.5) \mu\text{m}$ (av. = $14.9 \pm 1.46 \mu\text{m}$) long, wall verruculose, concolourous, pale brown, second cell from the base $(3\text{--})4.5\text{--}5.5 \mu\text{m}$ (av. = $4.8 \pm 0.36 \mu\text{m}$) long, third cell $(3\text{--})3.5\text{--}5(5.5) \mu\text{m}$ (av. = $4.6 \pm 0.54 \mu\text{m}$), fourth cell $4\text{--}5.5(6) \mu\text{m}$ (av. = $4.9 \pm 0.38 \mu\text{m}$); apical cell $(3\text{--})3.5\text{--}5.5 \mu\text{m}$ (av. = $4.4 \pm 0.85 \mu\text{m}$) long, hyaline, cylindrical to subcylindrical, thin and smooth walled; with 2–3 tubular apical appendages (mostly three), arising from the apical crest, unbranched, filiform, flexuous, $(9\text{--})11.5\text{--}20(21.5) \mu\text{m}$ (av. = $15.7 \pm 1.58 \mu\text{m}$) long; one basal appendage, tubular, centric appendage tubular, branched or unbranched, $(5.5\text{--})6\text{--}7.5 \mu\text{m}$ (av. = $6.9 \pm 1.74 \mu\text{m}$) long.

Culture characteristics — Colonies on PDA flat with entire margin, aerial mycelium white, cottony, fluffy; reverse white in the centre and faint yellow margin, colony diam 59–63 mm

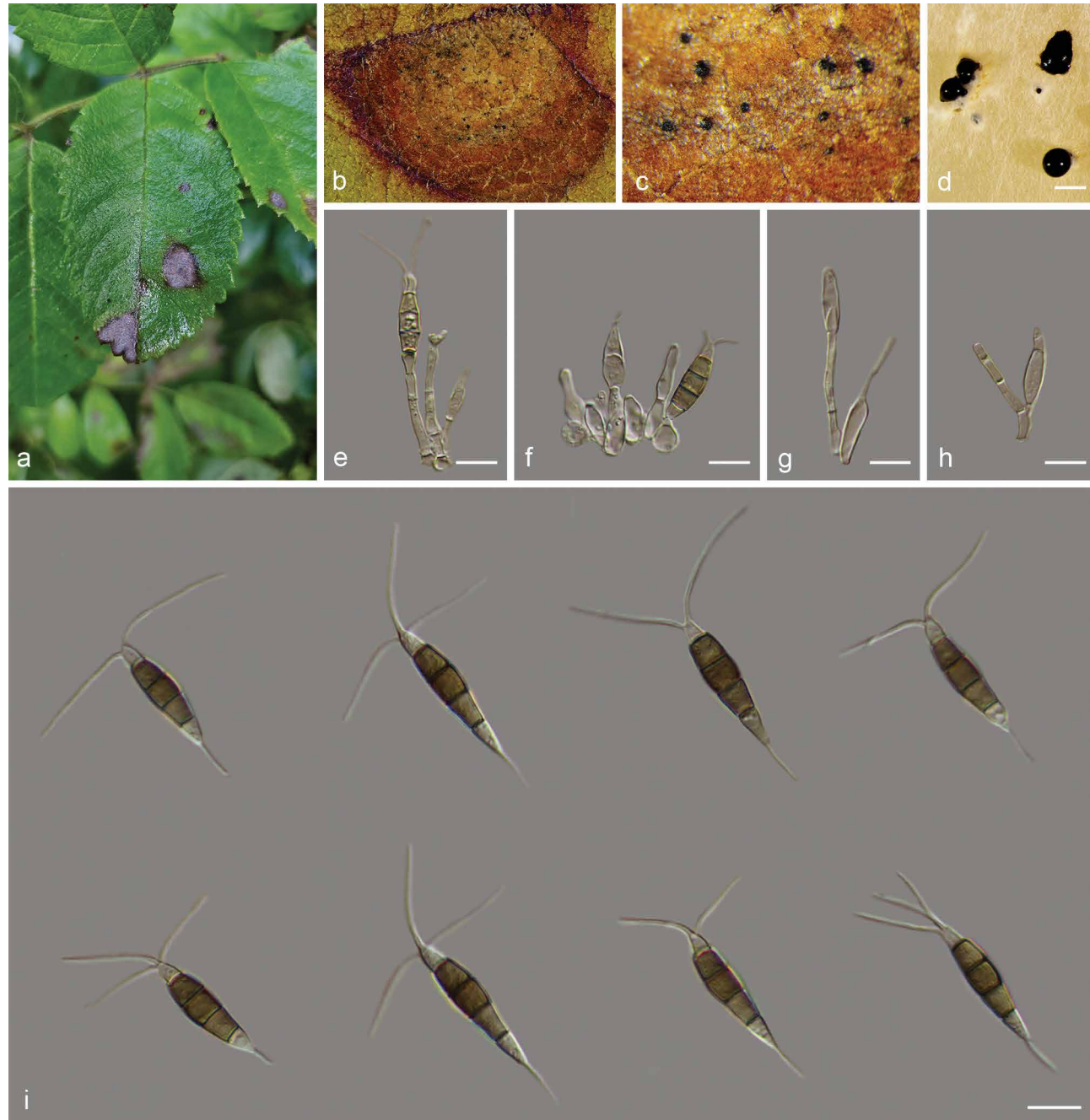


Fig. 13 *Pestalotiopsis rhodomyrtus* (BJFC-S1888). a. Disease symptoms; b–c. appearance of conidiomata on host substrate; d. conidiomata on PDA; e–h. conidiogenous cells with attached conidia; i. conidia. — Scale bars: d = 200 μm ; e–i = 10 μm .

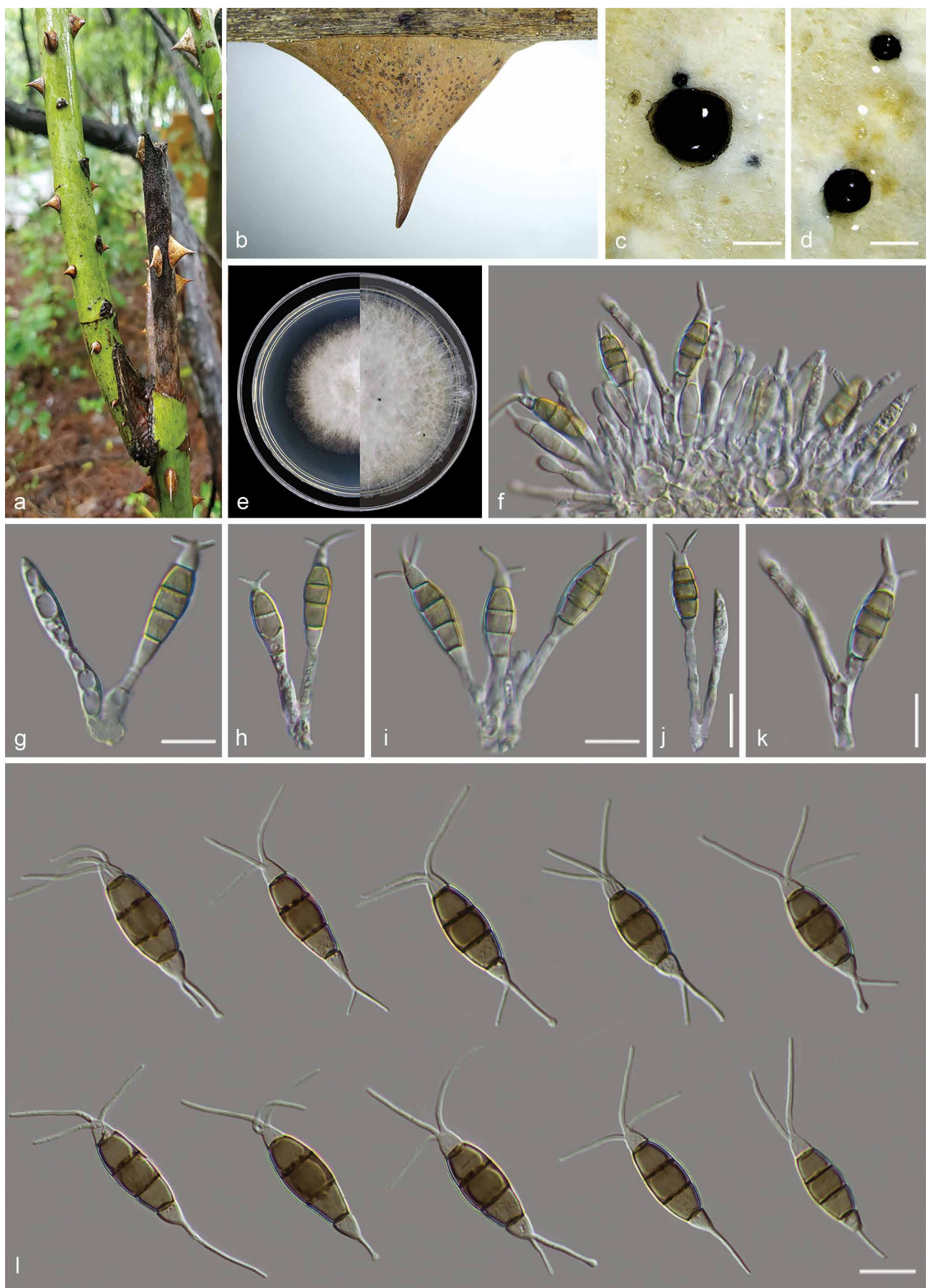


Fig. 14 *Pestalotiopsis tumida* (BJFC-S1891 holotype). a. Disease symptoms; b. appearance of conidiomata on host substrate; c–d. conidiomata on PDA; e. colonies on PDA at 3 d (left) and 15 d (right); f. conidiomata on *Rosa chinensis*; g–k. conidiogenous cells with attached conidia; l. conidia. — Scale bars: c–d = 200 µm; f–l = 10 µm.

diam in 15 d. Conidia in mass black. Conidiomata globose, irregularly distributed on the medium surface, exuding globose, black conidial masses.

Materials examined. CHINA, Henan Province, Nanyang City, Neixiang county, Mahuang Village, N33°20'14" E114°52'1", alt. 266 m, on leaves of *R. rugosa*, 7 Aug. 2020, Y.M. Liang & C. Peng (BJFC-S1888, cultures ROC 056, ROC 057, ROC 058); ibid. (cultures ROC 059, ROC 060, ROC 061, ROC 062); Gansu Province, Gannan Tibetan Autonomous Prefecture, Lintan County, Yeliguhan, N34°53'48" E103°35'2", alt. 2740 m, on spines of *R. multiflora*, 18 Aug. 2020, C. Peng & S. Jia (BJFC-S1889, cultures ROC 303, ROC 304, ROC 305, ROC 306); ibid. (cultures ROC 307, ROC 309, ROC 311); Hunan Province, Changsha City, Changsha County, N28°58'52" E113°34'38", alt. 61 m, on branches of *R. chinensis*, 10 Nov. 2020, C.M. Tian & N. Jiang (BJFC-S1890, cultures ROC 356, ROC 357, ROC 358, ROC 359).

Notes — *Pestalotiopsis rhodomyrtus* was initially described from *Rhodomyrtus tomentosa* in Guangxi Province, China (Song et al. 2013). In addition, this species was discovered on *Camellia sinensis* (Liu et al. 2017, Wang et al. 2019a). In this study, 18 isolates were identified as belonging to this species (Fig. 5) and this is the first report of this fungus on the host genus *Rosa*.

Compared with the description of the ex-type isolate HGUP 4230, isolate ROC 056 has longer apical and basal appendages (11.5–20 µm vs 7.5–14.9 µm and 6–7.5 µm vs 2.8–4.9 µm).

***Pestalotiopsis tumida* C. Peng & C.M. Tian, sp. nov.** — Myco-Bank MB 843814; Fig. 14

Etymology. Name refers to the basal appendage that is occasionally swollen at the tip.

Type. CHINA, Gansu Province, Tianshui City, Maiji District, Maiji Mounta, N34°20'32" E106°0'29", alt. 1601 m, on spines of *R. chinensis*, 15 Aug. 2020, C. Peng & S. Jia (holotype BJFC-S1891, ex-type cultures CFCC 55158 = ROC 110, ROC 108, ROC 109).

Sexual morph not observed. Asexual morph: *Acervular conidiomata* globose or irregular, superficial to semi-immersed, scattered or aggregated, visible as black acervuli on the host. *Conidiophores* branched, subcylindrical, hyaline. *Conidiogenous cells* discrete, cylindrical or ampulliform, hyaline, smooth-walled, collarate present and not flared, with prominent periclinal thickening, (7–)8–11.5(–12) × (1.5–)2–4.5 µm (av. = 10.4 ± 2.23 × 2.9 ± 0.83 µm). *Conidia* fusoid, ellipsoid, straight to slightly curved, 4-septate, (19–)19.5–23.5(–24) × 6.5–7.5 µm (av. = 21.4 ± 1.33 × 6.9 ± 0.58 µm); basal cell obconic with a truncate base, hyaline, minutely verruculose and thin-walled, (2.5–)3–4.5 µm (av. = 3.9 ± 0.58 µm) long; three median cells doliform to subcylindrical, (14–)14.5–18(–18.5) µm (av. = 16.6 ± 1.68 µm) long, wall verruculose, concolourous, light brown, second cell from the base (3.5–)4–5 µm (av. = 4.6 ± 0.36 µm) long, third cell (4–)4.5–6.5 µm (av. = 5.3 ± 0.68 µm), fourth cell (4.5–)5.5 µm (av. = 5.1 ± 0.34 µm); apical cell 4.5–6 µm (av. = 5.1 ± 0.49 µm) long, hyaline, cylindrical to subcylindrical, thin- and smooth

walled; with 2–3 tubular apical appendages (mostly three), arising from the apical crest, unbranched, filiform, flexuous, (10–)10.5–15.5(–16) µm (av. = 13.1 ± 2.07 µm) long; 1–2 basal appendages, tubular, centric appendage tubular, branched or unbranched, occasionally swollen at the tip, (6.5–)7–19(–19.5) µm (av. = 10.9 ± 3.44 µm) long, excentric appendage tubular, 6.5–7.5(–8) µm (av. = 7.3 ± 0.26 µm) long.

Culture characteristics — Colonies on PDA with aerial mycelium white, fluffy, reverse yellow pigment accumulation in the centre, surrounded by amber, pure white at the colony margin. Colony 56–60 mm diam in 15 d at 28 °C. Conidiomata globose, irregularly distributed on the medium surface, exuding globose, black conidial masses.

Additional materials examined. CHINA, Gansu Province, Tianshui City, Maiji District, Maiji Mounta, N34°20'36" E106°0'23", alt. 1557 m, on branches and spines of *R. chinensis*, 15 Aug. 2020, C. Peng & S. Jia (BJFC-S1892, cultures CFCC 55159 = ROC 234, ROC 235, ROC 236, ROC 237); ibid. (cultures ROC 238, ROC 240).

Notes — *Pestalotiopsis tumida* formed a distinct clade (ML/MP/BI = 100/100/1) in the multi-locus analyses and is sister to *Pes. intermedia* and *Pes. linearis*. *Pestalotiopsis tumida* (Fig. 5) can be distinguished from *Pes. intermedia* and *Pes. linearis* in ITS (two different unique fixed alleles in *Pes. intermedia* (531/533, 99.5 % with a single gap) and two in *Pes. linearis* (536/538, 99.5 % with no gaps)), *TEF* loci (six different unique fixed alleles in *Pes. intermedia* (526/532, 98.6 % with no gaps) and four in *Pes. linearis* (528/532, 99.2 % with no gaps)) and *TUB* loci (10 different unique fixed alleles in *Pes. intermedia* (443/553, 97.7 % with four gaps) and 18 in *Pes. linearis* (415/433, 95.7 % with three gaps)). Moreover, the conidial morphology of *Pes. tumida* is significantly different from these two species. *Pestalotiopsis tumida* differs from *Pes. intermedia* and *Pes. linearis* by shorter conidia (*Pes. tumida*: 19.5–23.5 µm vs *Pes. intermedia*: 24–28 µm, *Pes. linearis*: 24–33 µm). In addition, it is different from *Pes. linearis* in bearing shorter apical appendages (10.5–15.5 µm vs 24–33 µm) and longer basal appendages (7–19 µm vs 4–7 µm).

There are 11 species of *Pestalotiopsis* that have been recorded from *Rosa*, namely *Pes. adusta*, *Pes. algeriensis*, *Pes. aquatica*, *Pes. lespedezae*, *Pes. longisetula*, *Pes. macrochaeta*, *Pes. maculans*, *Pes. oleandri*, *Pes. populi-nigrae*, *Pes. rosae* and *Pes. suffocata* (Riley 1960, Guba 1961, Mathur 1979, Rai 1990, Zhu et al. 1991, Nag Raj 1993, Mendes et al. 1998, Sameva 2004, Wei et al. 2005, Kobayashi 2007, Ge et al. 2009). *Pestalotiopsis tumida* can be easily distinguished from *Pes. adusta*, *Pes. algeriensis*, *Pes. aquatica*, *Pes. longisetula* and *Pes. oleandri* by the colour of its median conidial cells. The median conidial cells of these five species are versicolourous while the three median conidial cells of *Pes. tumida* are concolourous. *Pestalotiopsis tumida* can be distinguished from other *Rosa* associated species by the size of its conidia and length of appendages (Table 4). Furthermore, the basal appendage

Table 4 Synopsis of *Pestalotiopsis* species with concolourous median conidium cells from *Rosa*.

Species	Conidia length (µm)	Conidia width (µm)	Middle cells length (µm)	Length of apical appendages (µm)	Length of basal appendages (µm)	Host	Country	References
<i>Pestalotiopsis lespedezae</i>	20.2–25	7.5–8.8	13.8–17.5	15–27.5	5–6.3	<i>Rosa canina</i>	India	Mathur (1979)
<i>Pes. macrochaeta</i>	24.8–33	6.6–7.6	13.0–21.2	15.3–34.2	7.1–11.8	<i>Rosa</i> sp.	Brazil	Mendes al. (1998)
<i>Pes. maculans</i>	19–27.5	6–8	10–15.5	16–24	4.2–5	<i>Rosa</i> sp.	Bulgaria	Sameva ((2004))
<i>Pes. populi-nigrae</i>	21.2–28.3	7.1–8.3	14.2–16.5	21.2–31.9	2.4–7.1	<i>Rosa hybrida</i>	Japan	Kobayashi (2007)
<i>Pes. rosae</i>	20.5–28.8	5–6.3	11.8–16.3	10–25	4–5.3	<i>Rosa</i> sp.	China	Ge et al. (2009)
<i>Pes. suffocata</i>	20.8–28.6	5.8–7.1	13.6–18.8	15.6–35.1	1.3–3.5	<i>Rosa</i> sp.	China	Ge et al. (2009)
<i>Pes. tumida</i>	19.5–23.5	6.5–7.5	14.5–18	10.5–15.5	7–19	<i>Rosa chinensis</i>	China	Present study

* Newly described taxon is in bold.

of *Pes. tumida* is occasionally swollen at the tip, a unique morphological character that distinguishes it from other species that have been recorded from *Rosa*.

Key to Pestalotiopsis species on Rosa spp.

1. Median conidial cells versicolourous 2
1. Median conidial cells concolourous 6
2. Length of apical appendages less than 12 µm 3
2. Length of apical appendages more than 12 µm 5
3. Basal appendages less than 3.5 µm 4
3. Basal appendages more than 3.5 µm .. *Pes. algeriensis*
4. Conidia not or slightly constricted at the septa, 16–22 × 5–7 µm, apical appendages 5–12 µm *Pes. adusta*
4. Conidia constricted at the septa, 18.9–28.3 × 4.7–7.1 µm, apical appendages 16.5–28.3 µm *Pes. oleandri*
5. Conidia 20.6–28.2 × 7.2–8.2 µm, apical appendages 12.8–23 µm, basal appendages 2–4 µm *Pes. aquatica*
5. Conidia 20.6–25.7 × 6.4–7.7 µm, apical appendages 20.6–36 µm, basal appendages 5.1–7.7 µm .. *Pes. longisetula*
6. Basal appendages less than 5 µm 7
6. Basal appendages more than 5 µm 9
7. Conidia 3–4-septate *Pes. rosae*
7. Conidia 4-septate 8
8. Conidia 21.8–28.3 × 6.6–8.3 µm, apical appendages 21.2–31.9 µm, basal appendages 1.5–3 µm *Pes. populi-nigrae*
8. Conidia 19–27.5 × 6–8 µm, apical appendages 16–24 µm, basal appendages 4.2–5 µm *Pes. maculans*
9. Conidial length less than 26 µm 10
9. Conidial length more than 26 µm 12
10. Basal appendages occasionally swollen at the tip *Pes. tumida*
10. Basal appendages not occasionally swollen at the tip 11
11. Conidia 19.7–26.3 × 4.9–6.7 µm, apical appendages 7.5–14.9 µm, basal appendages 2.8–4.9 µm *Pes. rhodomyrtus*
11. Conidia 20–25 × 7.5–8.5 µm, apical appendages 15–22.5 µm, basal appendages 3.7–7.5 µm *Pes. lespedeziae*
12. Basal appendages less than 5.5 µm *Pes. suffocata*
12. Basal appendages more than 5.5 µm 13
13. On PDA, reverse of colonies cinnamon-rufous, conidia 24.8–33 × 6.6–7.6 µm, apical appendages 15.3–34.2 µm, basal appendages 7.1–11.8 µm *Pes. macrochaeta*
13. On PDA, reverse of colonies white, conidia 26–27.5 × 7–8.5 µm, apical appendages 6–24 µm, basal appendages 5.5–8 µm *Pes. chamaeropis*

***Seimatosporium centrale* C. Peng & C.M. Tian, sp. nov.** — MycoBank MB 843816; Fig. 15

Etymology. Name refers to conidiomata produced in the centre of the colonies on PDA.

Type. CHINA, Gansu Province, Tianshui City, Maiji District, Dongcha Town, N34°19'34"E 106°34'27", alt. 1120 m, on spines of *R. chinensis*, 16 July 2019, C.M. Tian, Y.M. Liang & C. Peng (holotype BJFC-S1893, ex-type cultures CFCC 55166 = ROC 003, ROC 001, ROC 002).

Sexual morph not observed. Asexual morph: *Acervular conidiomata* solitary to gregarious, immersed to semi-immersed, unicellular, subglobose, visible as black acervuli on the spines of *R. chinensis*. *Conidiophores* branched at the base, hyaline. *Conidiogenous cells* discrete or integrated, cylindrical, subcylindrical or irregular, hyaline, smooth, thick-walled, (6–)7.5–21.5–23.5 × (2–)2.5–3(–3.5) µm (av. = 14.4 ± 3.23 × 2.7 ± 0.35 µm). *Conidia* straight or slightly curved, fusoid, cylindrical

or subcylindrical, concolourous, 3-septate, mostly constricted at the septa, transverse septa fairly thick, smooth-walled, (18.5–)19.5–23.5(–24) × (5–)5.5–7 µm (av. = 20.9 ± 1.58 × 6.1 ± 0.52 µm); basal cell obconic with a truncate base, hyaline to pale brown, (4–)4.5–5.5(–6) µm (av. = 5.0 ± 0.64 µm) long; middle cells cylindrical, pale brown, second cell from base (4–)4.5–5.5 µm (av. = 5.0 ± 0.39 µm), third cell from base (4.5–)5–6(–6.5) µm (av. = 5.4 ± 0.58 µm), together (9.5–)10–11.5(–12) µm (av. = 10.7 ± 0.88 µm) long; apical cell conical, pale brown, (3.5–)4–5 µm (av. = 4.2 ± 0.32 µm); apical appendage single, unbranched, centric, occasionally eccentric, 3.5–5.5(–7) µm (av. = 4.9 ± 0.67 µm) long; basal appendage single, unbranched, eccentric, (3–)4.5–5(–6) µm (av. = 5.0 ± 0.27 µm) long; mean conidium length/width ratio = 3.40 : 1.

Culture characteristics — Colonies on PDA with aerial mycelium white, dense, reverse with tawny pigment accumulation, being darker at the centre and paler at the edge. Colony 56–58 mm diam in 15 d at 28 °C. Conidiomata are observed around 25 d and are mostly produced in the centre of the colony. Conidiomata globose, exuding black conidial masses.

Additional materials examined. CHINA, Shaanxi Province, Baoji City, Fengxian County, Xinjia Mountain, N34°12'45"E 106°36'25", alt. 1609 m, on spines of *R. chinensis*, 16 July 2019, C.M. Tian, Y.M. Liang & C. Peng (BJFC-S1894, cultures CFCC 55169 = ROC 014, ROC 015, ROC 016); Gansu Province, Tianshui City, Maiji District, Maiji Mountain, N34°20'44"E 106°0'22", alt. 1601 m, on spines of *R. chinensis*, 15 Aug. 2020, C. Peng & S. Jia (BJFC-S1895, cultures ROC 145, ROC 146, ROC 147).

Notes — The nine isolates studied form a well-supported independent clade distinct from known *Seimatosporium* species (ML/MP/BI = 98/96/1). *Seimatosporium centrale* is most closely related to *Seim. botan*, *Seim. discosiooides*, *Seim. gracile* sp. nov. and *Seim. nonappendiculatum* sp. nov. (Fig. 6). Among them, *Seim. discosiooides* as pathogens occurring on some Rosaceae hosts, especially on *Rosa* spp. (Shoemaker 1964, Nag Raj 1993). A pairwise comparison of the ITS sequence showed seven nucleotide differences out of 557 nucleotides (98.7 % similarity, including two gaps) between *Seim. centrale* and *Seim. discosiooides*, while LSU showed six nucleotide differences out of 794 nucleotides (99.2 % similarity, without gaps). Meanwhile, *Seim. discosiooides* morphologically differs from our new species and other *Seimatosporium* species associated with *Rosa* by the absent of appendages. *Seimatosporium centrale* differs from *Seim. botan* in morphology, namely having wider conidia (5.5–7 µm vs 4–5 µm) and their mean conidium length/width ratio is quite distinct (3.4 : 1 in *Seim. centrale* vs 4.6 : 1 in *Seim. botan*). In addition, *Seim. botan* has two types of conidia (with only basal appendage and both apical and basal appendages) while *Seim. centrale* has only one conidial type (both apical and basal appendages). Furthermore, *Seim. centrale* can be distinguished from *Seim. gracile* by its extremely high mean conidium length/width ratio (3.40 : 1 vs 6.19 : 1) and from *Seim. nonappendiculatum* by the colour of its basal cell (pale brown vs hyaline).

Besides *Seim. discosiooides*, four species of *Seimatosporium* have been recorded from *Rosa*, namely *Seim. caninum*, *Seim. pseudorosae*, *Seim. salicinum* and *Seim. rosae* (Nag Raj 1993, Kobayashi 2007, Muñoz et al. 2008, Norphanphon et al. 2015, Hyde et al. 2016). *Seimatosporium centrale* has larger conidia than *Seim. pseudorosae* and *Seim. rosae* (19.5–23.5 × 5.5–7 µm vs 12–17.5 × 3–6 µm and 19.5–23.5 × 5.5–7 µm vs 10–16 × 3–4.5 µm). However, the apical appendages of *Seim. centrale* are noticeably shorter than those of the two species (3.5–5.5 µm vs 8–25 µm and 3.5–5.5 µm vs 1.5–15 µm). *Seimatosporium caninum* and *Seim. salicinum* can be distinguished from *Seim. centrale* based on the number of conidial septa. While *Seim. centrale* has 3-septate conidia, *Seim. salicinum* has 2–3-septate and *Seim. caninum* only has 2-septate conidia (Wanasinghe et al. 2018).

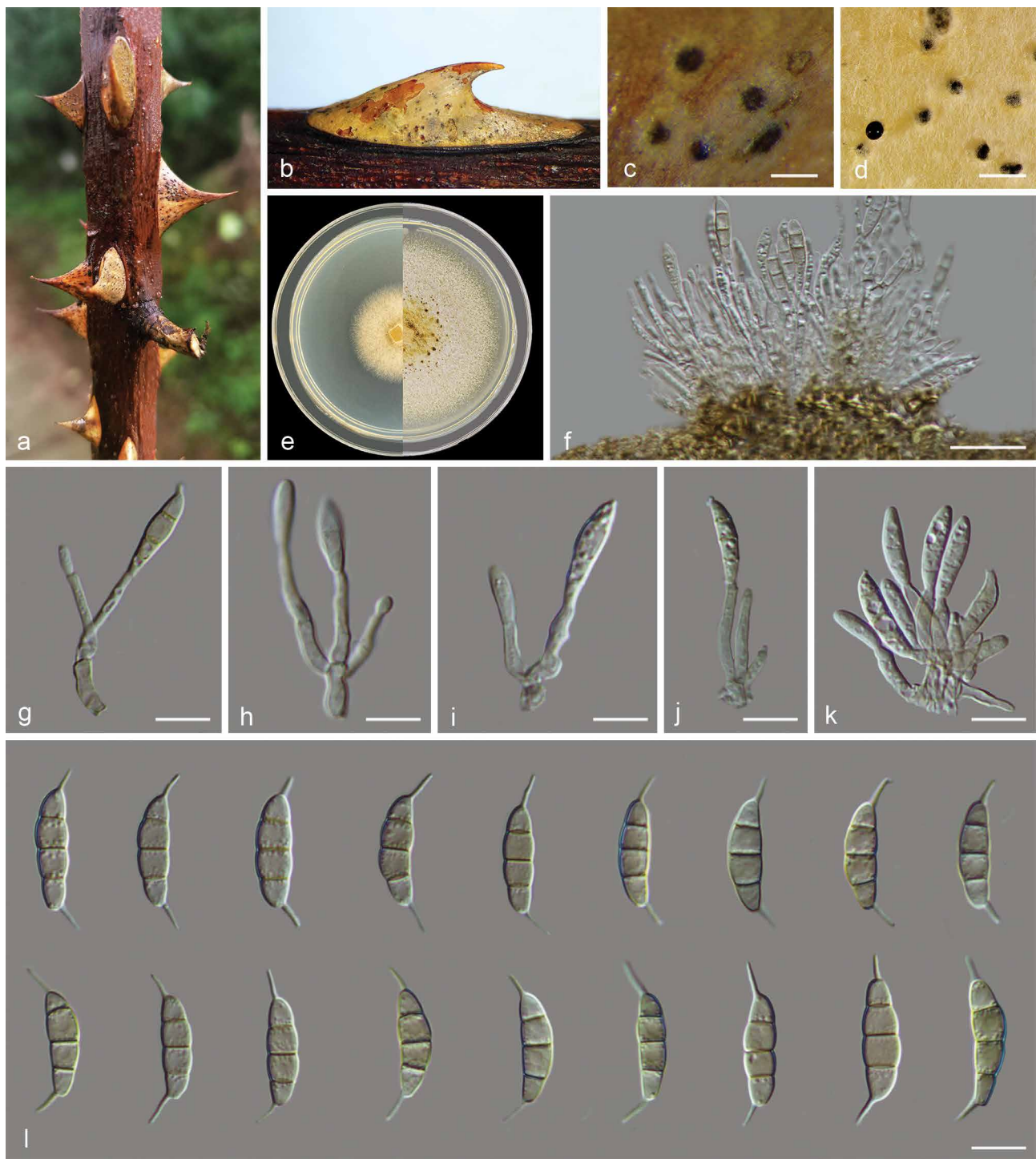


Fig. 15 *Seimatosporium centrale* (BJFC-S1893, holotype). a–b. Disease symptoms; c. appearance of conidiomata on host substrate; d. conidiomata on PDA; e. colonies on PDA at 3 d (left) and 15 d (right); f. longitudinal section through conidiomata; g–k. conidiogenous cells with attached conidia; l. conidia. — Scale bars: c–d = 200 µm; f = 20 µm; g–l = 10 µm.

***Seimatosporium gracile* C. Peng & C.M. Tian, sp. nov. — MycoBank MB 843818; Fig. 16**

Etymology. From Latin ‘gracile’ means slender/slim, which refers to the shape of the conidia.

Type. CHINA, Gansu Province, Tianshui City, Qingshui county, Shidong Mountain, N34°41'4" E106°21'34", alt. 1697 m, on spines of *R. xanthina*, 17 July 2019, C.M. Tian, Y.M. Liang & C. Peng (holotype BJFC-S1896, ex-type cultures CFCC 55167 = ROC 004, ROC 005, ROC 006).

Sexual morph not observed. Asexual morph: **Acervular conidiomata** solitary to gregarious, immersed when immature, becoming erumpent at maturity, subglobose, up to 95–337 µm diam, 56–104 µm high, visible as black conidiomata on the spines. **Conidiophores** irregularly branched, mostly branched at the

base, 1–3-septate, hyaline. **Conidiogenous cells** discrete or integrated, ampulliform, cylindrical or subcylindrical, hyaline, smooth, thick-walled, variable in size, (7–)8.5–21.5(–23) × 1.5–2(–3) µm (av. = $15.6 \pm 3.23 \times 1.6 \pm 0.18$ µm). **Conidia** straight or slightly curved, cymbiform or fusoid, concolourous, 3-septate, barely constricted at the septa, transverse septa dark brown and fairly thick, smooth-walled, (13.5–)14.5–19.5(–20) × 2.5–3(–3.5) µm (av. = $16.7 \pm 1.82 \times 2.7 \pm 0.25$ µm); basal cell obconic with or without a truncate base, pale brown to hyaline, (2.5–)3–4(–4.5) µm (av. = 3.6 ± 0.47 µm) long; middle cells cylindrical, pale brown, second cell from base (3–)3.5–4.5 µm (av. = 3.9 ± 0.37 µm), third cell from base 3.5–4(–4.5) µm (av. = 3.8 ± 0.27 µm), together 7–8(–9) µm (av. = 7.7 ± 0.43 µm) long; apical cell conical, pale brown, (2.5–)3–3.5(–4.5) µm

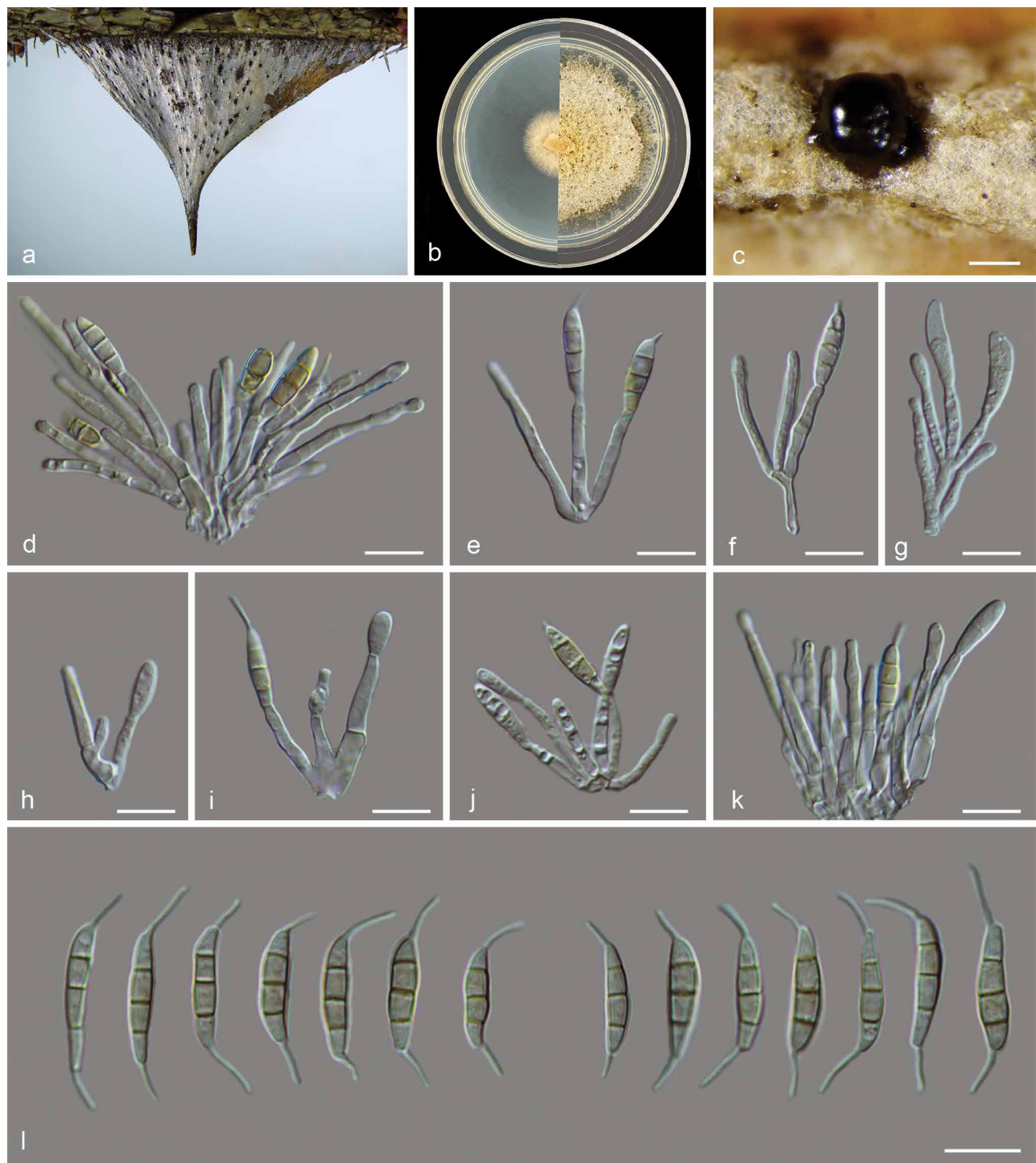


Fig. 16 *Seimatosporium gracile* (BJFC-S1896, holotype). a. Appearance of conidiomata on host substrate; b. colonies on PDA at 3 d (left) and 15 d (right); c. conidiomata formed on pine needles; d–k. conidiogenous cells with attached conidia; l. conidia. — Scale bars: c = 200 µm; d–l = 10 µm.

(av. = $3.2 \pm 0.28 \mu\text{m}$); apical appendage single, unbranched, centric, (3–)4–8(–8.5) µm (av. = $6.3 \pm 1.58 \mu\text{m}$) long; basal appendage single, unbranched, excentric, 4.5–8.5(–9) µm (av. = $6.1 \pm 1.22 \mu\text{m}$) long; mean conidium length/width ratio = 6.19 : 1.

Culture characteristics — Colonies on PDA flat with irregular margin, colony yellow or pale yellow in the centre with fluffy aerial mycelia and pale white margin; reverse tawny pigment accumulation formed in the shape of a concentric ring pattern. Colony 56–58 mm diam in 15 d at 28 °C. Conidiomata sparse, concentrically and irregularly distributed on the medium surface.

Additional materials examined. CHINA, Gansu Province, Tianshui City, Qingshui county, Shidong mountain, N34°41'4" E106°21'35", alt. 1699 m, on spines of *R. xanthina*, 17 July 2019, C.M. Tian, Y.M. Liang & C. Peng (BJFC-S1897, cultures ROC 007, ROC 008, ROC 009); ibid. (cultures ROC 010, ROC 011, ROC 012).

Notes — *Seimatosporium gracile* forms an independent clade (ML/MP/BI = 100/100/1) and is phylogenetically distinct from *Seim. nonappendiculatum* (described below) (Fig. 6). A comparison of the ITS region showed 0.35 % differences (two bp difference of 566 bp, with one single gap), 0.23 % bp differences (2 bp difference of 846 bp, with no gaps) in the LSU region, 2.1 % bp differences (7 bp difference of 326 bp, with no gaps) in *TEF*, 2.4 % bp differences (11 bp difference of 464 bp, with no gaps) in *TUB* and 0.38 % bp differences (4 bp difference of 1051 bp, with no gaps) in *RPB2*, which is evidence for new species rank. Moreover, the two species are morphologically distinct. *Seimatosporium gracile* differs from *Seim. nonappendiculatum* in the colour of its basal cell and presence or absence of appendages. While *Seim. gracile* has a pale brown basal cell with both apical and basal appendages, *Seim. nonappendiculatum* has a dark brown basal cell with only a basal appendage.

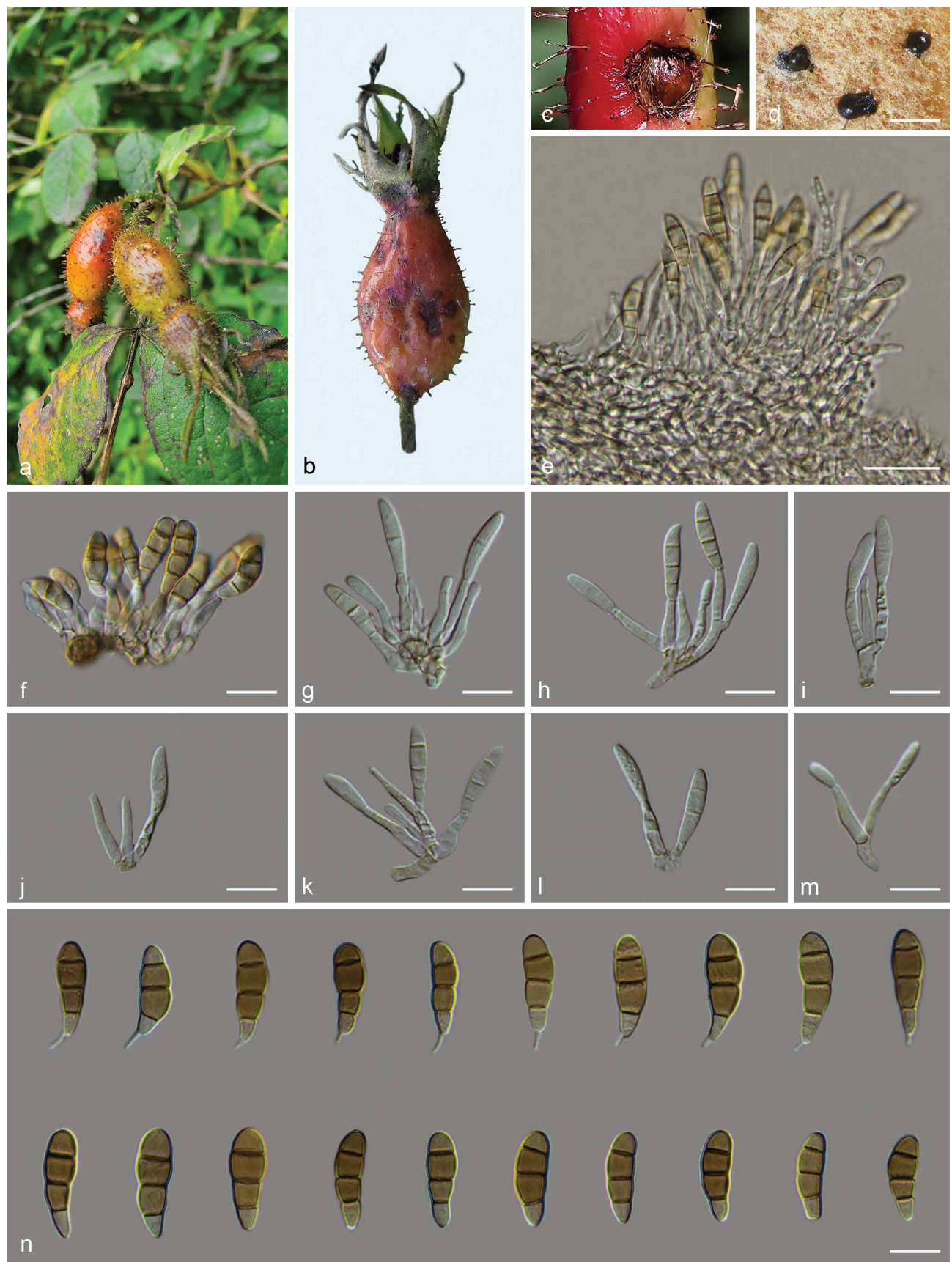


Fig. 17 *Seimatosporium nonappendiculatum* (BJFC-S1901, holotype). a–b. Disease symptoms; c. appearance of conidiomata on host substrate; d. conidiomata formed on PDA; e. longitudinal section through conidiomata; f–m. conidiogenous cells with attached conidia; n. conidia. — Scale bars: d = 200 µm; e = 20 µm; f–n = 10 µm.

diculatum has a hyaline basal cell with no appendages or only basal appendage. Furthermore, the typical characteristic of *Seim. gracile* is that the conidia are slender and has a markedly higher mean conidial length/width ratios (6.19 : 1) than other species that have been recorded from *Rosa* in this genus.

***Seimatosporium nonappendiculatum* C. Peng & C.M. Tian, sp. nov.** — MycoBank MB 843820; Fig. 17

Etymology. Referring to conidia lacking an apical appendage.

Typus. CHINA, Ningxia Hui Autonomous Region, Guyuan City, Jingyuan County, N35°23'53" E106°22'33", alt. 1786 m, on fruits of *R. laevigata*, 29 Aug. 2020, C. Peng (holotype BJFC-S1901, ex-type cultures CFCC 55168 = ROC 377, ROC 378).

Symptoms are marked by slightly collapsed lesions, with regular margin, black dark brown, round spots on fruits (Fig. 19a–c). Sexual morph not observed. Asexual morph: *Acervular conidiomata* solitary to gregarious, subglobose, globose or irregular, up to 287–436 µm diam, 135–160 µm high. *Conidiophores* cylindrical, branched at the base, 1–3-septate, hyaline, smooth-walled. *Conidiogenous cells* discrete or integrated, ampulliform, cylindrical or subcylindrical, hyaline, smooth, thick-walled, variable in size, (5–)6.5–13.5(–16) × (1.5–)2–2.5(–3) µm (av. = 9.9 ± 2.21 × 2.3 ± 0.25 µm). *Conidia* straight or curved, fusoid or pyriform, 3-septate, distoseptate or euseptate, with or without constrictions at the septa, transverse septa dark brown and fairly thick, smooth-walled, (17–)18–23.5(–24) × (5–)5.5–7 µm (av. = 20.3 ± 1.47 × 6.4 ± 0.52 µm); basal cell obconic with a truncate base, hyaline or almost hyaline, (3–)3.5–4.5 µm (av. = 3.9 ± 0.39 µm) long; middle cells cylindrical, pale to medium brown, second cell from base 3–5(–5.5) µm (av. = 4.3 ± 0.32 µm), third cell from base (3.5–)4–4.5(–5) µm (av. = 4.3 ± 0.44 µm), together (7–)8–10(–11) µm (av. = 8.7 ± 0.32 µm) long; apical cell obtuse or conical, pale brown, (3–)4.5–5.5 µm (av. = 4.8 ± 0.31 µm); apical appendage absent; basal appendage lacking or, when present, single, unbranched, excentric, 1.5–4 µm (av. = 2.9 ± 0.93 µm) long; mean conidium length/width ratio = 3.17 : 1.

Culture characteristics — Colonies on PDA flat with entire margin, colony yellow or pale yellow in the centre with fluffy aerial mycelia and pale white margin; reverse with yellow pigment. Colony 50–52 mm diam in 15 d at 25 °C. Conidiomata sparse, concentrically and irregularly distributed on the medium surface.

Additional material examined. CHINA, Ningxia Hui Autonomous Region, Guyuan City, Jingyuan County, N35°23'53" E106°22'36", alt. 1788 m, on fruits of *R. laevigata*, 29 Aug. 2020, C. Peng (BJFC-S1902, cultures ROC 379, ROC 380, ROC 381).

Notes — *Seimatosporium nonappendiculatum* forms an independent clade (ML/MP/BI = 89/93/1) and is phylogenetically distinct from *Seim. gracile* (Fig. 6). The differences between *Seim. nonappendiculatum* and *Seim. gracile* have been mentioned above (see *Seim. gracile*).

Seimatosporium nonappendiculatum is characterised by its fusoid to pyriform, 3-septate conidia with a hyaline basal cell, lacking an apical appendage or with an excentric basal appendage. These morphological characteristics can easily distinguish *Seim. nonappendiculatum* from other *Seimatosporium* species previously reported from *Rosa*. *Seimatosporium botan* which was collected from *Paeonia suffruticosa* in Japan also has two types of conidia (Hatakeyama & Harada 2004). *Seimatosporium botan* can produce conidia with only one basal appendage which morphologically resembles our new *Seimatosporium* species, but *Seim. botan* has longer basal appendages (4–8 µm vs 1.5–4 µm) and larger mean conidium length/width ratio (4.6 : 1 vs 3.17 : 1). The other conidial type of *Seim. botan*

bears appendages at both ends, which is very different from the conidia of *Seim. nonappendiculatum*. Besides *Seim. botan*, *Seim. graminitum*, *Seim. hebeiense* and *Seim. hysteroides* produce conidia with only a basal appendage (Shoemaker 1964, Hatakeyama & Harada 2004). *Seimatosporium nonappendiculatum* can be distinguished from these three species by its larger conidia (18–23.5 × 5.5–7 µm vs 12–18.5 × 3.5–5.5 µm, 18–23.5 × 5.5–7 µm vs 13.5–17.6 × 4.5–6.5 µm and 18–23.5 × 5.5–7 µm vs 12–18 × 5.5–6.5 µm). *Seimatosporium pseudoglandigenum* produces conidia without appendages which morphologically resemble the other conidial type of *Seim. nonappendiculatum* (Wijayawardene et al. 2016a). However, the conidia of *Seim. pseudoglandigenum* only has one conidial type. Although *Seim. nonappendiculatum* is similar to *Seim. pseudoglandigenum* in conidial size (18–23.5 × 5.5–7 µm vs 15–23 × 5–8 µm), *Seim. pseudoglandigenum* can be distinguished from our new species based on the colour of its apical conidial cells. While *Seim. nonappendiculatum* has pale brown apical cells and the apical cell is heterochromatic to the basal cells, *Seim. pseudoglandigenum* has hyaline apical cells and the apical cell is concolourous to the basal cells (Wijayawardene et al. 2016a).

***Seimatosporium parvum* C. Peng & C.M. Tian, sp. nov.** — MycoBank MB 843819; Fig. 18, 19

Etymology. From Latin *parva* 'small', referring to smaller conidia.

Typus. CHINA, Qinghai Province, Huangnan Tibetan Autonomous Prefecture, Zeku County, N37°18'51" E101°56'34", alt. 2890 m, on spines of *R. spinosissima*, 12 July 2019, C.M. Tian, Y.M. Liang & C. Peng (holotype BJFC-S1898, ex-type cultures CFCC 55164 = ROC 038, ROC 039, ROC 040).

Sexual morph: *Ascomata* 52–155 µm high × 102–254 µm diam, black, immersed, solitary or gregarious, fully or partly erumpent, globose, uniloculate. *Ostiole* 6.5–16.5 µm, single, dark grey to black. *Peridium* 22–68 µm wide, comprising 2 layers, outer most layer heavily pigmented, thick-walled, comprising dark brown cells of *textura angularis*, inner layer composed of hyaline, flattened cells of *textura angularis*. *Pseudoparaphyses* numerous, 1.6–2.7 µm wide, filamentous, branched. *Ascii* (86.5–91.5–99(–102.5) × (9–)10–11(–12.5) µm (av. = 96.7 ± 4.13 × 10.6 ± 1.16 µm), 8-spored, bitunicate, fissitunicate, clavate to cylindrical. *Ascospores* (21–)23.5–29(–30.5) × (3–)4.5–6(–7) µm (av. = 26.4 ± 2.21 × 5.4 ± 1.01 µm), overlapping biseriate, fusiform with narrow ends, mostly curved, 4–5-septate, constricted at the central septum, cells above central septum swollen, (3.5–)4.5–5.5(–6) × (4–)4.5–6 µm (av. = 5.1 ± 0.37 × 5.5 ± 1.02 µm). Asexual morph: *Acervuli conidiomata* solitary to gregarious, immersed when immature, becoming erumpent at maturity, unicellular, subglobose, up to 133–262 µm diam, 80–121 µm high, visible as black acervuli on the spines of *R. spinosissima*. *Conidiophores* cylindrical, branched at the base, smooth. *Conidiogenous cells* discrete or integrated, ampulliform, cylindrical or subcylindrical, hyaline, smooth, thick-walled, variable in size, (7–)9.5–24.5(–26.5) × (1–)1.5–2(–2.5) µm (av. = 16.5 ± 3.23 × 1.7 ± 0.97 µm). *Conidia* straight or slightly curved, cylindrical or subcylindrical, concolourous, 3-septate, without constrictions at the septa, transverse septa dark brown and fairly thick, smooth-walled, (10–)11–13.5(–14) × (2–)2.5–3.5(–4) µm (av. = 12.3 ± 0.51 × 2.9 ± 0.25 µm); basal cell obconic with a truncate base, pale brown to brown, (2–)2.5–3.5(–4) µm (av. = 2.6 ± 0.32 µm) long; middle cells cylindrical, pale brown to medium brown, second cell from base 2–3(–3.5) µm (av. = 2.7 ± 0.27 µm), third cell from base 2–3(–4) µm (av. = 2.4 ± 0.36 µm), together (5.5–)6–7(–8) µm (av. = 6.4 ± 0.41 µm) long; apical cell obtuse or conical, pale brown, (2–)2.5–3.5 µm (av. = 3.1 ± 0.31 µm); apical appendage single,



Fig. 18 Sexual morph of *Seimatosporium parvum* (BJFC-S1898, holotype). a. Disease symptoms; b. appearance of ascomata on host substrate; c–d. longitudinal section through ascomata; e. ascospores and pseudoparaphyses; f–g. ascospores; h–i. ascospores. — Scale bars: c–d = 50 µm; f–k = 10 µm.

unbranched, centric, (17)–19.5–22.5(–23) µm (av. = 21.3 ± 2.13 µm) long; basal appendage single, unbranched, excentric, (18)–19.5–28.5(–30) µm (av. = 25.8 ± 2.32 µm) long; mean conidium length/width ratio = 3.95 : 1.

Culture characteristics — Colonies on PDA flat with entire margin, colony yellow or pale yellow in the centre with fluffy aerial mycelia and pale white margin; reverse with yellow pigment. Colony 54–58 mm diam in 15 d at 28 °C. Conidiomata sparse, concentrically and irregularly distributed on the medium surface.

Additional materials examined. CHINA, Qinghai Province, Huangnan Tibetan Autonomous Prefecture, Zeku County, N37°18'60" E101°56'43", alt. 2899 m, on spines of *R. spinosissima*, 12 July 2019, C.M. Tian, Y.M. Liang & C. Peng (BJFC-S1899, cultures ROC 041, ROC 042, ROC 043); ibid., N37°18'56" E101°56'09", alt. 2910 m, on branches of *R. heleneae*, 13 July 2019, C.M. Tian, Y.M. Liang & C. Peng (BJFC-S1900, cultures CFCC 55165 = ROC 017, ROC 018, ROC 019, ROC 020).

Notes — *Seimatosporium parvum* is most closely related to *Seim. pseudorosae* which has also been reported from *Rosa* (Hyde et al. 2016) (Fig. 6). Pairwise comparison of the LSU sequence data reveals 7 bp difference from 668 (98.7 %, without gap region) between this species and *Seim. pseudorosae*.

Moreover, morphological differences between *Seim. parvum* and *Seim. pseudorosae* are obvious, namely *Seim. parvum* have smaller conidia (11–13.5 × 2.5–3.5 µm vs 12–17.5 × 4–6 µm). Furthermore, the basal appendages of *Seim. parvum* are longer than those of *Seim. pseudorosae* (19.5–28.5 µm vs 6–15 µm).

In addition to *Seim. pseudorosae*, *Seim. parvum* is separated from *Seim. rosae* which has also been reported from *Rosa* based on phylogenetic analysis (Norphanphoun et al. 2015) (Fig. 6). Furthermore, *Seim. parvum* differs from other *Seimatosporium* species associated with *Rosa* in producing thinner conidia (*Seim. parvum*: 2.5–3.5 µm vs *Seim. salicinum*: 4–6 µm and *Seim. rosae*: 3–4.5 µm) and having longer apical appendage (*Seim. parvum*: 19.5–22.5 µm vs *Seim. salicinum*: 9–14 µm and *Seim. rosae*: 5–10 µm). Although *Seim. caninum* is similar to *Seim. parvum* in conidial dimensions (9.5–12 × 4–5 µm vs 11–13.5 × 2.5–3.5 µm), the conidia of this species only have two septa and lack appendages, which make *Seim. caninum* easily distinguishable from other species of *Seimatosporium* (Nag Raj 1993).



Fig. 19 Asexual morph of *Seimatosporium parvum* (BJFC-S1898, holotype). a. Appearance of conidiomata on host substrate; b. appearance of conidiomata on host substrate; c. conidiomata formed on pine needles; d. colonies on PDA at 3 d (left) and 15 d (right); e–l. conidiogenous cells with attached conidia; m. conidia. — Scale bars: c = 200 μm ; e–m = 10 μm .

Key to *Seimatosporium* species on Rosa spp.

1. Conidia lacking appendages 2
1. Conidia with appendages at both ends 3
2. Conidia 2-septate *Seim. caninum*
2. Conidia 3-septate *Seim. discosiodes*
3. Appendages less than 8 µm 4
3. Appendages more than 8 µm 7
4. Conidia with appendages at both ends 5
4. Conidia without apical appendage, with or without basal appendage *Seim. nonappendiculatum*
5. Conidial length more than 15 µm 6
5. Conidial length less than 15 µm *Seim. rosae*
6. Mean conidium length/width ratio = 3.40 : 1, conidia 19.5–23.5 × 5.5–7 µm *Seim. centrale*
6. Mean conidium length/width ratio = 6.19 : 1, conidia 14.5–19.5 × 2.5–3 µm *Seim. gracile*
7. Mean conidium length/width ratio less than 6 8
7. Mean conidium length/width ratio more than 6 *Seim. parvum*
8. Conidia 3-septate, 12–17.5 × 3–6 µm *Seim. pseudorosae*
8. Conidia 2–3-septate, 11–17 × 4–6 µm *Seim. salicinum*

***Seiridium rosae* C. Peng & C.M. Tian, sp. nov.** — MycoBank MB 843821; Fig. 20

Etymology. The epithet reflects the name of the host plant genus *Rosa*.

Typus. CHINA, Ningxia Hui Autonomous Region, Guyuan City, Jingyuan County, N35°18'52" E106°21'53", alt. 2157 m, on branches of *R. rugosa*, 27 Aug. 2020, C.M. Tian, Y.M. Liang & C. Peng (holotype BJFC-S1903, ex-type cultures CFCC55174 = ROC 208, ROC 209).

Symptoms appeared as elongate and ovoid, red or dark red, raised, dehiscent lesions on twigs or branches (Fig. 20a–c). Sexual morph not observed. Asexual morph: *Acervular conidiomata* irregularly scattered over the surface, solitary to gregarious, immersed when immature, erumpent from tissue at maturity, subglobose to globose and occasionally irregular. *Conidiophores* septate, cylindrical, irregularly branched, mostly branched at the base. *Conidiogenous cells* discrete, hyaline, subcylindrical to cylindrical, smooth- and thin-walled, the size varies tremendously, (8–)12–64.5(–70) × (1–)1.5–2(–3) µm (av. = 27.8 ± 15.43 × 1.7 ± 0.16 µm). *Conidia* fusoid, straight or slightly curved, 5-septate, not striate, distoseptate without pores, bearing one or two basal and one or more apical appendages, (29–)31–35(–36.5) × (7–)8–9.5 µm (av. = 32.6 ± 0.83 × 8.8 ± 0.47 µm); basal cell obconic, hyaline, smooth-walled, with marginal frill, (3–)3.5–4.5 µm (av. = 4.1 ± 0.63 µm); four median cells brown, smooth-walled, cylindrical to doliform; second cell from base (4–)5.5–6.5(–7) µm (av. = 6.1 ± 0.21 µm); third cell (3–)4–5.5(–6) µm (av. = 4.9 ± 0.52 µm); fourth cell (3–)3.5–5.5(–6.5) µm (av. = 4.7 ± 0.68 µm), fifth cell (4–)6–7.5 µm (av. = 6.5 ± 0.48 µm), together (18–)20.5–24.5(–26) µm (av. = 22.8 ± 2.65 µm); apical cell conical, hyaline, smooth-walled, (3–)3.5–5.5(–7) µm (av. = 4.1 ± 1.05 µm) long; apical appendages single or multiple, centric, branched or unbranched, occasionally swollen at the tip, (27–)28.5–44.5(–46) µm (av. = 35.3 ± 4.68 µm); 1–2 basal appendages (mostly two), cylindrical, centric, occasionally eccentric, unbranched or branched, (2–)3–4.5 µm (av. = 3.7 ± 0.55 µm).

Culture characteristics — Colony on PDA with flattened mycelium, white, smoke grey in the centre, reverse with pale yellow pigments formed in concentric pattern. Colony 36–40 mm diam in 15 d at 25 °C, with concentrically distributed conidiomata.

Additional materials examined. CHINA, Ningxia Hui Autonomous Region, Guyuan City, Jingyuan County, N35°18'52" E106°21'55", alt. 2158 m, on branches of *R. rugosa*, 27 Aug. 2020, C.M. Tian, Y.M. Liang & C. Peng (cultures CFCC 55175 = ROC 267, ROC 268).

Notes — *Seiridium rosae* clustered in a well-supported independent clade (ML/MP/BI = 100/100/1) closely related to *Seir. aquaticum* and *Seir. venetum* (Fig. 7). *Seiridium rosae* can be distinguished from *Seir. venetum* in ITS (19 bp difference from 463 characters, with 95.8 % similarity, including 28 gaps) and TUB (7 bp difference from 365 characters, with 98.1 % similarity, including no gaps) sequences. Pairwise comparison of the ITS sequence data reveals 49 bp difference from 526 (90.6 % similarity, including 10 gaps) between our new species and the *Seir. aquaticum*. *Seiridium rosae* is distinct from *Seir. aquaticum* by its branched appendages, while *Seir. aquaticum* has conidia bearing single, short and unbranched appendage (Luo et al. 2019). Additionally, *Seir. rosae* has thinner conidia (8–9.5 µm vs 12–14 µm) and longer basal appendages (the basal appendages of *Seir. aquaticum* reduced to marginal frills) than *Seir. aquaticum* (Luo et al. 2019). *Seiridium venetum* can also produce conidia with branched apical appendages (Nag Raj 1985), but this species can be distinguished from *Seir. rosae* based on conidial dimensions (31–35 × 8–9.5 µm vs 20–30 × 6.5–8.5 µm).

Seiridium rosae morphologically resembles *Seir. pezizoides* (basionym: *Pestalotia pezizoides*) which was isolated from *Vitis* sp. in Italy and the USA having 5-distoseptate conidia with one or more, branched or unbranched apical appendages (Nag Raj 1985). However, *Seir. rosae* differs from *Seir. pezizoides* in having longer apical appendages (28.5–44.5 µm vs 8.5–27 µm) and shorter basal appendages (3–4.5 µm vs 5.5–14 µm). Besides, the conidia of *Seir. rosae* mostly bear two basal appendages while *Seir. pezizoides* only has one basal appendage (Nag Raj 1985, Marin-Felix et al. 2019). *Seiridium rosae* is also morphologically distinct from other *Seiridium* species associated with *Rosa* (i.e., *Seir. marginatum* and *Seir. rosarum*) (Jaklitsch et al. 2016, Wanasinghe et al. 2018). *Seiridium rosae* differs from *Seir. marginatum* in having smaller conidia (31–35 × 8–9.5 µm vs 38–42 × 8.8–10.2 µm), and differs from *Seir. rosarum* in having larger conidia (31–35 × 8–9.5 µm vs 22–28 × 7–9 µm) and longer conidiogenous cell (12–64.5 µm vs 5–20 µm) (Jaklitsch et al. 2016, Wanasinghe et al. 2018).

Key to *Seiridium* species on Rosa spp.

1. Conidia with one or more, branched or unbranched apical appendages *Seir. rosae*
1. Conidia with one unbranched apical appendage 2
2. Conidia 38.2–42 × 8.8–10.2 µm, appendages up to 52 µm long *Seir. marginatum*
2. Conidia 22–28 × 7–9 µm, appendages up to 12 µm long *Seir. rosarum*

***Sporocadus brevis* C. Peng & C.M. Tian, sp. nov.** — MycoBank MB 843822; Fig. 21

Etymology. The Latin 'brevis' meaning short, which refers to the conidial size.

Typus. CHINA, Gansu Province, Gannan Tibetan Autonomous Prefecture, Lintan County, Yeliguang, N34°53'43" E103°35'2", alt. 2808 m, on spines of *R. spinosissima*, 21 Aug. 2020, C. Peng & S. Jia (holotype BJFC-S1904, ex-type cultures CFCC 55170 = ROC 091, ROC 092, ROC 093).

Sexual morph not observed. Asexual morph: *Acervular conidiomata* solitary to gregarious, mostly irregular or subglobose, erumpent through the surface of bark when mature, up to 187–251 µm diam, visible as black acervuli on the spines. *Conidiophores* septate, branched at base, smooth, hyaline, mostly reduced to conidiogenous cells. *Conidiogenous cells* discrete or integrated, lageniform, filiform or ampulliform, sometimes irregular, hyaline, smooth, without annellations, (2.5–)3.5–19(–21) × 1–2(–2.5) µm (av. = 8.2 ± 3.62 × 1.6 ± 0.24 µm). *Conidia* straight or slightly curved, fusoid or obovoid, pale brown, mostly 2-septate, rarely 3-septate, septa fairly thick-walled and darker than

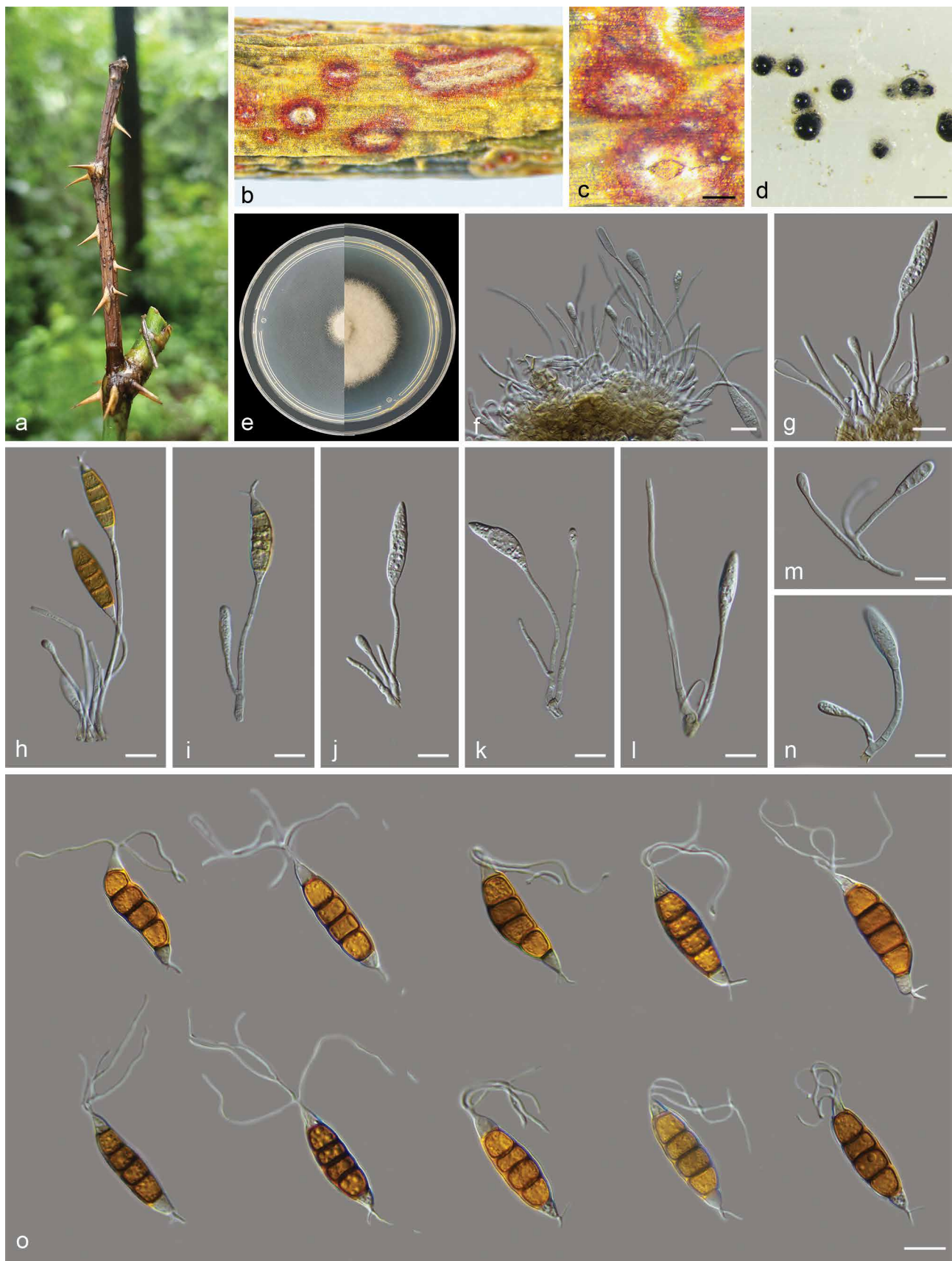


Fig. 20 *Seiridium rosae* (BJFC-S1903, holotype). a–b. Disease symptoms c. appearance of conidiomata on host substrate; d. conidiomata on PDA; e. colonies on PDA at 3 d (left) and 15 d (right); f–g. conidiomata on *Rosa rugosa*; h–n. conidiogenous cells with attached conidium; o. conidia. — Scale bars: c–d = 200 µm; h–o = 10 µm.



Fig. 21 *Sporocadus brevis* (BJFC-S1904, holotype). a. Disease symptoms; b–c. appearance of conidiomata on host substrate; d. conidiomata formed on pine needles; e. longitudinal section through conidiomata; f. colonies on PDA at 3 d (left) and 15 d (right); g–m. conidiogenous cells with attached conidia; n. conidia. — Scale bars: c–d = 200 µm; e = 50 µm; g–n = 10 µm.

the rest of the cell, wall smooth and occasionally slightly constricted at the septa, $(9\text{--}10)10\text{--}12(12.5) \times (6\text{--}6.5)7\text{--}7.5 \mu\text{m}$ (av. = $11.3 \pm 0.74 \times 6.4 \pm 0.22 \mu\text{m}$), lacking appendages; basal cell obconic with or without a truncate base, hyaline to pale brown, thick-walled, shorter than other cells, $1.5\text{--}3.5(4) \mu\text{m}$ (av. = $2.4 \pm 0.47 \mu\text{m}$) long; median cells doliform, each $(2\text{--}3)4.5(5) \mu\text{m}$ (av. = $3.7 \pm 0.43 \mu\text{m}$) long, pale to mid-brown; apical cell $(2.5\text{--}3)5(5.5) \mu\text{m}$ (av. = $4.2 \pm 0.68 \mu\text{m}$), short conic with a wide round apex, concolourous with the median cell in 2-septate conidia paler than median cells in 3-septate conidia; mean conidium length/width ratio = 1.76 : 1.

Culture characteristics — Cultures on PDA with aerial mycelium white, fluffy, reverse with a mottled tawny pigment. Colony 54–56 mm diam in 15 d at 28 °C. Conidiomata sparse and distributed irregularly on the medium surface.

Additional material examined. CHINA, Gansu Province, Gannan Tibetan Autonomous Prefecture, Lintan County, Yeliquan, N34°53'48" E103°35'2", alt. 2806 m, on spines of *R. spinosissima*, 21 Aug. 2020, C. Peng & S. Jia (BJFC-S1905, cultures ROC 094, ROC 095).

Notes — *Sporocadus brevis* is introduced based on multi-gene phylogenetic analysis, with five isolates clustering separately in a well-supported clade (ML/MP/BI = 100/100/1) (Fig. 8). *Sporocadus brevis* is most closely related to *Spo. trimorphus*, which was isolated from *R. canina* in Sweden (Liu et al. 2019), but distinguished based on ITS, *RPB2*, *TEF* and *TUB* loci from *Spo. trimorphus* by 34 bp in the concatenated alignment, in which 2 bp are distinct in the ITS region (from 506 characters, with 99.6 % sequence identity, including 1 gap), 5 bp in the *RPB2* region (from 832 characters, with 99.3 % sequence identity, no gaps), 11 bp in the *TEF* region (from 468 characters, with 97.6 % sequence identity, including 1 gap) and 16 bp in the *TUB* region (from 702 characters, with 97.7 % sequence identity, including 1 gap). Morphologically, *Spo. trimorphus* can produce conidia with appendages but the conidia of *Spo. brevis* lack appendages (Liu et al. 2019). Moreover, conidia of *Spo. brevis* are wider than those of *Spo. trimorphus* ($6.5\text{--}7 \mu\text{m}$ vs $3\text{--}4.5 \mu\text{m}$).



Fig. 22 *Sporocadus sorbi* (BJFC-S1906). a–b. Appearance of conidiomata on host substrate; c. conidiomata on PDA; d–g. conidiogenous cells with attached conidia; h. conidia. — Scale bars: c = 200 μm ; d–h = 10 μm .

In addition to *Sporocadus trimorphus*, *Spo. lichenicola*, *Spo. rosarum* and *Spo. rosigena* are also associated with *Rosa* spp. (Wanasinghe et al. 2018, Liu et al. 2019). *Sporocadus brevis* can be easily distinguished from these species by the conidial length (10–12 µm in *Spo. brevis* vs 18–25 µm in *Spo. lichenicola*) and width (6.5–7 µm in *Spo. brevis* vs 4–6 µm in *Spo. rosarum*, 3.5–6.5 µm in *Spo. rosigena*). Furthermore, the mean conidium length/width ratio of *Spo. brevis* is smaller than these four species (*Spo. brevis*: 1.76 : 1 vs *Spo. lichenicola*: 3 : 1, *Spo. rosarum*: 2.24 : 1, *Spo. rosigena*: 2.4 : 1 and *Spo. trimorphus*: 3.4 : 1).

***Sporocadus sorbi* (Wijayaw. et al.) F. Liu et al., Stud. Mycol. 92: 404. 2019 — Fig. 22**

Sexual morph not observed. Asexual morph: *Aceri*vular *conidiomata* solitary to gregarious, mostly subglobose, immersed to semi-immersed, up to 390–420 µm diam, 121–130 µm high, visible as black or dark red acervuli on the stems. *Conidiophores* septate, mostly branched at base, hyaline, smooth.

Conidiogenous cells discrete or integrated, sub-cylindrical or lageniform, variable in size, hyaline, smooth, with annellations, (7–)12–43.5(–48) × 1.5–2(–2.5) µm (av. = 17.2 ± 9.78 × 1.9 ± 0.34 µm). *Conidia* fusoid or obovoid, straight, 3-septate, transverse septa brown to dark brown, slightly constricted at the septa, wall smooth, (9.5–)11–15.5(–17) × (3–)3.5–5.5(–6) µm (av. = 13.7 ± 1.54 × 4.3 ± 0.21 µm), lacking appendages; basal cell obconic with or without a truncate base, hyaline to pale grey, 2–3(–3.5) µm (av. = 2.7 ± 0.38 µm) long; median cells mostly two, cylindrical, fairly thick-walled and pale brown, each 3–4.5(–5) µm (av. = 4.1 ± 0.54 µm) long; apical cell conic, hyaline or concolourous with median cells, 2–3(–4) µm (av. = 2.6 ± 0.32 µm) long; mean conidium length/width ratio = 3.18 : 1.

Culture characteristics — Colony on PDA with fluffy aerial mycelium, panniform, aerial mycelium white to pale brown, reverse umber coloured, being darker at the centre and paler at the edge. Colony 36–42 mm diam in 15 d at 25 °C. Conidiomata black, distributed circularly at the colony margin on the medium surface.

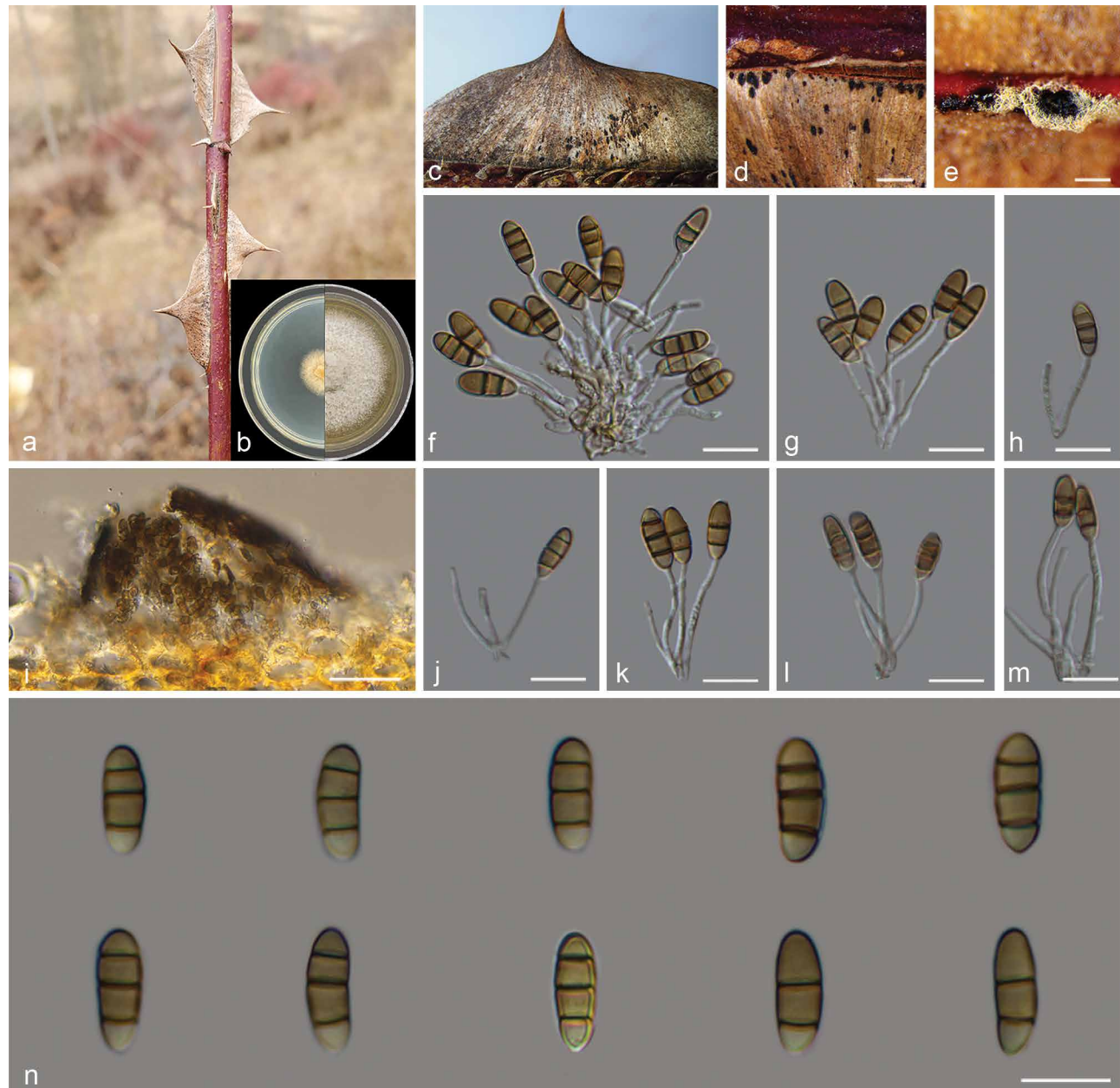


Fig. 23 *Sporocadus spiniger* (BJFC-S1908, holotype). a. Disease symptoms; b. colonies on PDA at 3 d (left) and 15 d (right); c–d. appearance of conidiomata on host substrate; e. conidiomata formed on pine needles; f–h, j–m. conidiogenous cells with attached conidia; i. longitudinal section through conidiomata; n. conidia. — Scale bars: e = 200 µm; f–h, j–m, n = 10 µm; i = 50 µm.

Materials examined. CHINA, Gansu Province, Lanzhou City, Yuzhong County, Xinglong Mountain, N35°48'2" E104°3'57", alt. 2160 m, on branches of *R. xanthina*, 26 Aug. 2020, C. Peng (BJFC-S1906, cultures ROC 102, ROC 103, ROC 105); Gansu Province, Gannan Tibetan Autonomous Prefecture, Lintan County, Yeliquan, N34°53'45" E103°35'2", alt. 2806 m, on spines of *R. xanthina*, 21 Aug. 2020, C. Peng & S. Jia (BJFC-S1907, cultures ROC 159, ROC 160, ROC 161).

Notes — *Sporocadus sorbi* was first reported from a dead leaf of *Sorbus torminalis* in Italy (Lawrence et al. 2018). In this study, six isolates of *Sporocadus* were identified as belonging to this species, and this is the first report of this fungus on *Rosa* plants, and in China.

Conidia of the ex-type (MFLUCC 14-0469) of *Spo. sorbi* are slightly wider than those of isolate ROC 101 (5.5–7.5 µm vs 3.5–5.5 µm), and it has shorter conidiogenous cells (8–20 µm vs 12–43.5 µm).

***Sporocadus spiniger* C. Peng & C.M. Tian, sp. nov.** — MycoBank MB 843823; Fig. 23

Etymology. Referring to the fact that this strain was isolated from spines.

Type. CHINA, Gansu Province, Lanzhou City, Yongdeng County, Dayou Town, N36°44'20" E102°49'27", alt. 2743 m, on spines of *R. omeiensis*, 25 Oct. 2020, C. Peng (holotype BJFC-S1908, ex-type cultures ROC 119, ROC 120, ROC 121).

Sexual morph not observed. Asexual morph: *Acervular conidiomata* solitary to gregarious, mostly irregular, occasionally subglobose, superficial to semi-immersed, up to 154–196 µm diam, 61–95 µm high, visible as black acervuli on the spines. *Conidiophores* septate, mostly branched at base, hyaline, smooth. *Conidiogenous cells* discrete, filiform or ampulliform, sometimes cylindrical and subcylindrical, hyaline, smooth, without annellations, (12–)14.5–30.5(–34) × 1–1.5 µm (av. = 23.8 ± 4.27 × 1.2 ± 0.18 µm). *Conidia* straight or slightly curved, clavate or subcylindrical, with round ends, pale brown, (2–)3-septate, septa darker than the rest of cell, wall smooth and slightly constricted at the septa, (12.5–)14.5–16.5(–17.5) × (4–)4.5–5(–5.5) µm (av. = 15.8 ± 0.54 × 4.9 ± 0.31 µm), lacking appendages; basal cell obconic with round base, hyaline to pale brown, paler than other cells, thick-walled, (2–)2.5–3.5(–4) µm (av. = 2.8 ± 0.21 µm) long; median cells doliiform, the second cell from base is slightly longer than the third cell in 3-septate conidia, 3.5–4.5 µm (av. = 4.2 ± 2.17 µm) vs 2.5–3 µm (av. = 2.7 ± 0.16 µm), pale to mid-brown; median cell 4.9–5.0 µm (av. = 5.0 ± 0.07 µm), pale brown in 2-septate conidia; apical cell in 2-septate conidia significantly longer than apical cell in 3-septate conidia, (5.5–)6–6.5 µm (av. = 6.2 ± 0.09 µm) vs (2–)2.5–3.5 µm (av. = 2.7 ± 0.31 µm), short conic with a wide round apex, concolourous with the median cells; mean conidium length/width ratio = 3.22 : 1.

Culture characteristics — Cultures on PDA with white aerial mycelium and regular margin, fluffy, reverse yellowish brown. Colony 48–52 mm diam in 15 d at 25 °C. Acervuli black, distributed irregularly at the colony margin on the medium surface.

Additional material examined. CHINA, Lanzhou City, Yongdeng County, Dayou Town, N36°44'17" E102°49'25", alt. 2745 m, on spines of *R. omeiensis*, 25 Oct. 2020, C. Peng (BJFC-S1909, cultures ROC 122, ROC 123, ROC 124, ROC 125).

Notes — Based on the multi-locus phylogenetic analysis, the seven isolates cluster separately in a well-supported clade (ML/MP/BI = 100/100/1) (Fig. 8). *Sporocadus spiniger* is most closely related to *Spo. brevis* and *Spo. trimorphus*, differentiated from them in ITS (three different unique fixed alleles in *Spo. brevis* (521/524, 99.4 % with no gaps) and three in *Spo. trimorphus* (503/506, 99.4 % with no gaps)), LSU loci (four bp in *Spo. brevis* (884/888, 99.5 % with a single gap) and eight bp in *Spo. trimorphus* (876/884, 99.0 % with no gaps)), *RPB2* loci (35 bp in *Spo. brevis* (812/847, 95.8 % with no gaps) and 39

bp in *Spo. trimorphus* (793/832, 95.3 % with no gaps)), *TEF* loci (40 bp in *Spo. brevis* (433/473, 91.5 % with 11 gaps) and 45 bp in *Spo. trimorphus* (427/472, 91.5 % with 11 gaps)) and *TUB* loci (45 bp in *Spo. brevis* (663/708, 93.6 % with 10 gaps) and 41 bp in *Spo. trimorphus* (667/708, 94.2 % with 10 gaps)). Moreover, *Spo. spiniger* differs from *Spo. brevis* in having longer conidia (14.5–16.5 µm vs 10–12 µm) and conidiogenous cells (14.5–30.5 µm vs 3.5–19 µm). The conidia are also wider than those of *Spo. trimorphus* (4.5–5 µm vs 3–4.5 µm).

Other species of *Sporocadus* that have been recorded from *Rosa* can be distinguished from this new species based on the number of septa and presence or absence of appendages. While *Spo. spiniger* has mostly 3-septate conidia without appendages, *Spo. lichenicola* has 4–5-septate conidia and *Spo. rosarum* has conidia with one apical appendage (Liu et al. 2019). *Sporocadus rosigena* mostly has 3-septate conidia without appendages that are morphologically similar to those of *Spo. spiniger* (Liu et al. 2019), but these two species have a distinctly different mean conidium length/width ratio (*Spo. spiniger*: 3.22 : 1 vs *Spo. rosigena*: 2.4 : 1).

***Sporocadus trimorphus* F. Liu et al., Stud. Mycol. 92: 406. 2018 — Fig. 24**

Sexual morph not observed. Asexual morph: *Acervular stromata* ostiolate, immersed or semi-immersed in plant tissues, slightly to strongly erumpent through the bark surface, sometimes delimited by a black or dark red marginal line, up to 207–269 µm diam, 82–144 µm high. *Conidiophores* septate, mostly branched at base, hyaline, smooth. *Conidiogenous cells* discrete or integrated, sub-cylindrical, lageniform or ampulliform, hyaline, smooth, with annellations, (11.5–)13–34(–38.5) × 1.5–2.5 µm (av. = 24.5 ± 6.43 × 2.0 ± 0.31 µm). *Conidia* fusoid or obovoid, straight, 3-septate, transverse septa fairly thick, wall smooth, (11–)12–16 × 4.5–5.5 µm (av. = 14.1 ± 1.22 × 4.8 ± 0.14 µm), bearing appendages; basal cell obconic with or without a truncate base, hyaline to pale brown, 2–3 µm (av. = 2.7 ± 0.41 µm) long; median cells mostly two, cylindrical, fairly thick-walled and pale brown, each (3–)3.5–4.5(–5) µm (av. = 4.1 ± 0.88 µm) long; apical cell conic, hyaline or concolourous with median cells, (1.5–)2–3.5(–4.5) µm (av. = 2.7 ± 0.28 µm) long; apical appendage lacking or, when present, single, unbranched, attenuated, tubular or flexuous, (6.5–)8–13.5 µm (av. = 11.3 ± 1.39 µm) long; basal appendage lacking or, when present, unbranched, tubular or flexuous, centric or excentric, (7–)9–12(–13.5) µm (av. = 10.4 ± 1.27 µm) long; mean conidium length/width ratio = 2.94 : 1.

Culture characteristics — On PDA, colonies initially white, irregular, lacking aerial mycelium, fast growing, reaching up to 60–62 mm diam in 15 d. Colonies pale white to pale grey after 15 d, lacking aerial mycelium. Conidiomata distributed sparsely over the medium surface.

Material examined. CHINA, Gansu Province, Lanzhou City, Yuzhong County, Xinglong Mountain, N35°47'37" E104°3'53", alt. 2168 m, on branches of *R. xanthina*, 25 Aug. 2020, C. Peng (BJFC-S1910, cultures CFCC 55171 = ROC 112, ROC 113, ROC 114, ROC 115, ROC 116).

Notes — *Sporocadus trimorphus* was first described from *R. canina* in Sweden (Liu et al. 2019). In this study, five isolates were identified as belonging to this species and this species is also reported for the first time from China. *Sporocadus trimorphus* is characterised by three conidial types, i.e., non-appendaged, either apical or basal appendaged, and both apical and basal appendaged conidia (Liu et al. 2019).

Compared with the description of the ex-type isolate CBS 114203, isolate CFCC 55171 has shorter apical appendages (8–13.5 µm vs 2–20 µm), slightly wider conidia (4.5–5.5 µm vs 3–4.5 µm) and longer conidiogenous cells (13–34 µm vs 4.5–14 µm).

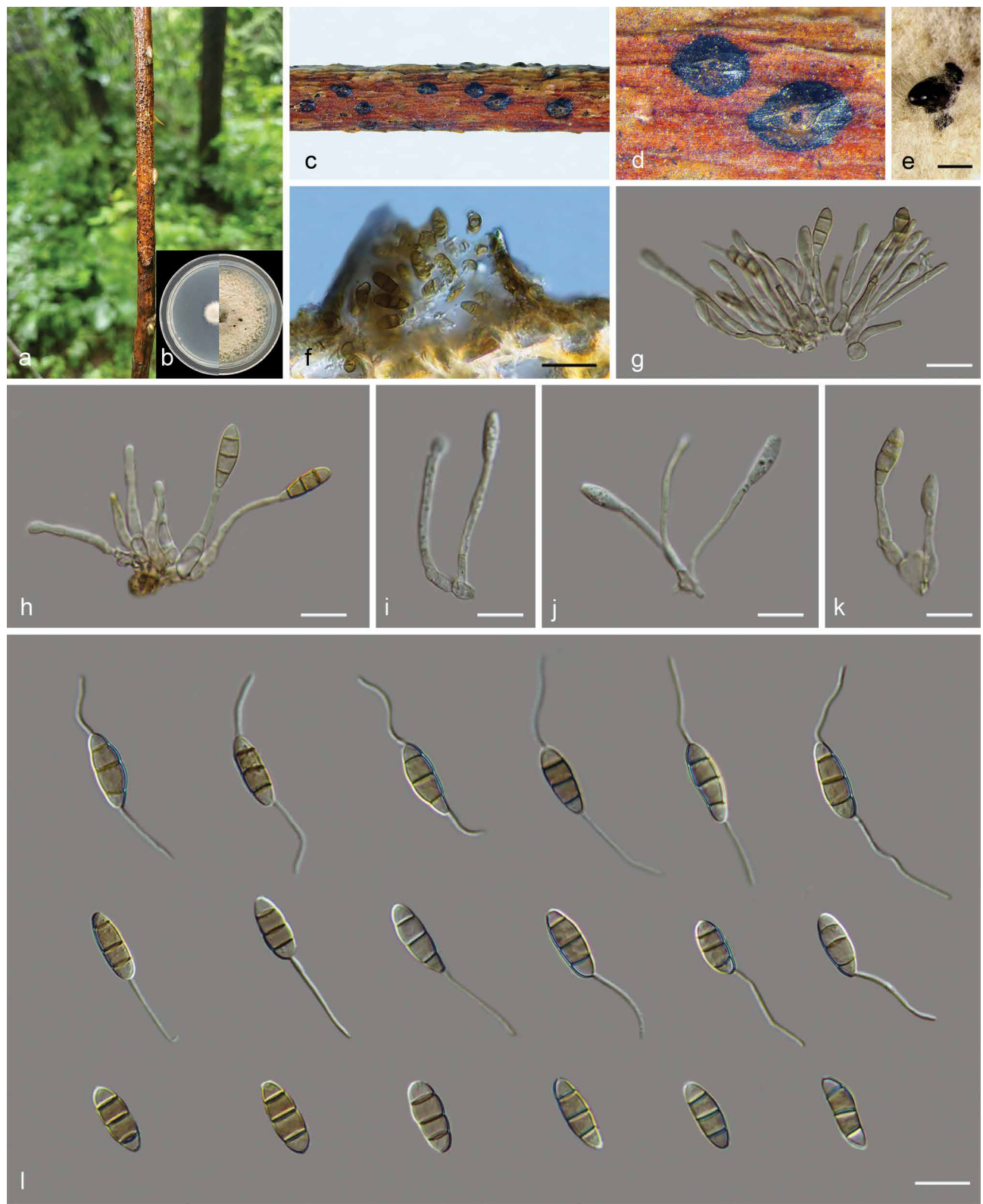


Fig. 24 *Sporocadus trimorphus* (BJFC-S1910). a. Disease symptoms; b. colonies on PDA at 3 d (left) and 15 d (right); c–d. appearance of conidiomata on host substrate; e. conidiomata on PDA; f. longitudinal section through conidiomata; g–k. conidiogenous cells with attached conidia; l. conidia. — Scale bars: e = 200 µm; f = 20 µm; g–l = 10 µm.

Key to Sporocadus species on Rosa spp.

1. Conidia with appendages	2
1. Conidia lacking appendages	6
2. Conidia 3–5-septate	<i>Spo. lichenicola</i>
2. Conidia 3-septate	3
3. Mean conidium length/width ratio less than 3	4
3. Mean conidium length/width ratio more than 3	5
4. Conidia 10–12 × 6.5–7 µm	<i>Spo. brevis</i>
4. Conidia 10–15 × 3.5–6.5 µm	<i>Spo. rosigena</i>
5. Conidia 11–15.5 × 3.5–5.5 µm, conidiogenous cells 11.0–28.5 × 1.0–1.7 µm	<i>Spo. sorbi</i>
5. Conidia 14.5–16.5 × 4.5–5 µm, conidiogenous cells 14.5–30.5 × 1.0–1.5 µm	<i>Spo. spiniger</i>
6. Conidia of two types, i.e., non-appendaged or only basal appendaged	<i>Spo. rosarium</i>
6. Conidia of three types, i.e., non-appendaged, either apical or basal appendaged, or both apical and basal appendaged conidia	<i>Spo. trimorphous</i>

Prevalence

Pestalotiopsis was the most prevalent genus (45 isolates, 35.2 % of the total isolates from *Rosa*), followed by *Seimatosporium* (33 isolates, 26.2 %) and *Sporocadus* (23 isolates, 18.3 %). The isolation rate of the other genera varied from 3.1 % to 13.5 % (Fig. 25). *Pestalotiopsis* was also the most abundant genus in all tissues investigated and had the highest isolation rate from all tissues. *Seiridium* was the genus with the lowest richness among all tissues, isolated only from branches (Fig. 26).

Fifteen species present in six genera (*Monochaetia*, *Neopestalotiopsis*, *Pestalotiopsis*, *Seimatosporium*, *Seiridium* and *Sporocadus*) were identified. *Pestalotiopsis chamaeropis* and *Pes. rhodomyrtus* (18 isolates, 14 % of the isolates from *Rosa*) were the two most prevalent species, followed by *Seim. parvum* (10 isolates, 8 %). *Neopestalotiopsis concentrica*, *Seim. centrale* and *Seim. gracile* have the same isolation rate of 7 %. In the current study, *N. concentrica*, *N. subepidermalis*, *Pes. rhodomyrtus* and *Seim. parvum* were isolated from spines/branches of two and three species of *Rosa*. Each of the remaining 11 species of *Sporocadaceae* was only isolated from one *Rosa* species (Fig. 29).

The isolation rate of *Seimatosporium* in fruits and *Pestalotiopsis* in leaves was 100 %. These data reveal low generic and species diversity in these plant organs. In contrast, the branches had the highest genus diversity among all organs in this study, except for *Seimatosporium*, the other five genera were isolated from branches. Although the generic diversity of spines was slightly lower than that of branches, the number of strains isolated from the spines and the species diversity of spines was the highest of all tissues and was much higher than that of any other tissues (Fig. 26, 27).

Analysis of the abundance of *Sporocadaceae* species on *Rosa* species revealed seven species from *R. chinensis*, four from *R. rugosa*, three from *R. xanthina* and two from *R. spinosissima*, respectively (Fig. 29), with only one species on the remaining *Rosa* species, namely *R. multiflora* (*Pes. rhodomyrtus*), *R. helenae* (*Seim. parvum*), *R. laevigata* (*Seim. nonappendiculatum*) and *R. omeiensis* (*Spo. spiniger*) (Fig. 29). These findings might be due to the smaller sampling size of *R. multiflora*, *R. helenae*, *R. laevigata* and *R. omeiensis* obtained, since symptomatic branches were far less commonly observed than for the other *Rosa* species.

DISCUSSION

In this study, many *Rosa* specimens were collected from six major rose production areas (Gansu, Henan, Hunan, Ningxia, Qinghai and Shaanxi) in China, and 126 pestalotioid strains were obtained elsewhere. Multi-locus phylogenetic and morphological analyses revealed 15 species belonging to six genera in *Sporocadaceae*, namely *Monochaetia*, *Neopestalotiopsis*, *Pestalotiopsis*, *Seimatosporium*, *Seiridium* and *Sporocadus*.

Seimatosporium species have been extensively studied on several hosts (Tanaka et al. 2011, Liu et al. 2019), but not yet on *Rosa* spp. Up to now, five species of *Seimatosporium* have been recorded from *Rosa*, namely *Seim. caninum* on *R. canina*, *Seim. pseudorosae* on *R. villosa*, *Seim. salicinum* on *R. multiflora* and *R. spinosissima*, *Seim. rosae* on *R. canina*, *R. kalmiussica*, *R. mucosa* and *R. pomifera*, *Seim. discosiodes* on *R. blanda*, *R. heliophila*, *R. moschata*, *R. multiflora* and *R. rugosa* (Weiss 1950, Nag Raj 1993, Cho & Shin 2004, Kobayashi 2007, Li et al. 2016, Crous et al. 2018, Liu et al. 2019). Among them, *Seim. salicinum* has been recorded in China (Tai 1979). In this study, a total of four new *Seimatosporium* species were introduced from *Rosa* in China. *Seimatosporium* is the genus which has the most species found and has a relatively high isolation rate (26.2 %) (Fig. 25). *Seimatosporium* species from *Rosa* spp. in previous and present studies show quite a difference based on morphology and DNA sequence data. *Seimatosporium rosae* is distinguished from the four new species in this study based on DNA phylogenetic data (Fig. 6) and the number of conidial septa (3–6-septate vs 3-septate). Although *Seim. pseudorosae* is closely related to *Seim. parvum* in this study (Fig. 6), these two species can be clearly distinguished by the size of their conidia and the length of their appendages. There are no sequence data available for *Seim. caninum* and *Seim. salicinum* for comparison, but the morphological characteristics of *Seim. caninum* (appendages lacking, 2-septate conidia) clearly distinguish it from other *Seimatosporium* species (Nag Raj 1993). *Seimatosporium salicinum* also produces 2-septate conidia (Sutton 1975, Nag Raj 1993), and this morphological characteristic distinguishes it from our four new species. Except for *Seim. salicinum* (the main hosts are *Salix* spp. and *Rosaceae* plants) (Nag Raj 1993, Tanaka et al. 2011), the other species from *Rosa* spp. are rarely recorded on other hosts (Nag Raj 1993, Muñenko et al. 2008, Li et al. 2016, Bonthond et al. 2018). Currently, seven *Seimatosporium* species have been reported from China besides our new species and *Seim. salicinum*. However, none of them occur on *Rosa* spp., i.e., *Seim. botan*, *Seim. graminitum* and *Seim. hebeiensis* on *Paeonia suffruticosa*, *Seim. lonicerae* on *Pinus tabulaeformis*, *Seim. rhododendri* on *Rhododendron aureum*, *Seim. piceae* on *Picea jezoensis* and *Seim. maria* (Tai 1979, Wang 1985, Nag Raj 1993, Guo 2004, Duan et al. 2011). Among these species, *Seim. botan* can produce conidia with only basal appendages (Hatakeyama & Harada 2004), which is similar to *Seim. nonappendiculatum*, to which it formed a sister clade. *Seimatosporium graminitum* and *Seim. hebeiensis* produce conidia lacking appendages and are therefore similar to *Seim. nonappendiculatum*. However, they differ significantly in their conidial dimensions. Having conidia with only basal appendages or without appendages, makes *Seim. nonappendiculatum* unique in the *Sporocadaceae*, and phylogenetically it clustered closer *Sporocadus* (conidia lacking appendages) than other *Seimatosporium* species (Fig. 2). The most typical morphological characteristics of *Seim. piceae* is that the length of the appendages is longer than the conidia itself (Wang 1985), which is most similar to the new species *Seim. parvum* (Fig. 6), but the conidia and appendages of *Seim. parvum* are significantly shorter than *Seim. picea* (14.3–15 × 4.21–4.34 µm vs 18–23 × 5–7 µm). In addition, the conidial dimensions of the other two new species,

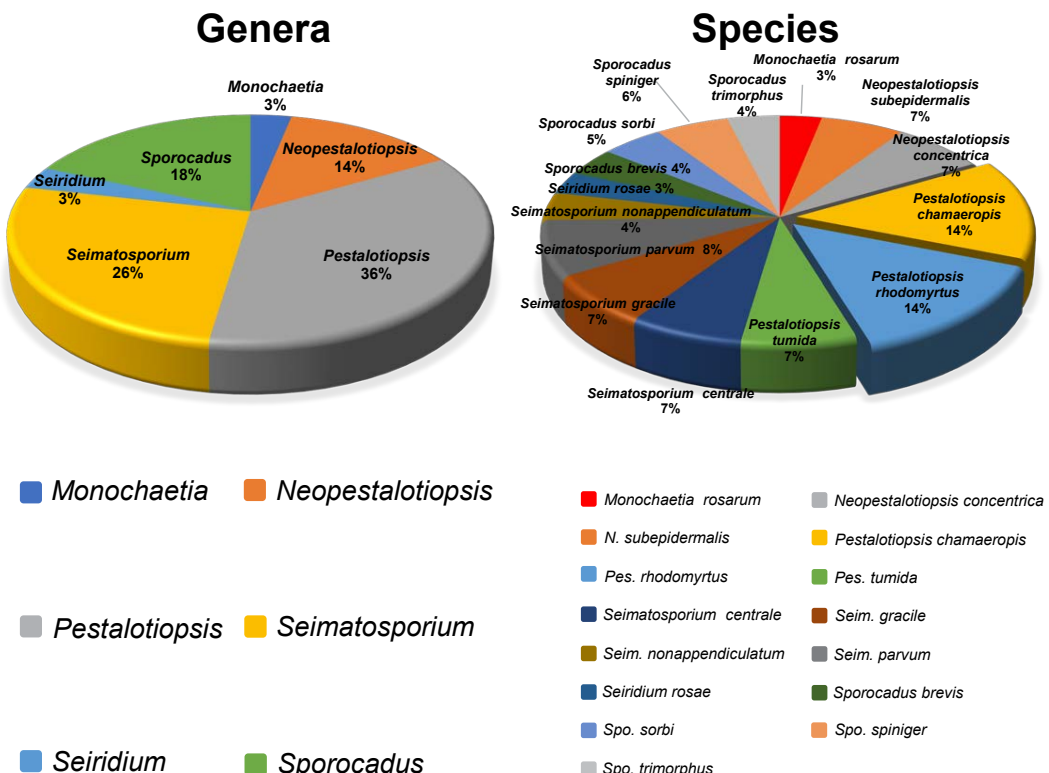


Fig. 25 Overall isolation rate (%) of Sporocadaceae genera and species.

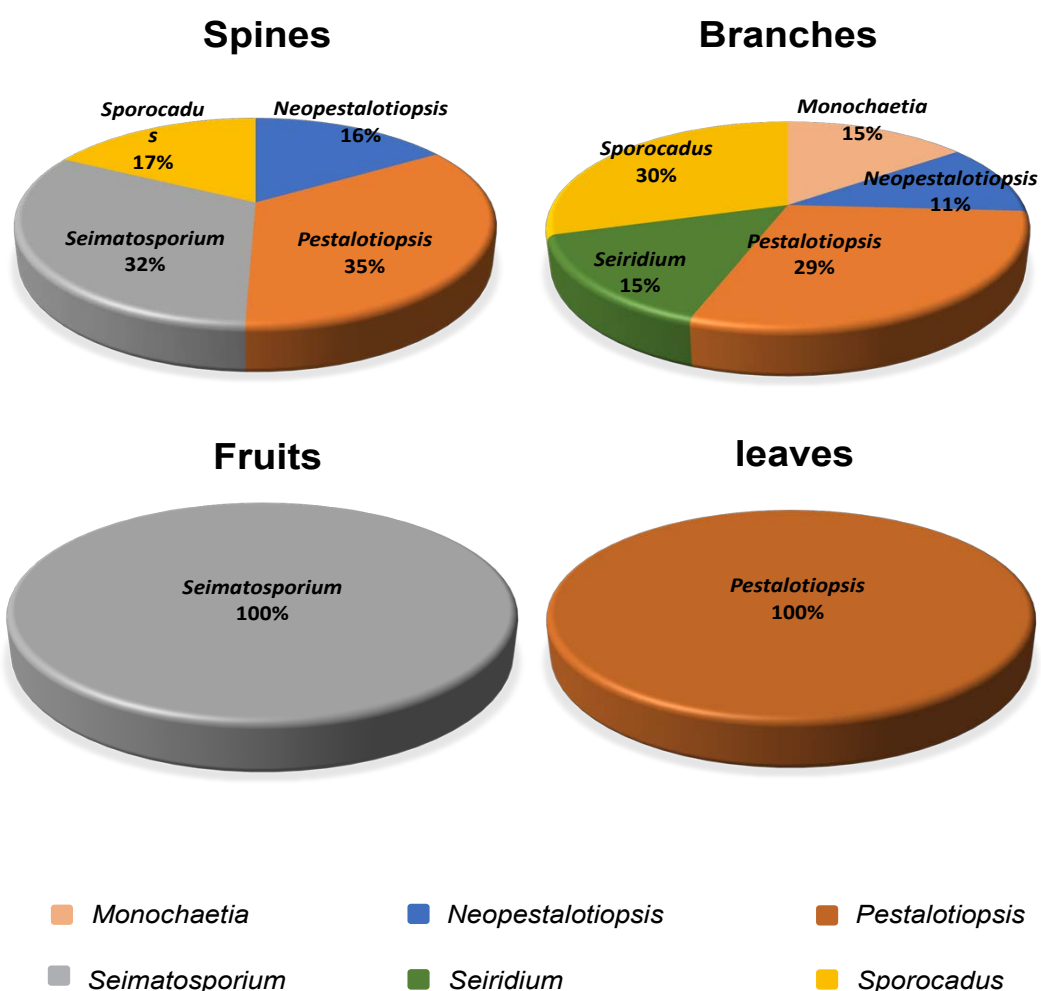


Fig. 26 Isolation rate (%) of Sporocadaceae genera from each Rosa organ.

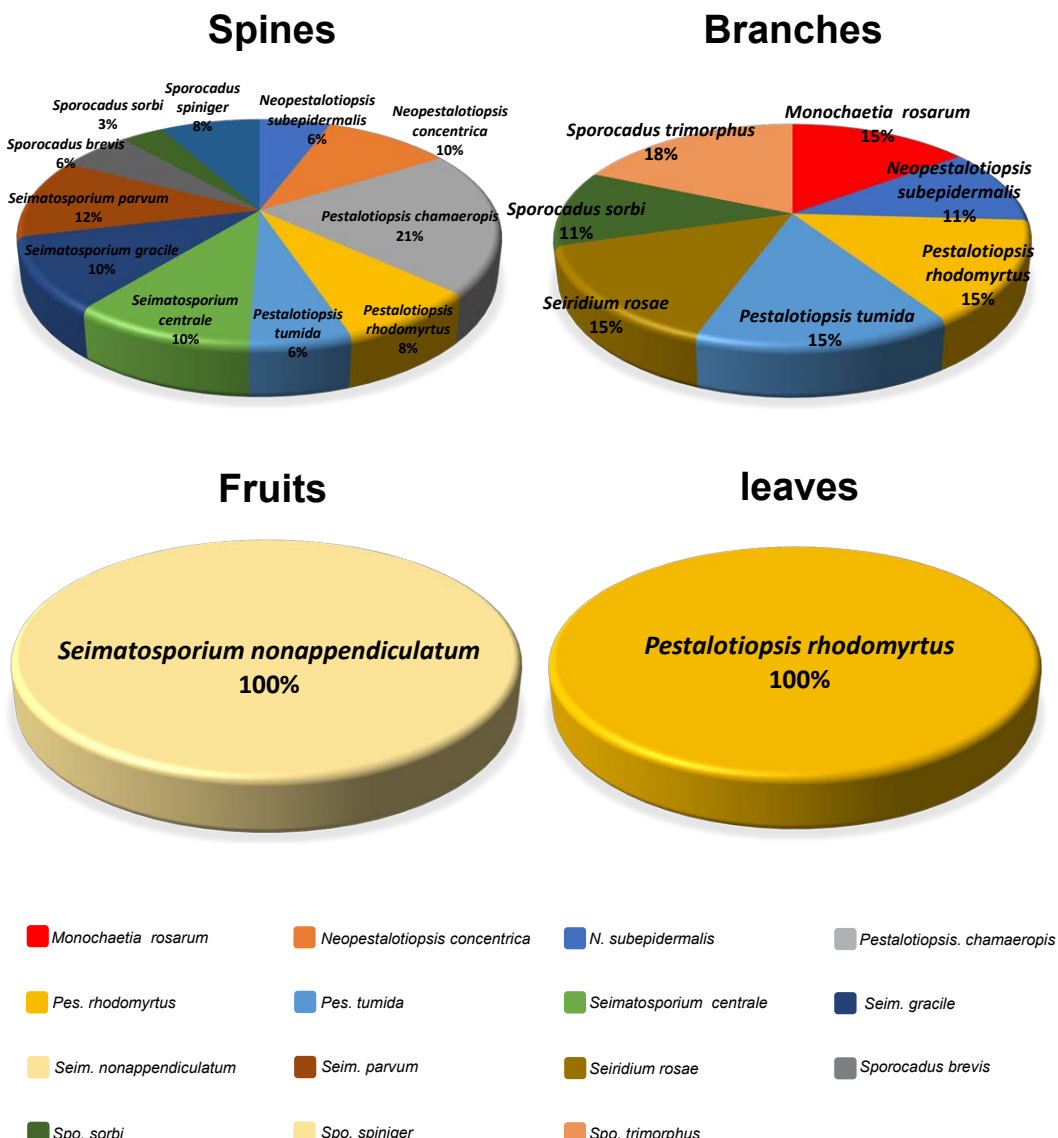


Fig. 27 Isolation rate (%) of Sporocadaceae species from each *Rosa* organs.

Seim. centrale and *Seim. gracile*, are significantly different from those species currently recorded in China.

Sporocadus is the type of Sporocadaceae and generally characterised by non-appendaged, 3-septate conidia (Liu et al. 2019). *Sporocadus* has long been assumed to be a synonym of *Seimatosporium* (Sutton 1975), but was confirmed to be a separate genus based on multigene phylogeny and conidial morphology (Brockmann 1976, Nag Raj 1993, Liu et al. 2019, Wijayawardene et al. 2020). However, in this study, although ITS-Blast is useful to locate species at the generic and family level, relatively weak in distinguishing *Seimatosporium* from *Sporocadus*, and even less so at the species level. Therefore, analysing these two genera at the family level is necessary to classify species into the correct genus (Fig. 2). Corresponding to the taxonomic classification determined by multi-locus phylogenetic analyses (Fig. 2), most *Sporocadus* species also exhibit characteristic morphological characters, including their non-appendaged and 3-septate conidia. In previous studies, most of these features have been used to delimit this genus (Brockmann 1976, Nag Raj 1993). It is worth to note that the presence or absence of conidial appendages is not a stable taxonomic character for the genus (Liu et al. 2019). For example, the conidia of *Seim. discosiooides* and *Seim. germanicum* are also non-appendaged (Shoemaker 1964, Liu et al. 2019). Liu et al. (2019) introduced *Spo. trimorphus* and the conidia

of this species have three types, i.e., non-appendaged which is the typical morphological characteristics of this genus; both apical and basal appendaged conidia which is the typical characteristics of *Seimatosporium* and either apical or basal appendaged conidia. This was also the first time that species with appendaged conidia were observed in *Sporocadus*, which renders morphology-based identifications more difficult, and underlines the necessity of molecular data for accurate identification. This study also found *Spo. trimorphus* on *R. xanthina*, which is also a first report from China. The other important morphological characteristic of this genus is 3-septate conidia (Nag Raj 1993). However, the number of conidial septa is far too unstable a feature to determine generic delineations. Liu et al. (2019) were the first to suggest that *Sporocadus* species could produce 2-septate conidia and introduced five species with this conidial type, namely *Spo. biseptatus*, *Spo. incanus*, *Spo. rosarum*, *Spo. rosigena* and *Spo. rotundatus*. Although the newly described species *Spo. brevis* can also produce conidia with two septa, this species is phylogenetically distinct from these five species (Fig. 8) and has significantly wider conidia (Table 5). To our knowledge, this study represents the first resolution of *Sporocadus* species in China based on multi-locus sequence data. A total of four species of *Sporocadus* were identified in this study, and the isolation rate is similar to that of *Seimatosporium* (Fig. 25). Besides *Spo. brevis* and

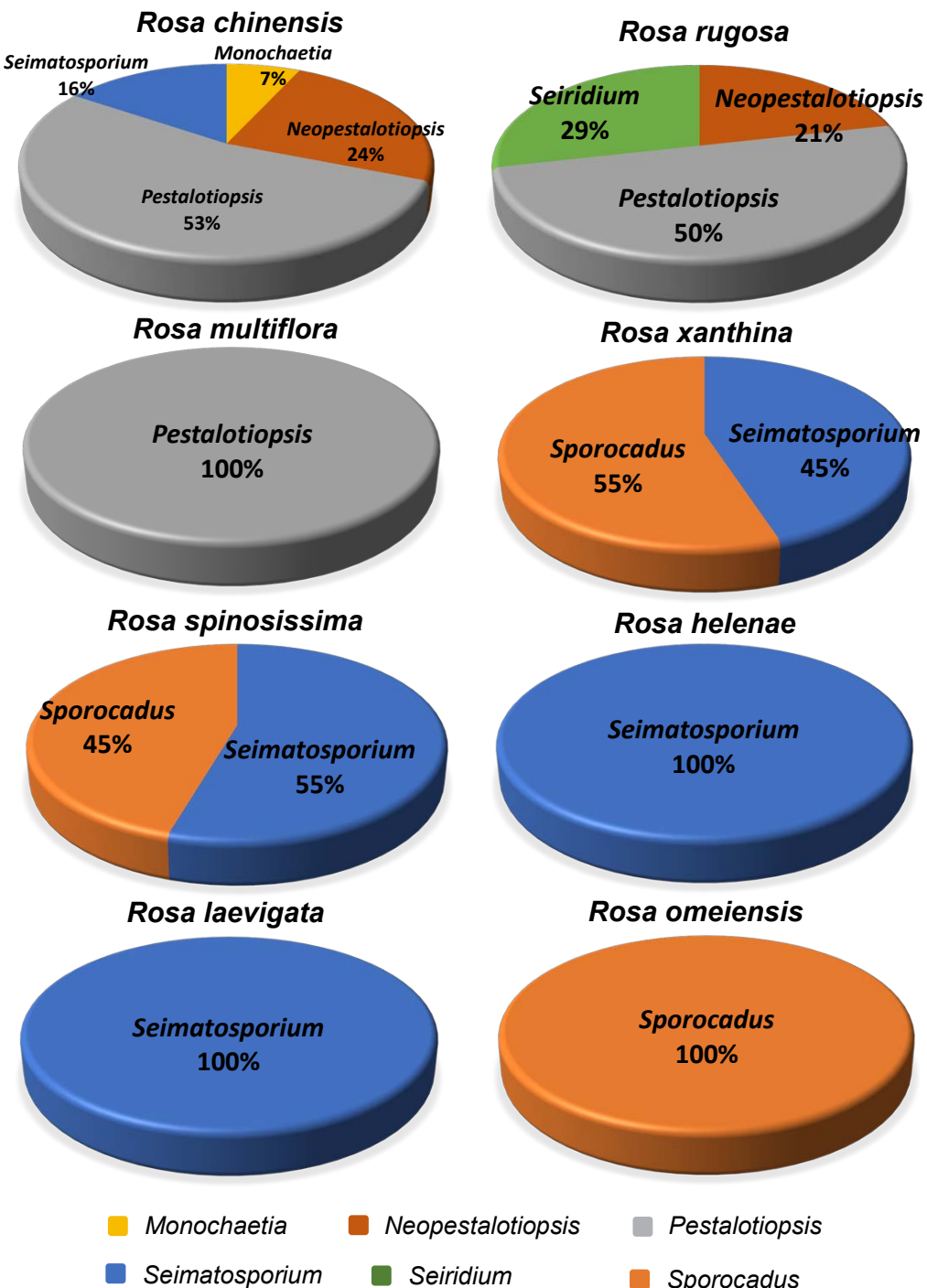


Fig. 28 Isolation rate (%) of Sporocadaceae genera from each *Rosa* sp.

Spo. trimorphus, this study also described a new species *Spo. spiniger*, and represents the first report of *Spo. sorbi* on *Rosa* globally. Currently, only one *Sporocadus* species has been reported from China, namely *Spo. lichenicola*, the type species of the genus (Tai 1979). The hosts of this species include many *Rosa* plants and can cause leaf spot or brown spot of *R. xanthina* in China (Tai 1979, Wu 1992, Chen 2003). Based on multigene phylogenetic analyses, *Spo. lichenicola* is also separated from the two new species (Fig. 8). Moreover, the conidia of *Spo. lichenicola* are 4–5-septate, which is also an important morphological characteristic distinguishing it from other species in *Sporocadus* (Norphanphoun et al. 2015). In addition to *Spo. lichenicola*, relatively little has been recorded about *Sporocadus* species associated with *Rosa*. Liu et al. (2019) transferred four *Seimatosporium* species associated with *Rosa* to *Sporocadus* based on molecular systematics and mor-

phological characteristics, namely *Spo. rosarum* (synonyms: *Seim. rosarum*, *Seim. pseudorosarum* and *Seim. rosigenum*) and *Spo. rosigena* (basionym: *Seim. rosicola*). *Sporocadus rosarum* forms a large sister clade with the two new species and *Spo. trimorphus* (Fig. 8), but the conidia of *Spo. rosarum* have an apical appendage, which makes it easy to distinguish them from other species of *Sporocadus* (Wanasinghe et al. 2018, Liu et al. 2019). *Sporocadus rosigena* is separated from the two new species in this study based on DNA phylogeny (Fig. 8) and there are also differences in conidial dimensions. It is remarkable that *Seim. caninum* isolated from *R. chinensis* has the typical morphological characteristics of *Sporocadus*, that is, with conidia lacking appendages (Sutton 1975). The feature of 2-septate conidia distinguishes *Seim. caninum* from other species in *Seimatosporium* and most of the members in *Sporocadus*. As described above, six *Sporocadus* species

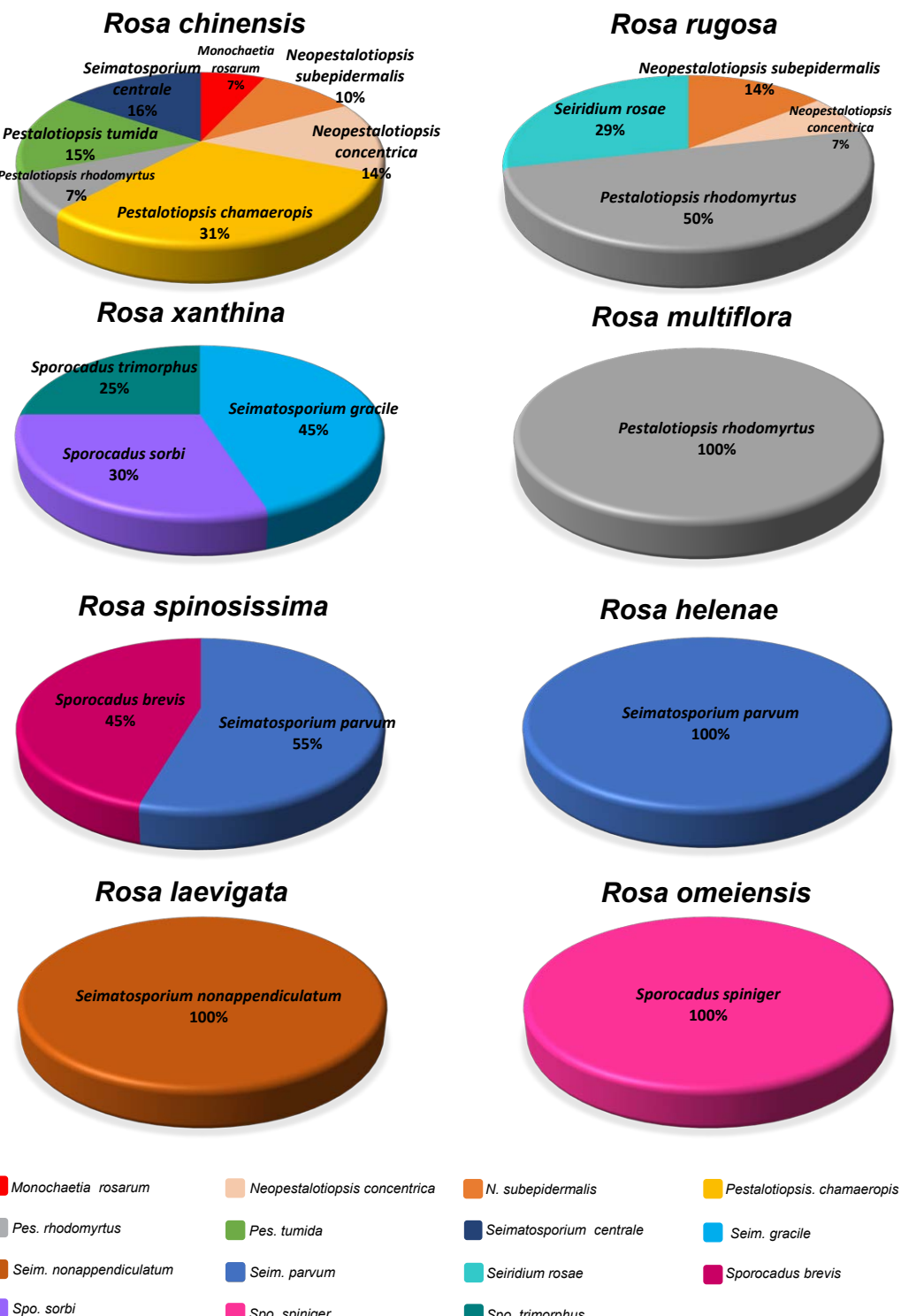


Fig. 29 Isolation rate (%) of Sporocadaceae species from each Rosa sp.

(including the new species described here) can produce 2-septate conidia similar to those of *Seim. caninum*, but the conidia of *Seim. caninum* are smaller than those of other species (Table 5). Therefore, since related sequence data of *Seim. caninum* are unavailable, further research is needed to resolve which genus it belongs to.

Pestalotiopsis is the genus with the highest isolation rate in this study, namely 29.6 % (Fig. 25), which is basically in line with expectations, because *Pestalotiopsis*, as an important plant pathogen, has many records and can parasitise more than 50 plant families in China (Tai 1979, Chen 2003, Ge et al. 2009). Cash crops such as palm, eucalypts, guava and tea trees have suffered serious damage due to species of *Pestalotiopsis* (Ge et al. 2009, Maharachchikumbura et al. 2013a, Wang et al.

2019a, b). This genus also has many records on *Rosa* plants. In China, five species of *Pestalotiopsis* have been recorded from *Rosa*, namely *Pes. rosae* and *Pes. suffocata* that are parasitic on *R. chinensis*, *Pes. oleandri* that is parasitic on *R. laevigata*, *Pes. longisetula* that is parasitic on *R. henryi* and *Pes. aquatica* that is saprophytic on *R. chinensis* (Zhu et al. 1991, Wei et al. 2005, Ge et al. 2009). Beyond that, there are six species of *Pestalotiopsis* recorded from *Rosa* in different countries (Riley 1960, Guba 1961, Mathur 1979, Rai 1990, Nag Raj 1993, Mendes et al. 1998, Sameva 2004, Kobayashi 2007). In this study, *Pes. chamaeropis* and *Pes. rhodomyrtus* are newly reported from *Rosa*. For the newly described species, *Pes. tumida* isolated from *R. chinensis*, morphological differences distinguish this species and other known species

Table 5 Synopsis of *Seimatosporium caninum* and species with 2-septate conidia in *Sporocadus*.

Species	Length of conidia (μm)	Width of conidia (μm)	Host	Country	References
<i>Seimatosporium caninum</i>	9.5–12	4.5–5.5	<i>Quercus incana</i>	India	Sutton (1975)
<i>Sporocadus biseptatus</i>	12.5–19.5	4.5–9	Unknown	Unknown	Liu et al. (2019)
<i>Spo. brevis</i>	10–12	6.5–7	<i>Rosa spinosissima</i>	China	Present study
<i>Spo. incanus</i>	11.5–20	4.5–6.5	<i>Prunus dulcis</i>	Spain	Liu et al. (2019)
<i>Spo. rosarum</i>	9.0–14.0	4.0–6.0	<i>Rosa canina</i>	Europe	Liu et al. (2019)
<i>Spo. rosigena</i>	10.0–15.0	3.5–6.5	<i>Vitis vinifera</i> <i>Rosa canina</i> <i>Rhododendron</i> sp. <i>Rubus fruticosus</i>	Iran Italy Latvia Netherlands	Liu et al. (2019) Liu et al. (2019) Liu et al. (2019) Liu et al. (2019)
<i>Spo. rotundatus</i>	9.0–16.5	4.5–7.5	<i>Arceuthobium pusillum</i>	Canada	Liu et al. (2019)

* Newly described taxon is in **bold**.

recorded on *Rosa*, especially in terms of the conidial dimensions and length of the appendages, as well as shape of basal appendages. The results of our study suggest that the species diversity of *Pestalotiopsis* on *Rosa* in China may be higher than what was previously expected.

Neopestalotiopsis was separated from *Pestalotiopsis* based on its versicolourous median conidium cells and indistinct conidiophores (Maharachchikumbura et al. 2014, Liu et al. 2017, 2019). In this study, two new species of *Neopestalotiopsis* were introduced from *Rosa* based on the phylogenetic analyses and morphological characteristics, namely *N. concentrica* and *N. subepidermalis*. Five *Neopestalotiopsis* species associated with *Rosa* have been recorded, namely *N. clavispora*, *N. palmarum*, *N. rosae*, *N. rosicola* and *N. versicolor* (Liu et al. 2010, Feng et al. 2014, Maharachchikumbura et al. 2014, Jiang et al. 2018, Vu et al. 2019). For these five species, *N. clavispora*, *N. palmarum*, *N. rosicola* and *N. versicolor* have been reported in China and cause leaf blotch, stem canker of *R. chinensis* and leaf spot disease of many other hosts (Ge et al. 2009, Feng et al. 2014, Jiang et al. 2018), but these four species are phylogenetically separated from our new species (Fig. 4) and there are also differences in their conidial morphology. *Neopestalotiopsis rosae* is morphologically quite distinct from other taxa in the genus (has appendages which do not arise from the apical crest, but at different regions in the upper half of the apical cell; Maharachchikumbura et al. 2014). With the increase of collections and DNA data, *N. clavispora*, *N. palmarum*, *N. rosae* and *N. versicolor* appear to be widely distributed in different countries where they cause severe diseases on different hosts, e.g., *N. rosae* causes dieback, crown rot, fruit rot and root rot of many economically important plants including *Eucalyptus*, *Fragaria*, *Paeonia* and *Vitis* (Maharachchikumbura et al. 2014, Rebollar-Alviter et al. 2020, Santos et al. 2020, Cosseboom & Hu 2021), and *N. clavispora* can infect more than 50 plant species belonging to 27 families in China and about 17 other

countries, resulting in severe leaf diseases (Qiu et al. 2020). For this reason, the two new species isolated from *Rosa* may present dangerous pathogens for other hosts, and further work is needed to better understand the role and distribution of these two new *Neopestalotiopsis* species. For other pestalotiopsis-like species associated with *Rosa*, as mentioned above, some *Pestalotiopsis* spp. on *Rosa* (*Pes. adusta*, *Pes. algeriensis*, *Pes. aquatica*, *Pes. longisetula* and *Pes. oleandri*) have the typical morphological characteristics of *Neopestalotiopsis*, namely versicolourous median conidium cells (Guba 1961, Mordue & Holliday 1971, Zhu et al. 1991, Wei et al. 2005, Ge et al. 2009, Cardoso et al. 2017). However, due to the lack of related DNA sequence data, their taxonomy still needs to be resolved. However, our two new *Neopestalotiopsis* species can be distinguished from these five *Pestalotiopsis* species based on their conidial and appendage morphology (Table 6). This study also encountered the same problem as previous studies on *Neopestalotiopsis* compared to other genera, namely the short branch length and low support rate of the current phylogenetic tree based on ITS, TEF and TUB (Liu et al. 2017, Norphanphoun et al. 2019). More gene regions will have to be introduced in future studies to provide better support for species in the genus.

Many species of *Pestalotiopsis* and *Neopestalotiopsis* have overlapping morphological characteristics, and it is difficult to identify them solely based on morphology (Maharachchikumbura et al. 2014, Liu et al. 2017). Some morphological characteristics are unstable and vary with host range, culture and other environmental conditions (Maharachchikumbura et al. 2011, Norphanphoun et al. 2019). But at the same time, conidial morphology can still provide a good reference for species distinction of pestalotioid fungi (Crous et al. 2012). Therefore, the combination of morphology and molecular systematics based on sequence data has become an important means to solve the classification of pestalotiopsis-like and support the introduction

Table 6 Synopsis of two new *Neopestalotiopsis* species and species with versicolourous median conidium cells in *Pestalotiopsis*.

Species	Length of conidia (μm)	Width of conidia (μm)	Length of apical appendages (μm)	Length of basal appendages (μm)	Host	Country	References
<i>Neopestalotiopsis concentrica</i>	14–18.5	4.5–5	19–26	3.5–5.5	<i>Rosa rugosa</i>	China	Present study
<i>N. subepidermalis</i>	20–25	7.5–9	27–32.5	7–7.5	<i>Rosa rugosa</i>	China	Present study
<i>Pestalotiopsis adusta</i>	16–22.4	4.7–6.6	5–12	3.5	<i>Rosa indica</i>	India	Rai (1990)
<i>Pes. algeriensis</i>	20.5–31.3	6.3–8.0	13.3–17.8	3–6.3	<i>Rosa sempervirens</i>	Algeria	Nag Raj (1993)
<i>Pes. aquatica</i>	20.6–28.2	7.2–8.2	12.8–23	2–4	<i>Rosa</i> sp.	China	Ge et al. (2009)
<i>Pes. longisetula</i>	20.6–25.7	6.4–7.7	20.6–36	5.1–7.7	<i>Rosa henryi</i> <i>Rosa</i> sp.	China China	Ge et al. (2009) Ge et al. (2009)
<i>Pes. oleandri</i>	15–22.6	5–7.5	14–16.5	6.1–11.5	<i>Rosa laevigata</i> <i>Rosa</i> sp.	China China	Ge et al. (2009) Zhu et al. (1991)

* Newly described taxa are in **bold**.

Table 7 *Monochaetia* species that have been recorded in China in previous studies.

Species	Host	Location	Collector	References
<i>Monochaetia caryotae</i>	<i>Caryota ochlandra</i>	Guangxi, China	Y.X. Chen & G. Wei	Chen et al. (2002)
<i>M. castaneae</i>	<i>Castanea mollissima</i>	Sichuan, China	N. Jiang	Jiang et al. (2021)
<i>M. elaeocarpi</i>	<i>Elaeocarpus serratus</i>	Hainan, China	Z.W. Wang & G. Wei	Chen et al. (2002)
<i>M. concentrica</i>	<i>Rosa xanthina</i>	Jilin, China	P.K. Qi	Tai (1979)
<i>M. cycadis</i>	<i>Cycas revoluta</i>	Guangxi, China	G. Wei	Chen et al. (2002)
<i>M. diospyri</i>	<i>Diospyros lotus</i>	–	–	Chen et al. (2002)
<i>M. garciniae</i>	<i>Garcinia tinctoria</i>	Hainan, China	Z.W. Wang & G. Wei	Chen et al. (2002)
<i>M. hirta</i>	<i>Castanopsis fabri</i>	Hainan, China	Z.W. Wang & G. Wei	Chen et al. (2002)
<i>M. kansensis</i>	<i>Castanea mollissima</i> <i>Quercus dentata</i> <i>Q. dentata</i>	– Henan, China Gansu, China	– M.Q. Wang Y.R. Meng	Chen et al. (2002) Tai (1979) Meng (2003)
<i>M. monochaeta</i>	<i>Q. dentata</i> <i>Q. variabilis</i> <i>Q. variabilis</i>	Gansu, China Jiangsu, China Jiangsu, China	Y.R. Meng – Q.Y. Shen	Meng et al. (2003) Teng (1963) Tai (1979)
<i>M. natrassii</i>	<i>Camellia sinensis</i>	Hong Kong	–	Sutton et al. (1980)
<i>M. nodosporella</i>	<i>Castanopsis delavayi</i>	Yunnan, China	Zhao & Li	Zhao & Li (1994)
<i>M. sabinae</i>	<i>Sabina chinensis</i>	Guangxi, China	G. Wei	Chen et al. (2002)
<i>M. saccardoi</i>	<i>Q. variabilis</i>	Jiangsu, China	–	Teng (1963)
<i>M. salaccae</i>	<i>Salacca secunda</i>	Yunnan, China	G. Wei	Chen et al. (2002)
<i>M. seiridioides</i>	<i>R. xanthina</i>	Henan, China	M.Q. Wang	Tai (1979)
<i>M. turgida</i>	<i>Pyrus communis</i>	Guangdong, China	Z. Tu	Tai (1979)

of new species (Crous et al. 2012, Maharachchikumbura et al. 2014, Liu et al. 2019).

Monochaetia has undergone a lot of changes since it was introduced, and many species have been transferred to other genera, such as *Diploceras*, *Monochaetinula*, *Sarcostroma*, *Seimatosprium* and *Seiridium* (De Silva et al. 2018, Liu et al. 2019). However, species of *Monochaetia* are morphologically conserved at present and the typical morphological characteristic of this genus is that conidia have a single centric apical and basal appendage (if present) (De Silva et al. 2018, Liu et al. 2019). Previous reports on the hosts of *Monochaetia* were mainly concentrated on *Fagaceae* (especially *Castanea* and *Quercus* spp.) (De Silva et al. 2018, Liu et al. 2019). In this study one new species, *M. rosarum*, was isolated from *Rosa* and can be distinguished from other phylogenetically allied species based on conidial dimensions. In addition, there are currently four species of *Monochaetia* that have been recorded from *Rosa*, namely *M. concentrica*, *M. rosae-caninae*, *M. seiridioides* and *M. turgida* (Guba 1961, Tai 1979, Chen 2003). Except for *M. rosae-caninae*, three other species have also been recorded in China (Tai 1979, Chen 2003). The species associated with *Rosa* have relatively wide host ranges mainly concentrated in the *Rosaceae*, excluding the *Fagaceae* (Weiss 1950, Sutton 1980, Nag Raj 1993), and the choice of host may also be affected by the geographical environment. For example, *M. turgida*, has been recorded on *Rosa* spp. in India, on *Crataegus* spp. in the USA, and on *Pyrus* spp. in China (Mathur 1979, Tai 1979, Nag Raj 1993). Besides the three species on *Rosa* mentioned above (*M. concentrica*, *M. seiridioides* and *M. turgida*), 16 species of *Monochaetia* have been recorded from China (Table 7). Among them, Chen et al. (2002) introduced seven *Monochaetia* species based on morphology and host, i.e., *M. caryotae* on *Caryota ochlandra*, *M. cycadis* on *Cycas revoluta*, *M. elaeocarpi* on *Elaeocarpus serratus*, *M. garciniae* on *Garcinia tinctoria*, *M. hirta* on *Castanopsis fabri*, *M. sabinae* on *Sabina chinensis* and *M. salaccae* on *Salacca secunda*, and all these species are endemic to China. Although sequence data for these species are not available and reliance only on morphology and host data in *Monochaetia* taxonomy is far from

perfect, the ongoing discovery of this genus from other hosts except for *Fagaceae* in China will deepen our understanding of the species in this genus. It is worth mentioning that Zhao & Li (1994) have described a species *M. nodosporella*, the hosts of which include also *Castanopsis* spp. Characteristics of this species are quite different from morphological characters of *Monochaetia*, including 4-celled distoseptate conidia with two olivaceous-brown median cells, lacking appendages. Considering the limited sampling and the lack of sequence data, the taxonomy of *M. nodosporella* remains unresolved and will be treated once DNA sequence data have been obtained. Aside from the species associated with *Rosa* and the Chinese endemic species mentioned above, the remaining species recorded in China have a relatively small range of host plants mainly on *Castanea* and *Quercus*, and are geographically widespread (Tai 1979, Zhao & Li 1994, Chen et al. 2002). For example, *M. monochaeta* and *M. kansensis* have also been recorded in many countries besides China, but the hosts are basically *Quercus* and *Castanea* (Ellis & Everhart 1893, Weiss 1950, Guba 1961, Nag Raj 1993, Cho & Shin 2004, Kobayashi 2007). Therefore, for the new species *M. rosarum* described in this study, many specimens still need to be collected to improve our understanding of its host range and distribution.

Seiridium generally produces 5-septate conidia with a single centric apical and single excentric basal appendage (Bonhond et al. 2018, Liu et al. 2019). Nees (1817) established *Seiridium* based on *Seir. marginatum* which was collected from rose stems in Germany, and this is also the earliest record of pestalotioid fungi on the *Rosa* plants. Presently, besides the type species *Seir. marginatum*, only one *Seiridium* species has been recorded from *Rosa*, namely *Seir. rosarum*, which is distributed in Europe and Australia (Sutton 1980, Nag Raj 1993, Jaklitsch et al. 2016). In this study, a new species *Seir. rosae* was introduced from *R. multiflora* in China. The newly described species can be distinguished from most *Seiridium* species by its numerous appendages, which are branched, while in *Seiridium* appendages are fewer and generally unbranched (Maharachchikumbura et al. 2014). However, conidial appendages are branched, which is not unique to *Seir. rosae* in *Seiridium* and is also typical for

Table 8 Synopsis of species with branched appendages in *Seiridium*.

Species	Length of conidia (μm)	Width of conidia (μm)	Length of apical appendages (μm)	Length of basal appendages (μm)	Host	Country	References
<i>Seiridium indicum</i>	22–30.8	7.7–8.8	4.4–11	1–1.8	<i>Spirea micrantha</i>	India	Nag Raj (1993)
<i>Seir. pezizoides</i>	28–33.5	7–8	8.5–27	5.5–14	<i>Vitis vinifera</i>	Italy	Marin-Felix et al. (2019)
<i>Seir. rosae</i>	31–35	8–9.5	28.5–44.5	3–4.5	<i>Rosa rugosa</i>	China	Present study
<i>Seir. venetum</i>	20–30	6.5–8.5	10–35	2–5	<i>Cornus sanguinea</i>	Italy	Nag Raj (1993)

* Newly described taxa is in **bold**.

Table 9 *Seiridium* species that have been recorded in China in previous studies.

Species	Host	Location	Collector	References
<i>Seiridium camelliae</i>	<i>Camellia reticulata</i>	Yunnan, China	Y.M. Zhang	Maharachchikumbura et al. (2015)
<i>Seir. ceratosporum</i>	<i>Vitis vinifera</i>	Yunnan, China	—	Bonthond et al. (2018)
<i>Seir. chinense</i>	<i>Trachycarpus fortunei</i>	Shaanxi, China	N. Jiang & C.M. Tian	Jiang et al. (2018)
<i>Seir. cupressi</i>	<i>Vitis</i> sp.	Zhejiang, China	—	Teng (1996)
<i>Seir. eriobotryae</i>	<i>Eriobotrya japonica</i>	Guangxi, China	G. Wei	Chen et al. (2002)
<i>Seir. manilkarae</i>	<i>Manilkara zapota</i>	Yunnan, China	G. Wei	Chen et al. (2002)
<i>Seir. pezizoides</i>	<i>Camellia oleifera</i>	Hunan, China	J.X. Yu	Yu et al. (2018)
<i>Seir. unicorn</i>	<i>Eriobotrya japonica</i> <i>Malus mandshurica</i> <i>M. prunifolia</i> <i>M. pumila</i> <i>Pyrus ussuriensis</i> <i>Sorbus alnifolia</i> <i>V. vinifera</i>	Jiangsu, China Jilin, China Jilin, China Yunnan, China Jilin, China Jilin, China Jiangsu, China	F.L. Tai Miura P.K. Qi L.D. Lin P.K. Qi Miura L. Ling	Tai (1979) Tai (1979) Tai (1979) Tai (1979) Tai (1979) Tai (1979) Tai (1979)
<i>Seir. venetum</i>	<i>Cornus</i> sp.	Yunnan, China	—	Tai (1979)

Seir. indicum, *Seir. pezizoides* and *Seir. venetum* (Pavgi & Singh 1970, Maharachchikumbura et al. 2015, Marin-Felix et al. 2019). *Seiridium rosae* is easily distinguishable from these three species based on conidial morphology (Table 8). It is worth mentioning that *Seiridium* is the most important pathogen group in *Sporocadaceae* (Bonthond et al. 2018). *Seiridium* is the main pathogen of cypress canker and causes huge economic losses worldwide (Boesewinkel 1983, Graniti 1986, 1993, 1998, Barnes et al. 2001, Tsopelas et al. 2007). There are currently nine species of *Seiridium* recorded in China, with diverse hosts (Table 9). However, thus far China still has no record of *Seiridium* spp. on *Cupressaceae*.

In this study, the species diversity of *Sporocadaceae* on the stems and spines of *Rosa* was significantly higher than that on the leaves and fruits. Nevertheless, a new species *Seim. nonappendiculatum* was isolated from the fruits of *Rosa laevigata* and *Pes. rhodomyrtus*, that was first reported on *Rosa*, was isolated from leaves of *Rosa rugosa*. Therefore, the leaves and fruits of *Rosa* plants might harbour many more species of pestalotioid fungi yet unknown to science. This study represents the first systematic investigation, morphological and molecular characterisation of *Sporocadaceae* on *Rosa*. The findings of this study reveal taxonomic, morphological and biological diversity of *Sporocadaceae* associated with different *Rosa* spp. in China. Other than expanding our knowledge of the genetic diversity and hosts of *Sporocadaceae* on *Rosa*, it provides crucially important information to understand the ecology of the *Sporocadaceae* associated with *Rosa*. Further study is needed to test the pathogenicity of these species and understand their biological and epidemiological characteristics to contribute towards better disease management.

Acknowledgements This study is financed by National Natural Science Foundation of China (Project No.: 31670647).

Declaration on conflict of interest The authors declare that there is no conflict of interest.

REFERENCES

- Akinsanmi OA, Nisa S, Jeff-Ego OS, et al. 2017. Dry flower disease of macadamia in Australia caused by *Neopestalotiopsis macadamiae* sp. nov. and *Pestalotiopsis macadamiae* sp. nov. *Plant Disease* 101: 45–53.
- Alberto F, Giorgio G, Dalia A. 2022. *Neopestalotiopsis siciliana* sp. nov. and *N. rosae* causing stem lesion and dieback on avocado plants in Italy. *Journal of Fungi* 8: 562.
- Ariyawansa HA, Hyde KD. 2018. Additions to *Pestalotiopsis* in Taiwan. *Mycosphere* 9: 999–1013.
- Bagsic I, Linde M, Debener T. 2016. Genetic diversity and pathogenicity of *Sphaceloma rosarum* (teleomorph *Elsinoë rosarum*) causing spot anthracnose on roses. *Plant Pathology* 65: 978–986.
- Barber PA, Crous PW, Groenewald JZ, et al. 2011. Reassessing *Vermisporium* (*Amphisphaeriaceae*), a genus of foliar pathogens of eucalypts. *Persoonia* 27: 90–118.
- Barnes I, Roux J, Wingfield MJ, et al. 2001. Characterization of *Seiridium* spp. associated with cypress canker based on β-tubulin and histone sequences. *Plant Disease* 85: 317–321.
- Bezerra JDP, Machado AR, Firmino AL, et al. 2018. Mycological diversity description I. *Acta Botanica Brasilica* 32: 656–666.
- Boesewinkel H. 1983. New records of the three fungi causing cypress canker in New Zealand, *Seiridium cupressi* (Guba) comb. nov. and *S. cardinale* on *Cupressocyparis* and *S. unicorn* on *Cryptomeria* and *Cupressus*. *Transactions of the British Mycological Society* 80: 544–547.
- Bonthond G, Sandoval-Denis M, Groenewald JZ, et al. 2018. *Seiridium* (*Sporocadaceae*): an important genus of plant pathogenic fungi. *Persoonia* 40: 96–118.
- Brockmann I. 1976. Untersuchungen über die Gattung *Discostroma* Clements (Ascomycetes). *Sydowia* 28: 275–338.
- Bruneau A, Starr JR, Joly S. 2007. Phylogenetic relationships in the genus *Rosa*: new evidence from chloroplast DNA sequences and an appraisal of current knowledge. *Systematic Botany* 32: 366–378.
- Cardoso JK, Nanami DS, Zanutto CA, et al. 2017. Description and identification of two new diseases of guariroba palm (*Syagrus oleracea*) in Brazil. *Journal of Phytopathology* 165: 610–619.

- Chaiwan N, Wanasinghe DN, Mapook A, et al. 2020. Novel species of Pestalotiopsis fungi on Dracaena from Thailand. *Mycology* 11: 306–315.
- Chen MM. 2003. Forest fungi phytogeography: Forest fungi phytogeography of China, North America, and Siberia and international quarantine of tree pathogens. Pacific Mushroom Research and Education Center Sacramento USA.
- Chen SF, Li GQ, Liu JQ, et al. 2016. Characteristics of Lasiodiplodia theobromae from Rosa rugosa in South China. *Crop Protection* 79: 51–55.
- Chen YX, Wei G, Chen WP. 2002. New species of Monochaetia and Seiridium in China. *Mycosistema* 21: 503–510.
- Chen YY, Maharachchikumbura SSN, Liu JK. 2017. Fungi from Asian Karst formations I. Pestalotiopsis photinicola sp. nov., causing leaf spots of Photinia serrulata. *Mycosphere* 8: 103–110.
- Cho WD, Shin HD. 2004. List of plant diseases in Korea. Korean Society of Plant Pathology, Korea.
- Collado J, Platas G, Bills GF, et al. 2006. Studies on Morinia: Recognition of Morinia longiappendiculata sp. nov. as a new endophytic fungus, and a new circumscription of Morinia pestalozzoides. *Mycologia* 98: 616–627.
- Cosseboom SD, Hu M. 2021. Diversity, pathogenicity, and fungicide sensitivity of fungal species associated with late-season rots of wine grape in the Mid-Atlantic United States. *Plant Disease* 105: 3101–3110.
- Crous PW, Boers J, Holdom D, et al. 2022. Fungal Planet description sheets: 1383–1435. *Persoonia* 48: 261–371.
- Crous PW, Carris LM, Giraldo A, et al. 2015a. The genera of fungi-fixing the application of the type species of generic names-G 2: Allantophomopsis, Latorua, Macrodiplodiopsis, Macrohilum, Milospium, Protostegia, Pyricularia, Robillarda, Rotula, Septoriella, Torula, and Wojnowicia. *IMA Fungus* 6: 163–198.
- Crous PW, Denman S, Taylor JE, et al. 2013. Cultivation and diseases of Proteaceae: Leucadendron, Leucospermum and Protea. CBS Biodiversity Series 13. CBS-KNAW Fungal Biodiversity Centre.
- Crous PW, Gams W, Stalpers JA, et al. 2004. MycoBank: an online initiative to launch mycology into the 21st century. *Studies in Mycology* 50: 19–22.
- Crous PW, Liu F, Cai L, et al. 2018. Allelochaeta (Sporocadaceae): pigmentation lost and gained. *Fungal Systematics and Evolution* 2: 273–309.
- Crous PW, Phillips A, Baxter A. 2000. Phytopathogenic fungi from South Africa: 73–75. Department of Plant Pathology Press, University of Stellenbosch, South Africa.
- Crous PW, Shivas RG, Quaedvlieg W, et al. 2014a. Fungal Planet description sheets: 214–280. *Persoonia* 32: 184–306.
- Crous PW, Summerell BA, Shivas RG, et al. 2011a. Fungal Planet description sheets: 92–106. *Persoonia* 27: 130–162.
- Crous PW, Summerell BA, Swart L, et al. 2011b. Fungal pathogens of Proteaceae. *Persoonia* 27: 20–45.
- Crous PW, Verkley G, Christensen M, et al. 2012. How important are conidial appendages? *Persoonia* 28: 126–137.
- Crous PW, Verkley G, Groenewald J, et al. 2019a. Fungal Biodiversity. Westerdijk Laboratory Manual Series no. 1. Utrecht, Westerdijk Fungal Biodiversity Institute, Utrecht, the Netherlands.
- Crous PW, Wingfield MJ, Cheewangkoon R, et al. 2019b. Foliar pathogens of eucalypts. *Studies in Mycology* 94: 125–298.
- Crous PW, Wingfield MJ, Chooi YH, et al. 2020. Fungal Planet description sheets: 1042–1111. *Persoonia* 44: 301–459.
- Crous PW, Wingfield MJ, Le Roux JJ, et al. 2015b. Fungal Planet description sheets: 371–399. *Persoonia* 35: 264–327.
- Crous PW, Wingfield MJ, Schumacher RK, et al. 2014b. Fungal Planet description sheets: 281–319. *Persoonia* 33: 212–289.
- De Silva NI, Maharachchikumbura SSN, Bhat DJ, et al. 2018. Monochaetia sinensis sp. nov. from Yunnan Province in China. *Phytotaxa* 375: 059–069.
- Dean RA, Lichens-Park A, Kole C. 2014. Genomics of plant-associated fungi: monocot pathogens. Berlin, Heidelberg, Germany.
- Debener T. 2019. The Beast and the Beauty: What do we know about Black Spot in roses? *Critical Reviews in Plant Sciences* 38: 313–326.
- Diogo E, Gonçalves CI, Silva AC, et al. 2021. Five new species of Neopestalotiopsis associated with diseased Eucalyptus spp. in Portugal. *Mycological Progress* 20: 1441–1456.
- Doyle JJ, Doyle JL. 1990. Isolation of plant DNA from fresh tissue. *Focus* 12: 39–40.
- Duan YB, Yu ZZ, Kang YB. 2011. First report of leaf spot disease of peony caused by Seimatosporium botan in China. *Plant Disease* 95: 226.
- Eken C, Spanbayev A, Tulegenova Z, et al. 2009. First report of Truncatella angustata causing leaf spot on Rosa canina in Kazakhstan. *Australasian Plant Disease Notes* 4: 44–45.
- Ellis JB, Everhart BM. 1893. New species of fungi from various localities. *Proceedings of the Academy of Natural Sciences of Philadelphia* 45: 440–466.
- Eriksson O. 1986. Notes on ascomycete systematics, Nos. 1–224. *Systema Ascomycetum* 5: 113–174.
- Eriksson O. 1987. Notes on ascomycete systematics. Nos. 225–463. *Systema Ascomycetum* 9: 11–165.
- Feng F, Zhou G, Li H. 2019. First report of Colletotrichum siamense causing anthracnose on Rosa chinensis in China. *Plant Disease* 103: 1422–1422.
- Feng Y, Liu B, Sun B. 2014. First report of leaf blotch caused by Pestalotiopsis clavispora on Rosa chinensis in China. *Plant Disease* 98: 1009–1009.
- Fougère-Danezan M, Joly S, Bruneau A, et al. 2015. Phylogeny and biogeography of wild roses with specific attention to polyploids. *Annals of Botany* 115: 275–291.
- Freitas EFS, Da Silva M, Barros MVP, et al. 2019. Neopestalotiopsis hadroliae sp. nov., a new endophytic species from the roots of the endangered orchid Hadrolaelia jongheana in Brazil. *Phytotaxa* 416: 211–220.
- Fu M, Crous PW, Bai Q, et al. 2019. Colletotrichum species associated with anthracnose of Pyrus spp. in China. *Persoonia* 42: 1–35.
- Ge QX, Chen YX, Xu T. 2009. Flora Fungorum Sinicorum. Vol. 38. Pestalotiopsis. Science Press, Beijing, China. [In Chinese.]
- Geng K, Zhang B, Song Y, et al. 2013. A new species of Pestalotiopsis from leaf spots of Licuala grandis from Hainan, China. *Phytotaxa* 88: 49–54.
- Goonasekara ID, Maharachchikumbura SSN, Wijayawardene NN, et al. 2016. Seimatosporium quercina sp. nov. (Discosporaceae) on Quercus robur from Germany. *Phytotaxa* 255: 240–280.
- Graniti A. 1986. Seiridium cardinale and other cypress cankers 1. EPPO Bulletin 16: 479–486.
- Graniti A. 1993. Seiridium blight of cypress-another ecological disaster? *Plant Disease* 77: 1–6.
- Graniti A. 1998. Cypress canker: a pandemic in progress. *Annual Review of Phytopathology* 36: 91–114.
- Gu M, Hu D, Han B, et al. 2021. Pestalotiopsis abietis sp. nov. from Abies fargesii in China. *Phytotaxa* 509: 93–105.
- Gualberto GF, Catarino ADM, Sousa TF, et al. 2021. Pseudopestalotiopsis gilvanii sp. nov. and Neopestalotiopsis formicarum leaves spot pathogens from guarana plant: a new threat to global tropical hosts. *Phytotaxa* 489: 121–139.
- Guba EF. 1961. Monograph of Monochaetia and Pestalotia. Harvard University Press, Cambridge, Massachusetts, USA.
- Guo LD. 2004. Endophytic Fungi II. New records from pine in China. *Mycosistema* 23: 24–27.
- Guo Y, Crous PW, Bai Q, et al. 2020. High diversity of Diaporthe species associated with pear shoot canker in China. *Persoonia* 77: 132–162.
- Hatakeyama S, Harada Y. 2004. A new species of Discostroma and its amorph Seimatosporium with two morphological types of conidia, isolated from the stems of Paeonia suffruticosa. *Mycoscience* 45: 106–111.
- Hernández-Restrepo M, Groenewald JZ, Crous PW, et al. 2016. Taxonomic and phylogenetic re-evaluation of Microdochium, Monographella and Idriella. *Persoonia* 36: 57–82.
- Hongsanan S, Maharachchikumbura SSN, Hyde KD, et al. 2017. An updated phylogeny of Sordariomycetes based on phylogenetic and molecular clock evidence. *Fungal Diversity* 84: 25–41.
- Huanluek N, Jayawardena RS, Maharachchikumbura SSN, et al. 2021. Additions to pestalotioid fungi in Thailand: Neopestalotiopsis hydeana sp. nov. and Pestalotiopsis hydei sp. nov. *Phytotaxa* 479: 23–43.
- Huelsenbeck JP, Ronquist F. 2001. MrBayes: Bayesian inference of phylogenetic trees. *Bioinformatics* 17: 754–755.
- Hyde KD, Hongsanan S, Jeewon R, et al. 2016. Fungal diversity notes 367–490: taxonomic and phylogenetic contributions to fungal taxa. *Fungal Diversity* 80: 1–270.
- Hyde KD, Jeewon R, Chen YJ, et al. 2020. The numbers of fungi: is the descriptive curve flattening. *Fungal Diversity* 103: 219–271.
- Jaklitsch WM, Gardiennet A, Voglmayr H. 2016. Resolution of morphology-based taxonomic delusions: Acrocordiella, Basiseptospora, Blagiaskospora, Clypeosphaeria, Hymenoplectella, Leptotyphula, Pseudapiospora, Requienella, Seiridium and Strickeria. *Persoonia* 37: 82–105.
- Jayawardena R, Hyde KD, Chethana K, et al. 2018. Mycosphere notes 102–168: Saprotrophic fungi on Vitis in China, Italy, Russia and Thailand. *Mycosphere* 9: 1–114.
- Jayawardena RS, Liu M, Maharachchikumbura SSN. 2016. Neopestalotiopsis vitis sp. nov. causing grapevine leaf spot in China. *Phytotaxa* 258: 63–74.
- Jia J, Li X, Zhang W, et al. 2019. First report of Botryosphaeria dothidea associated with stem canker on Rosa chinensis in China. *Plant Disease* 103: 3280.
- Jiang N, Bonhond G, Fan XL, et al. 2018. Neopestalotiopsis rosicola sp. nov. causing stem canker of Rosa chinensis in China. *Mycotaxon* 133: 271–283.
- Jiang N, Fan XL, Tian CM. 2021. Identification and characterization of leaf-inhabiting fungi from Castanea plantations in China. *Journal of Fungi* 7: 64.
- Jiang N, Liang YM, Tian CM. 2019. Morphological and phylogenetic evidences reveal a new Seiridium species in China. *Phytotaxa* 418: 287–293.
- Jin J. 2020. Investigation and application of Rosa resources in Guizhou, China. *Seed* 39: 61–65. [In Chinese.]
- Kang JC, Hyde KD, Kong RY. 1999. Studies on Amphisphaeriales: the Amphisphaeriaceae (sensu stricto). *Mycological Research* 103: 53–64.

- Katoh K, Rozewicki J, Yamada KD. 2019. MAFFT online service: multiple sequence alignment, interactive sequence choice and visualization. *Briefings in Bioinformatics* 20: 1160–1166.
- Katoh K, Standley DM. 2013. MAFFT multiple sequence alignment software version 7: improvements in performance and usability. *Molecular Biology and Evolution* 30: 772–780.
- Kobayashi T. 2007. Index of fungi inhabiting woody plants in Japan. Zenkoku Noson Kyoiku Kyokai, Tokyo, Japan.
- Kumar V, Cheewangkoon R, Gentekaki E. 2019. Neopestalotiopsis alpapicalis sp. nov. a new endophyte from tropical mangrove trees in Krabi Province (Thailand). *Phytotaxa* 393: 251–262.
- Lawrence DP, Travadon R, Baumgartner K. 2018. Novel *Seimatosporium* species from grapevine in northern California and their interactions with fungal pathogens involved in the trunk-disease complex. *Plant Disease* 102: 1081–1092.
- Li GJ, Hyde KD, Zhao RL, et al. 2016. Fungal diversity notes 253–366: taxonomic and phylogenetic contributions to fungal taxa. *Fungal Diversity* 78: 1–237.
- Li L, Yang Q, Li H. 2021. Morphology, phylogeny, and pathogenicity of pestalotioid species on *Camellia oleifera* in China. *Journal of Fungi* 7: 1080.
- Li WJ, Maharachchikumbura SSN, Li QR. 2015. Epitypification of *Broomella vitalbae* and introduction of a novel species of *Hyalotiella*. *Cryptogamie, Mycologie* 36: 93–108.
- Liu AR, Chen SC, Wu SY, et al. 2010. Cultural studies coupled with DNA based sequence analyses and its implication on pigmentation as a phylogenetic marker in Pestalotiopsis taxonomy. *Molecular Phylogenetics and Evolution* 57: 528–535.
- Liu F, Bonhond G, Groenewald JZ, et al. 2019. Sporocadaceae, a family of coelomycetous fungi with appendage-bearing conidia. *Studies in Mycology* 92: 287–415.
- Liu F, Hou L, Raza M, et al. 2017. Pestalotiopsis and allied genera from *Camellia*, with description of 11 new species from China. *Scientific Reports* 7: 866.
- Liu LL. 2016. Review on the research and utilization of the genus *Rosa* in China. *Agricultural Science and Technology*: 1–5.
- Liu JK, Hyde KD, Jones EB, et al. 2015. Fungal diversity notes 1–110: taxonomic and phylogenetic contributions to fungal species. *Fungal Diversity* 72: 1–197.
- Liu X, Tibpromma S, Zhang F, et al. 2021. Neopestalotiopsis cavernicola sp. nov. from Gem Cave in Yunnan Province, China. *Phytotaxa* 512: 1–27.
- Luo ZL, Hyde KD, Liu J, et al. 2019. Freshwater Sordariomycetes. *Fungal Diversity* 99: 451–660.
- Ma XY, Maharachchikumbura SSN, Chen BW, et al. 2019. Endophytic pestalotioid taxa in *Dendrobium* orchids. *Phytotaxa* 419: 268–286.
- Maharachchikumbura SSN, Camporesi E, Liu ZY, et al. 2015. Seiridium venetum redescribed, and *S. camelliae*, a new species from *Camellia reticulata* in China. *Mycological Progress* 14: 85.
- Maharachchikumbura SSN, Chukeatirote E, Guo LD, et al. 2013a. Pestalotiopsis species associated with *Camellia sinensis* (tea). *Mycotaxon* 123: 47–61.
- Maharachchikumbura SSN, Guo LD, Cai L, et al. 2012. A multi-locus backbone tree for Pestalotiopsis, with a polyphasic characterization of 14 new species. *Fungal Diversity* 56: 95–129.
- Maharachchikumbura SSN, Guo LD, Chukeatirote E, et al. 2011. Pestalotiopsis-morphology, phylogeny, biochemistry and diversity. *Fungal Diversity* 50: 167–187.
- Maharachchikumbura SSN, Hyde KD, Groenewald JZ, et al. 2014. Pestalotiopsis revisited. *Studies in Mycology* 79: 121–186.
- Maharachchikumburaa SSN, Zhang YM, Wang Y, et al. 2013b. Pestalotiopsis anacardiacearum sp. nov. *Amphisphaeriaceae* has an intricate relationship with *Penicillaria jocosatrix*, the mango tip borer. *Phytotaxa* 99: 49–57.
- Marin-Felix Y, Hernandez-Restrepo M, Iturrieta-Gonzalez I, et al. 2019. Genera of phytopathogenic fungi: GOPHY 3. *Studies in Mycology* 94: 1–124.
- Mathur RS. 1979. The Coelomycetes of India. Bishen Singh Mahendra Pal Singh.
- Mendes M, Da Silva V, Dianese J. 1998. Fungos em Plants no Brasil. Embrapa-SPI/Embrapa-Cenargen, Brasilia.
- Meng YR. 2003. Diseases of economic plants in Gansu province. Gansu Science and Technology Press. Lanzhou, China. [In Chinese.]
- Moghadam JN, Khaledi E, Abdollahzadeh J, et al. 2022. *Seimatosporium marivanicum*, *Sporocadus kurdistanicus*, and *Xenoseimatosporium kurdistanicum*: three new pestalotioid species associated with grapevine trunk diseases from the Kurdistan Province, Iran. *Mycological Progress* 21: 427–446.
- Mordue J. 1986. Another unusual species of Pestalotiopsis: *P. montellicoides* sp. nov. *Transactions of the British Mycological Society* 86: 665–668.
- Mordue J, Holliday P. 1971. Pestalotiopsis palmarum. [Descriptions of Fungi and Bacteria]. IMI Descriptions of Fungi and Bacteria No. 319.
- Moslemi A, Taylor PW. 2015. Pestalotiopsis chamaeropis causing leaf spot disease of round leaf mint-bush (*Prostanthera rotundifolia*) in Australia. *Australasian Plant Disease Notes* 10: 1–5.
- Mułenko W, Majewski T, Ruszkiewicz-Michalska M. 2008. A preliminary checklist of micromycetes in Poland. W. Szafer Institute of Botany, Polish Academy of Sciences, Poland.
- Munoz M, Faust JE, Schnabel G. 2019. Characterization of *Botrytis cinerea* from commercial cut flower roses. *Plant Disease* 103: 1577–1583.
- Nag Raj T. 1985. Redisposals and redescriptions in the *Monochaetia-Seiridium*, Pestalotia-Pestalotiopsis complexes. I: The correct name for the type species of Pestalotiopsis. II: Pestalotiopsis besseyii (Guba) comb. nov. and Pestalosphaeria varia sp. nov. III: *Monochaetia ilicina* (Sacc.) comb. nov. IV: On *Monochaetia miersi*. *Mycotaxon* 22: 43–75.
- Nag Raj T. 1993. Coelomycetous anamorphs with appendage-bearing conidia. Mycologue Publications, Waterloo, Canada.
- Nees C. 1817. Das system der Pilze und Schwämme. Stahelsche Buchhandlung, Würzburg, Germany.
- Norphanphon C, Jayawardena RS, Chen Y, et al. 2019. Morphological and phylogenetic characterization of novel pestalotioid species associated with mangroves in Thailand. *Mycosphere* 10: 531–578.
- Norphanphon C, Maharachchikumbura SSN, Daranagama A, et al. 2015. Towards a backbone tree for *Seimatosporium*, with *S. physocarpi* sp. nov. *Mycosphere* 6: 385–400.
- Nozawa S, Seto Y, Watanabe K. 2019. First report of leaf blight caused by Pestalotiopsis chamaeropis and Neopestalotiopsis sp. in Japanese andromeda. *Journal of General Plant Pathology* 85: 449–452.
- Pan M, Zhu H, Bonhond G, et al. 2020. High diversity of *Cytospora* associated with canker and dieback of Rosaceae in China, with 10 new species described. *Frontiers in Plant Science* 11: 690.
- Patouillard N. 1886. Quelques champignons de la Chine, récoltés par M. l'abbé Delavay dans la province du Yunnan. *Revue Mycologique* 8: 179–182.
- Pavigi M, Singh U. 1970. Parasitic fungi from North India. IX. *Sydowia* 24: 113–119.
- Peregrine WTH, Ahmad KB. 1982. Brunei: A first annotated list of plant diseases and associated organisms. *Phytopathological Papers* 27: 1–87.
- Prasannath K, Shivas RG, Galea, VJ, et al. 2021. Neopestalotiopsis species associated with flower diseases of *Macadamia integrifolia* in Australia. *Journal of Fungi* 7: 771.
- Qiu F, Xu G, Zheng FQ, et al. 2020. First report of Neopestalotiopsis clavispore causing leaf spot on macadamia (*Macadamia integrifolia*) in China. *Plant Disease* 104: 288–289.
- Rai M. 1990. New records of fungi from India. *Indian Journal of Mycology and Plant Pathology* 20: 199–201.
- Ran S, Maharachchikumbura SSN, Ren Y, et al. 2017. Two new records in Pestalotiopsidaceae associated with Orchidaceae disease in Guangxi Province, China. *Mycosphere* 8: 121–130.
- Rayner RW. 1970. A mycological colour chart. CMI and British Mycological Society, Kew, Surrey, UK.
- Rebollar-Alviter A, Silva-Rojas HV, Fuentes-Aragón D, et al. 2020. An emerging strawberry fungal disease associated with root rot, crown rot and leaf spot caused by Neopestalotiopsis rosae in Mexico. *Plant Disease* 104: 2054–2059.
- Riley EA. 1960. A revised list of plant diseases in Tanganyika Territory.
- Samarakoon M. 2016. Evolution of Xylariomycetidae (Ascomycota: Sordariomycetes). *Mycosphere* 7: 1746–1761.
- Sameva EF. 2004. New records of anamorphic fungi from Bulgaria. *Micologia Balcanica* 1: 55–57.
- Samuels G, Müller E, Petrini O. 1987. Studies in the Amphisphaeriaceae (sensu lato). III: New species of *Monographella* and *Pestalosphaeria*, and two new genera. *Mycotaxon* 28: 473–499.
- Santos GS, Mafia RG, Aguiar AM, et al. 2020. Stem rot of eucalyptus cuttings caused by Neopestalotiopsis spp. in Brazil. *Journal of Phytopathology* 168: 311–321.
- Santos J, Hilário S, Pinto G, et al. 2022. Diversity and pathogenicity of pestalotioid fungi associated with blueberry plants in Portugal, with description of three novel species of Neopestalotiopsis. *European Journal of Plant Pathology* 162: 539–555.
- Senanayake IC, Maharachchikumbura SSN, Hyde KD, et al. 2015. Towards unravelling relationships in Xylariomycetidae (Sordariomycetes). *Fungal Diversity* 73: 73–144.
- Shoemaker R. 1964. *Seimatosporium* (= *Cryptostictis*) parasites of *Rosa*, *Vitis*, and *Cornus*. *Canadian Journal of Botany* 42: 411–421.
- Silva AC, Diogo E, Henriques J, et al. 2020. Pestalotiopsis pini sp. nov., an emerging pathogen on stone pine (*Pinus pinea* L.). *Forests* 11: 805.
- Silvério ML, Cavalcanti MA, Silva GA. 2016. A new epipolar species of Neopestalotiopsis from Brazil. *Agrotropica* 28: 151–158.

- Silvestro D, Michalak I. 2012. raxmlGUI: a graphical front-end for RAxML. *Organisms Diversity & Evolution* 12: 335–337.
- Smith GJ, Liew EC, Hyde KD. 2003. The Xylariales: a monophyletic order containing 7 families. *Fungal Diversity* 13: 185–218.
- Smith H, Wingfield M, Coutinho T, et al. 1996. *Sphaeropsis sapinea* and *Botryosphaeria dothidea* endophytic in *Pinus* spp. and *Eucalyptus* spp. in South Africa. *South African Journal of Botany* 62: 86–88.
- Song Y, Geng K, Hyde KD, et al. 2013. Two new species of Pestalotiopsis from Southern China. *Phytotaxa* 126: 22–32.
- Spaulding P. 1949. Foreign diseases of forest trees of the world: an annotated list. US Department of Agriculture, USA.
- Sutton BC. 1975. Coelomycetes. V. *Coryneum*. *Mycological Papers* 138: 1–224. Commonwealth Mycological Institute, Kew.
- Sutton BC. 1980. The coelomycetes. Fungi imperfecti with pycnidia, acervuli and stromata. Commonwealth Mycological Institute, Kew.
- Swart L, Taylor J, Crous PW, et al. 1999. Pestalotiopsis leaf spot disease of Proteaceae in Zimbabwe. *South African Journal of Botany* 65: 239–242.
- Swofford DL. 2003. PAUP*: Phylogenetic Analysis Using Parsimony (*and other methods) version 4.0b10. Sinauer Associates, Sunderland, MA, USA.
- Tai FL. 1979. *Sylloge Fungorum Sinicorum*. Science Press, Academia Sinica. Beijing, China. [In Chinese.]
- Tamura K, Stecher G, Peterson D, et al. 2013. MEGA6: molecular evolutionary genetics analysis version 6.0. *Molecular Biology and Evolution* 30: 2725–2729.
- Tanaka K, Endo M, Hirayama K, et al. 2011. Phylogeny of *Discosia* and *Seimatosporium*, and introduction of *Adisciso* and *Immersidiscosia* genera nova. *Persoonia* 26: 85–98.
- Taylor J. 2000. Proteaceae pathogens: the significance of their distribution in relation to recent changes in phytosanitary regulations. *Acta Horticulturae* 545: 253–264.
- Teng SC. 1963. Fungi of China. Science Press. Beijing, China. [In Chinese.]
- Teng SC. 1996. Fungi of China. Ithaca, Mycotaxon, Ltd., NY, USA.
- Tibpromma S, Hyde KD, McKenzie EH, et al. 2018. Fungal diversity notes 840–928: micro-fungi associated with Pandanaceae. *Fungal Diversity* 93: 1–160.
- Tibpromma S, Mortimer PE, Karunarathna SC, et al. 2019. Morphology and multi-gene phylogeny reveal Pestalotiopsis pinicola sp. nov. and a new host record of *Cladosporium anthropophilum* from edible pine (*Pinus armandii*) seeds in Yunnan province, China. *Pathogens* 8: 285.
- Tsopelas P, Barnes I, Wingfield M, et al. 2007. *Seiridium cardinale* on Juniperus species in Greece. *Forest Pathology* 37: 338–347.
- Ul Haq I, Ijaz S, Khan NA, et al. 2021. Genealogical concordance of phylogenetic species recognition-based delimitation of Neopestalotiopsis species associated with leaf spots and fruit canker disease affected guava plants. *Pakistan Journal of Agricultural Sciences* 58: 1301–1313.
- Vieira WA, Michereff SJ, De Morais MA, et al. 2014. Endophytic species of *Colletotrichum* associated with mango in northeastern Brazil. *Fungal Diversity* 67: 181–202.
- Vu D, Groenewald M, De Vries M, et al. 2019. Large-scale generation and analysis of filamentous fungal DNA barcodes boosts coverage for kingdom fungi and reveals thresholds for fungal species and higher taxon delimitation. *Studies in Mycology* 92: 135–154.
- Wanasinghe DN, Phukhamsakda C, Hyde KD, et al. 2018. Fungal diversity notes 709–839: taxonomic and phylogenetic contributions to fungal taxa with an emphasis on fungi on Rosaceae. *Fungal Diversity* 89: 1–236.
- Wang G. 1985. New species and records of fungi from Changbai mountain, China (I). *Bulletin of Botanical Research* 5: 137–139. [In Chinese.]
- Wang S. 2021. Relationships between species richness patterns of *Rosa* L. and environmental factors in China. *Acta Ecologica Sinica* 42: 1–8.
- Wang S, Mi X, Wu Z, et al. 2019a. Characterization and pathogenicity of pestalotiopsis-like species associated with gray blight disease on *Camellia sinensis* in Anhui province, China. *Plant Disease* 103: 2786–2797.
- Wang Y, Xiong F, Lu Q, et al. 2019b. Diversity of pestalotiopsis-like species causing Gray Blight Disease of tea plants (*Camellia sinensis*) in China, including two novel Pestalotiopsis species, and analysis of their pathogenicity. *Plant Disease* 103: 2548–2558.
- Watanabe K, Motohashi K, Ono Y. 2010. Description of Pestalotiopsis pallidotheiae: a new species from Japan. *Mycoscience* 51: 182–188.
- Watanabe K, Nozawa S, Hsiang T. 2018. The cup fungus Pestalopezia brunneopruinosa is Pestalotiopsis gibbosa and belongs to Sordariomycetes. *PLoS one* 13: 1–12.
- Weiss F. 1950. Index of plant diseases in the United States. Parts I, II, III. U.S. Department of Agriculture, Plant Disease Survey Special Publication.
- Wei JG, Phan CK, Wang L, et al. 2013. Pestalotiopsis yunnanensis sp. nov., an endophyte from *Podocarpus macrophyllus* (Podocarpaceae) based on morphology and ITS sequence data. *Mycological Progress* 12: 563–568.
- Wei JG, Xu T, Guo LD, et al. 2005. Endophytic Pestalotiopsis species from southern China. *Mycosistema* 24: 481–493.
- Wijayawardene NN, Goonasekara I, Camporesi E, et al. 2016a. Two new *Seimatosporium* species from Italy. *Mycosphere* 7: 204–213.
- Wijayawardene NN, Hyde KD, Al-Ani LKT, et al. 2020. Outline of fungi and fungus-like taxa. *Mycosphere* 11: 1060–1456.
- Wijayawardene NN, Hyde KD, Wanasinghe DN, et al. 2016b. Taxonomy and phylogeny of dematiaceous coelomycetes. *Fungal Diversity* 77: 1–316.
- Wu W. 1992. Two new *Seimatosporium* species from China. *Journal of Hebei Academy of Sciences* 2: 61–64.
- Wu ZY, Raven PH, Hong DY (eds). 2003. Flora of China. Vol. 9 (Pittosporaceae through Connaraceae). Science Press, Beijing, and Missouri Botanical Garden Press, St. Louis.
- Yang Q, Zeng XY, Yuan J, et al. 2021. Two new species of Neopestalotiopsis from southern China. *Biodiversity Data Journal* 9: e70446.
- Yu J, Wu Y, He Z, et al. 2018. Diversity and antifungal activity of endophytic fungi associated with *Camellia oleifera*. *Mycobiology* 46: 85–91.
- Zhang M, Li J, Wu H, et al. 2014. First report of *Chaetomella raphigera* causing leaf spot on *Rosa chinensis* in China. *Plant Disease* 98: 569–569.
- Zhang Y, Jiang Y, Zu W. 2009. Resources of the genus *Rosa* in China and their application prospects in gardens. *Seed* 28: 1–9. [In Chinese.]
- Zhang YM, Maharanachikumbura SSN, McKenzie EH. 2012a. A novel species of Pestalotiopsis causing leaf spots of *Trachycarpus fortunei*. *Cryptogamie, Mycologie* 33: 311–318.
- Zhang YM, Maharanachikumbura SSN, Tian Q. 2013. Pestalotiopsis species on ornamental plants in Yunnan Province, China. *Sydwia* 65: 113–128.
- Zhang YM, Maharanachikumbura SSN, Wei JG. 2012b. Pestalotiopsis camelliae, a new species associated with grey blight of *Camellia japonica* in China. *Sydwia* 64: 335–344.
- Zhang ZX, Liu RY, Liu SB, et al. 2022. Morphological and phylogenetic analyses reveal two new species of Sporocadaceae from Hainan, China. *MycoKeys* 88: 171–192.
- Zhao G, Li N. 1994. A new species of *Monochaetia* (Coelomycetes) from China. *Mycotaxon* 52: 187–191.
- Zhu PL, Ge QX, Xu T. 1991. Seven new combinations of Pestalotiopsis from China. *Acta Mycologica Sinica* 10: 273–279.

Supplementary material

Fig. S1 Phylogenetic tree of *Monochaetia* resulting from maximum likelihood (ML) analysis of the ITS sequence alignment. Nodes are labelled with bootstrap values from RAxML/Parsimony bootstrap/Bayesian posterior probabilities values. Nodes receiving below 50 bootstrap values and 0.5 probability values are not labelled. The scale bar represents the expected number of changes per site. Isolates collected in this study are in **bold** and blue.

Fig. S2 Phylogenetic trees based on maximum likelihood (ML) analyses for species in *Neopestalotiopsis*. a. ITS region; b. *TEF* gene region; c. *TUB* gene region. Nodes are labelled with bootstrap values from RAxML/Parsimony bootstrap/Bayesian posterior probabilities values. Nodes receiving below 50 bootstrap values and 0.5 probability values are not labelled. The scale bar represents the expected number of changes per site. Isolates collected in this study are in **bold** and blue.

Fig. S3 Phylogenetic trees based on maximum likelihood (ML) analyses for species in *Pestalotiopsis*. a. ITS region; b. *TEF* gene region; c. *TUB* gene region. Nodes are labelled with bootstrap values from RAxML/Parsimony bootstrap/Bayesian posterior probabilities values. Nodes receiving below 50 bootstrap values and 0.5 probability values are not labelled. The scale bar represents the expected number of changes per site. Isolates collected in this study are in **bold** and blue.

Fig. S4 Phylogenetic trees based on maximum likelihood (ML) analyses for species in *Seimatosporium*. a. ITS region; b. LSU gene region. Nodes are labelled with bootstrap values from RAxML/Parsimony bootstrap/Bayesian posterior probabilities values. Nodes receiving below 50 bootstrap values and 0.5 probability values are not labelled. The scale bar represents the expected number of changes per site. Isolates collected in this study are in **bold** and blue.

Fig. S5 Phylogenetic trees based on maximum likelihood (ML) analyses for species in *Seiridium*. a. ITS region; b. *RPB2* gene region; c. *TEF* gene region; d. *TUB* gene region. Nodes are labelled with bootstrap values from RAxML/Parsimony bootstrap/Bayesian posterior probabilities values. Nodes receiving below 50 bootstrap values and 0.5 probability values are not labelled. The scale bar represents the expected number of changes per site. Isolates collected in this study are in **bold** and blue.

Fig. S6 Phylogenetic trees based on maximum likelihood (ML) analyses for species in *Sporocadus*. a. ITS region; b. LSU gene region; c. *RPB2* gene region; d. *TEF* gene region; e. *TUB* gene region. Nodes are labelled with bootstrap values from RAxML/Parsimony bootstrap/Bayesian posterior probabilities values. Nodes receiving below 50 bootstrap values and 0.5 probability values are not labelled. The scale bar represents the expected number of changes per site. Isolates collected in this study are in **bold** and blue.